USGS
science for a changing world

Prepared in cooperation with the East Bay Municipal Utility District

Lithostratigraphic, Borehole-Geophysical, Hydrogeologic, and Hydrochemical Data from the East Bay Plain, Alameda County, California

Data Series 890

U.S. Department of the Interior
U.S. Geological Survey

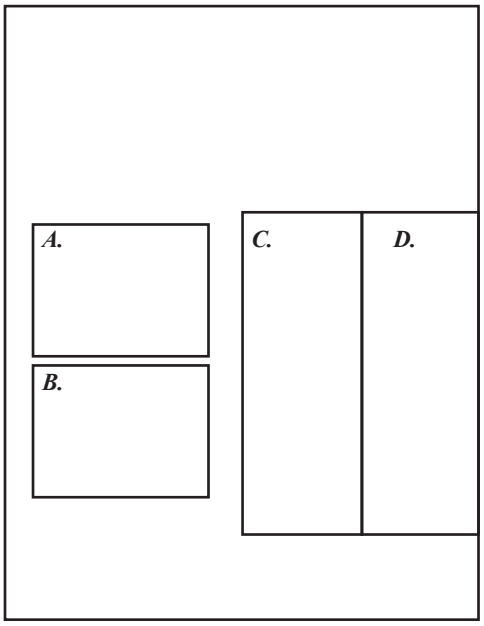

Front cover.

A. U.S. Geological Survey hydrologist analyzing slug-test data (Rhett Everett, U.S. Geological Survey)

B. Dual stage extensometer (Michelle Sneed, U.S. Geological Survey)

C. Portion of core EBAY_45 showing predominantly coarse-grained sediment (U.S. Geological Survey)

D. Portion of core EBAY_23 showing predominantly fine-grained sediment (U.S. Geological Survey)

Back cover

Two U.S. Geological Survey Research Drilling Program drill rigs operating simultaneously (Michelle Sneed, U.S. Geological Survey)

Lithostratigraphic, Borehole-Geophysical, Hydrogeologic, and Hydrochemical Data from the East Bay Plain, Alameda County, California

By Michelle Sneed, Patricia v.P. Orlando, James W. Borchers, Rhett Everett, Mike Solt, Mary McGann, Heather Lowers, and Shannon Mahan

Prepared in cooperation with the East Bay Municipal Utility District

Data Series 890

U.S. Department of the Interior
U.S. Geological Survey

U.S. Department of the Interior
SALLY JEWELL, Secretary

U.S. Geological Survey
Suzette M. Kimball, Acting Director

U.S. Geological Survey, Reston, Virginia: 2015

Suggested citation:
Sneed, Michelle, Orlando, P.v.P., Borchers, J.W., Everett, Rhett, Solt, Mike, McGann, Mary, Lowers, Heather, and Mahan, Shannon, 2015, Lithostratigraphic, borehole-geophysical, hydrogeologic, and hydrochemical data from the East Bay Plain, Alameda County, California: U.S. Geological Survey Data Series 890, 56 p., http://dx.doi.org/10.3133/ds890.

ISSN 2327–638X

Contents

Figures

Tables

Tables—Continued

Tables—Continued

Conversion Factors, Abbreviations, and Acronyms

Inch/Pound to SI

Multiply	By	To obtain
	Length	
inch (in.)	2.54	centimeter (cm)
inch (in.)	25.4	millimeter (mm)
inch (in.)	25400	micrometer (µm)
foot (ft)	0.3048	meter (m)
mile (mi)	1.609	kilometer (km)
	Area	
square foot (ft^2)	929.0	square centimeter (cm^2)
square foot (ft^2)	0.09290	square meter (m^2)
square inch (in^2)	6.452	square centimeter (cm^2)
square mile (mi^2)	259.0	hectare (ha)
square mile (mi^2)	2.590	square kilometer (km^2)
	Volume	
million gallons (Mgal)	3,785	cubic meter (m^3)
cubic inch (in^3)	16.39	cubic centimeter (cm^3)
cubic inch (in^3)	0.01639	liter (L)
cubic foot (ft^3)	0.02832	cubic meter (m^3)
acre-foot (acre-ft)	1,233	cubic meter (m^3)
	Flow rate	
million gallons per day (Mgal/d)	0.04381	cubic meter per second (m^3/s)
	Mass	
ounce, avoirdupois (oz)	28.35	gram (g)
ounce, avoirdupois (oz)	28,349.5	milligram (mg)
	Pressure	
atmosphere, standard (atm)	101.3	kilopascal (kPa)
bar	100	kilopascal (kPa)
pound per square foot (lb/ft^2)	0.04788	kilopascal (kPa)
pound per square inch (lb/in^2)	6.895	kilopascal (kPa)

Conversion Factors, Abbreviations, and Acronyms—Continued

Multiply	By	To obtain
	Density	
pound per cubic foot (lb/ft^3)	16.02	kilogram per cubic meter (kg/m^3)
pound per cubic foot (lb/ft^3)	0.01602	gram per cubic centimeter (g/cm^3)
	Hydraulic conductivity	
foot per day (ft/d)	0.3048	meter per day (m/d)
foot per second (ft/s)	0.3048	meter per second (m/s)
	Radioactivity	
picocurie per liter (pCi/L)	0.037	becquerel per liter

Temperature in degrees Celsius (°C) may be converted to degrees Fahrenheit (°F) as follows:
°F=(1.8×°C)+32

Vertical coordinate information is referenced to the North American Vertical Datum of 1988 (NAVD 88).

Horizontal coordinate information is referenced to the North American Datum of 1983 (NAD 83).

Altitude, as used in this report, refers to distance above the vertical datum.

Specific conductance is given in microsiemens per centimeter at 25 degrees Celsius (µS/cm at 25 °C).

Concentrations of chemical constituents in water are given either in milligrams per liter (mg/L) or micrograms per liter (µg/L).

Abbreviations and Acronyms

ASR	aquifer storage and recovery
ASTM	American Society for Testing and Materials
BGP	Bayside Groundwater Project
DIC	dissolved inorganic carbon
EBAY	East Bay Bayside Monitoring Site
EBMUD	East Bay Municipal Utility District
EBMY	East Bay Mud Yard
EBSP	East Bay Stenzel Park
EDS	energy dispersive spectroscopy
EXT1	East Bay Extensometer-1 Monitoring Site
EXT2	East Bay Extensometer-2 Monitoring Site
fbls	feet below land surface
GAMA	Groundwater Ambient Monitoring and Assessment

Abbreviations and Acronyms—Continued

ICP-MS	inductively coupled plasma-mass spectroscopy
INAA	instrumental neutron activation by abbreviated count
IRSL	infrared stimulated luminescence
kV	kilovolts
MSCL	multi-sensor core logger
mV	millivolts
nA	nanoamp
NAWQA	National Water-Quality Assessment
NOSAMS	National Ocean Sciences AMS Facility
NTRU	nephelometric turbidity ratio units
NWIS	National Water Information System
NWQL	National Water Quality Laboratory
OSL	optically stimulated luminescence
psu	practical salinity units
PVC	polyvinyl chloride
R_2	coefficient of determination
SCPT	seismic cone penetration test
SEM	scanning electron microscopy
TDS	total dissolved solids
TRIGA	Training, Research, Isotopes, General Atomics
UAMSL	University of Arizona Accelerator Mass Spectrometry Lab
USGS	U.S. Geological Survey
UWIL	University of Waterloo Environmental Isotope Lab
V_p	velocity of P waves
V_s	velocity of S waves
XRD	X-ray diffraction
YMPB	Yucca Mountain Project Branch

Lithostratigraphic, Borehole-Geophysical, Hydrogeologic, and Hydrochemical Data from the East Bay Plain, Alameda County, California

By Michelle Sneed, Patricia v.P. Orlando, James W. Borchers, Rhett Everett, Mike Solt, Mary McGann, Heather Lowers, and Shannon Mahan

Abstract

The U.S. Geological Survey, in cooperation with the East Bay Municipal Utility District, carried out an investigation of aquifer-system deformation associated with groundwater-level changes at the Bayside Groundwater Project near the modern San Francisco Bay shore in San Lorenzo, California. As a part of the Bayside Groundwater Project, East Bay Municipal Utility District proposed an aquifer storage and recovery program for 1 million gallons of water per day. The potential for aquifer-system compaction and expansion, and related subsidence, uplift, or both, resulting from aquifer storage and recovery activities were investigated and monitored in the Bayside Groundwater Project. In addition, baseline analysis of groundwater and substrata properties were performed to assess the potential effect of such activities. Chemical and physical data, obtained from the subsurface at four sites on the east side of San Francisco Bay in the San Lorenzo and San Leandro areas of the East Bay Plain, Alameda County, California, were collected during the study. The results of the study were provided to the East Bay Municipal Utility District and other agencies to evaluate the chemical and mechanical responses of aquifers underlying the East Bay Plain to the future injection and recovery of imported water from the Sierra Nevada of California.

Among 4 sites, 14 piezometers and 2 extensometers were installed in 6 boreholes, which ranged in depth from 460 to 1,040 feet. The lithology of drill cuttings, collected at 5- or 10-foot intervals, was described for grain size and any other noticeable features, such as wood or shell fragments. Borehole geophysical logging was performed at each site in the deepest borehole, immediately following drilling.

Drill-core samples, totaling 284 feet, were collected at the Bayside site. The drill-core sediment was subsampled to determine pore-water chemistry, vertical hydraulic conductivity, and physical and mechanical properties at different depths. Depositional environment and age were determined by luminescence geochronology and fossil identification. The elemental composition of the drill-core sediments was determined by inductively coupled plasma mass spectroscopy and instrumental neutron activation by abbreviated count analysis. Mineral composition was determined by X-ray diffraction and scanning electron microscopy analysis.

Groundwater samples were collected from all 14 piezometers as part of either the USGS Groundwater Ambient Monitoring and Assessment or the USGS National Water Quality Assessment program for water-quality analyses. Sample analytes included nutrients, major and minor ions, trace elements, isotopic ratios of hydrogen and oxygen in water, carbon-14, and tritium.

Water-level and aquifer-system-compaction measurements, which indicated diurnal and seasonal fluctuations, were made at the Bayside Groundwater Project site. Slug tests were performed at the Bayside piezometers and nine pre-existing wells to estimate hydraulic conductivity.

Introduction

Aquifer-system deformation associated with groundwater-level changes was investigated cooperatively by the U.S. Geological Survey (USGS) and the East Bay Municipal Utility District (EBMUD) at the Bayside Groundwater Project (BGP) in San Lorenzo, California, near the San Francisco Bay shore (*fig. 1*). As a part of the BGP, EBMUD has proposed an aquifer storage and recovery (ASR) program for injecting 1 million gallons of imported water per day. This water will be stored in a 98-foot (ft) -thick sequence of coarse-grained sediment (referred to in this report as the "Deep aquifer") underlying the East Bay Plain and the neighboring groundwater basin. Water from the Deep aquifer could be used directly to help meet short-term needs arising from drought, seismic, and other water-supply emergencies. In addition, water imported from the Sierra Nevada could be injected, stored, and later recovered from the Deep aquifer for public supply. Land-surface uplift and subsidence at the ASR site and surrounding areas resulting from the expansion

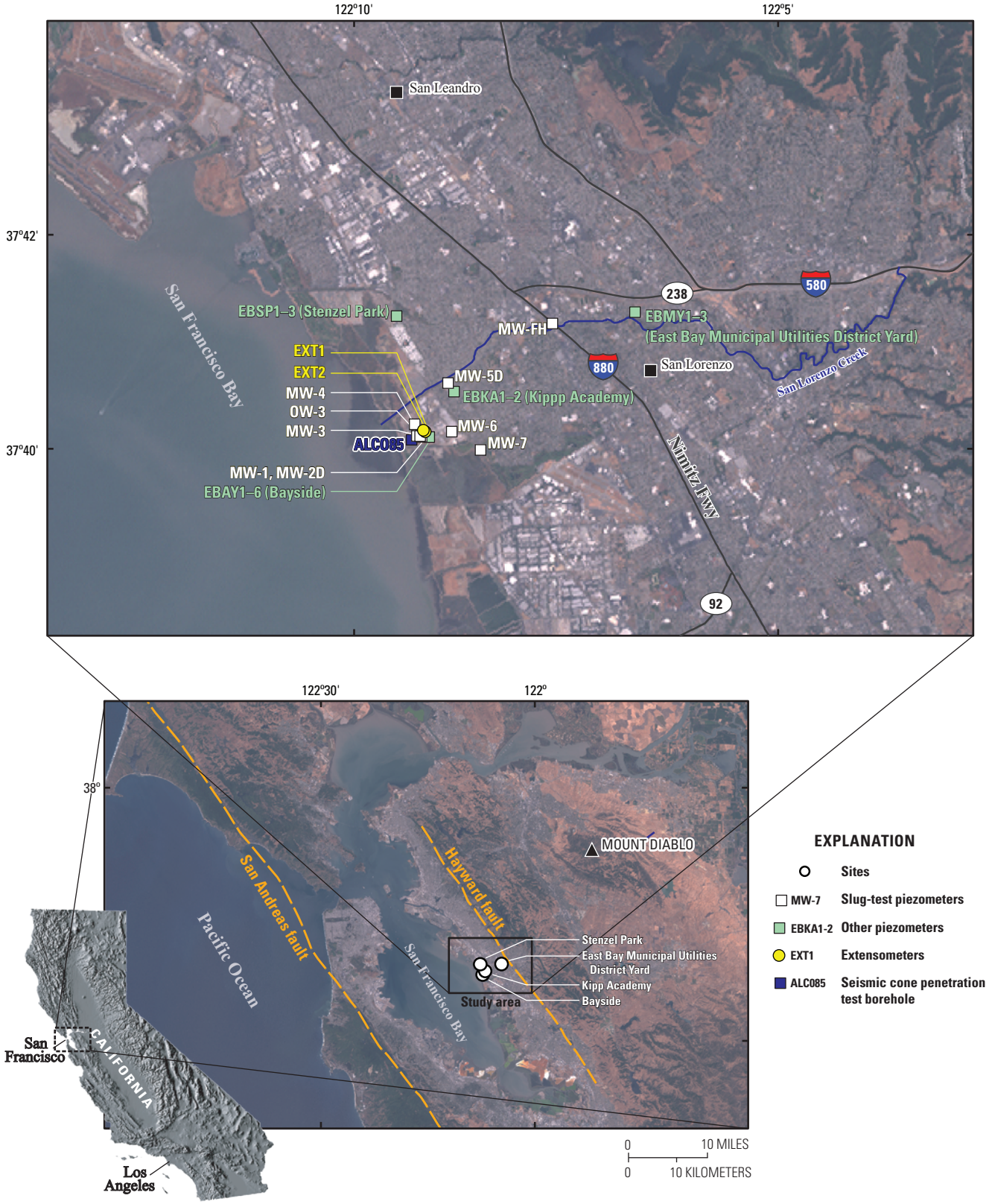

Figure 1. Map showing tThe piezometer, extensometer, and slug-test locations, East Bay Plain, Alameda County, California.

and compression of the aquifer system associated with water injection and pumping during ASR cycles could occur. In addition, the introduction of imported water that has a different chemical composition from native water could alter the chemical equilibrium between the groundwater and the substrate. Chemical analyses of the groundwater and sediments were performed at select sites in order to establish a baseline of water quality.

The Deep aquifer is overlain by about 500 ft of clayey, fine-grained sediments and underlain by comparable sediments. These sediments are similar to the clayey sediments found in the nearby Santa Clara Valley, where inelastic compaction resulted in about 14 ft of subsidence near San Jose from 1910 to 1995 due to overdraft of the aquifer (Galloway and others, 1999). The Deep aquifer is an important regional resource, and EBMUD is required to demonstrate that ASR activities will not cause permanent land subsidence or adversely affect nearby groundwater management or salinity levels. Because local relief is low, subsidence in the East Bay area could induce coastal flooding and create difficulty conveying winter storm runoff from urbanized areas.

The objectives of this investigation were to monitor and analyze aquifer-system compaction and expansion, and any related subsidence or uplift, resulting from proposed ASR activities at the BGP and to establish a baseline of groundwater quality prior to injection. For this purpose, 14 piezometers and 2 extensometers were constructed to monitor groundwater levels, groundwater chemistry, and aquifer-system compaction. This information is needed by the EBMUD for the planning and implementation of large-scale injection and recovery operations.

As an initial step to achieve this objective, the USGS drilled three boreholes at one site (Bayside) next to the BGP. Inside one of the boreholes, refered to as the East Bay Bayside Monitoring Site (EBAY), six piezometers (EBAY 1–6) were constructed, and in the other two boreholes (East Bay Extensometer-1 Monitoring Site, or EXT1, and East Bay Extensometer-2 Monitoring Site, or EXT2), a dual-stage extensometer was installed at depths of about 700 and 1,040 ft. Additional boreholes were drilled at three sites near the BGP —the East Bay MUD Yard (EBMY), Stenzel Park (EBSP), and Kipp Academy (EBKA)—and constructed with two or three piezometers each (*table 1*). These piezometers and extensometers were constructed for the purpose of monitoring pore-fluid pressure changes and aquifer-system deformation, respectively, which could result from the proposed ASR program.

Table 1. Summary of sites, boreholes, piezometers, and types of data collected for the Bayside Groundwater Project with table and figure references.

[**Abbreviations**: fbls, feet below land surface; MUD, Municipal Utility District; —, no data]

Site name	Borehole name (depth in fbls)	Piezometers (number in each borehole)	Extensometer	Lithological and geophysical logs	Water level and aquifer-system compaction	Slug tests	Water-quality data	Core analysis
Bayside	EBAY (1,040)	6	—	Fig. 2*A*	Fig. 4*A*	Table 2, 5	Table 2, 6–10	Table 11–27
Bayside	EXT1 (1,040)	0	Fig. 3	Fig. 2*B*	Fig. 4*B*	—	—	—
Bayside	EXT2 (696)	0	Fig. 3	Fig. 2*C*	Fig. 4*B*	—	—	Table 11–27
Bayside	ALC085	0	—	—[1]	—	—	—	—[1]
East Bay MUD yard	EBMY (460)	3	—	Fig. 2*D*	—	—	Table 2, 6–10	—
Kipp academy	EBKA (460)	2	—	Fig. 2*E*	—	—	Table 2, 6–10	—
Stenzel park	EBSP (680)	3	—	Fig. 2*F*	—	—	Table 2, 6–10	—
Slug site 1	MW-FH	1	—	—	—	Table 2, 5	—	—
Slug site 2	MW-1	1	—	—	—	Table 2, 5	—	—
Slug site 3	MW-2D	2	—	—	—	Table 2, 5	—	—
Slug site 4	OW3	1	—	—	—	Table 2, 5	—	—
Slug site 5	MW-3	1	—	—	—	Table 2, 5	—	—
Slug site 6	MW-4	1	—	—	—	Table 2, 5	—	—
Slug site 7	MW-5D	1	—	—	—	Table 2, 5	—	—
Slug site 8	MW-6	1	—	—	—	Table 2, 5	—	—
Slug site 9	MW-7	1	—	—	—	Table 2, 5	—	—

[1]Data for this borehole is presented in Bennett and others, 2009.

Purpose and Scope

The purpose of this report is to present chemical and physical data obtained from the subsurface at four sites in the East Bay Plain of Alameda County–East Bay Bayside (EBAY, EXT1, EXT2, and ALC085); East Bay MUD Yard (EBMY); Stenzel Park (EBSP); and Kipp Academy (EBKA). The data included lithologic descriptions, geophysical logs, and results of groundwater-quality analyses from each of the four sites. In addition, analyses of drill-core sediments, extensometer measurements, and groundwater-level measurements from the Bayside sites are presented. Furthermore, slug-test results from the Bayside and nine other pre-existing wells are presented. These data are for use by EBMUD and other agencies to evaluate the response of aquifers underlying the East Bay Plain to the injection and recovery of imported water from the Sierra Nevada.

The scope of the report includes descriptions of drilling and constructing piezometers and a dual-stage extensometer, collecting and analyzing chemical and physical data from the subsurface, performing and analyzing slug tests from selected new and existing wells, and measuring groundwater levels and compaction at the Bayside site. A second phase of this project has been proposed and includes production of a report that documents the hydromechanical analyses of the data presented in this report and of any high-quality data collected subsequent to publication of this report.

Previous Studies

The EBMUD has carried out a series of studies to evaluate the geologic and hydraulic properties of local deep aquifers. The purpose of these studies was to determine the yield of wells in these aquifers and to assess their suitability for injection and recovery of imported water. Most of this work has been site specific and related to the installation and performance of injection and recovery wells (Fugro West, Inc., 1998, 1999), although a regional assessment of subsurface geohydrologic conditions has been completed (CH2M-Hill Inc., 2000). Izbicki and others (2003) presented additional data and a comprehensive understanding of the geohydrology and geochemistry of the aquifer system to assist water-resources managers in the planning and implementation of large-scale injection and recovery operations in aquifers underlying the East Bay Plain. Catchings and others (2006) used seismic imaging to better understand the subsurface stratigraphy and structures and their effects on groundwater and earthquake hazards. Brocher and others (2007) characterized seismic hazards at Bayside by using shear-wave and compressional-wave suspension logging. Bennett and others (2009) used seismic cone-penetration tests (SCPT) at Bayside to determine stratification, soil type, shear-wave velocity, density, consistency, and penetration resistence. Water-quality and quality-assurance samples were collected at the six EBAY piezometers at the Bayside site in June 2007 and analyzed as part of the USGS Groundwater Ambient Monitoring and Assessment (GAMA) program (Ray and others, 2009).

Description of the Study Area

The study area is on the east side of the San Francisco Bay in the San Lorenzo and San Leandro areas of the East Bay Plain (*fig. 1*), which consists of about 120 square miles (mi^2) of tidal marshes and alluvial lowlands. San Lorenzo Creek is the principal stream in the study area, draining 44 mi^2, originating in the Diablo Range, and flowing westward to the San Francisco Bay. The study area has a Mediterranean climate with mild, wet winters and warm, dry summers. The average annual temperature is 13.2 degrees Celsius (ºC): average winter temperatures (December–February) are about 9ºC, and average summer (June–August) temperatures are about 15ºC. Most precipitation falls as rain between November and March, and precipitation averages 23 inches (in.) annually (Muir, 1997). In 1999, the East Bay Plain had a population of more than 900,000 (San Francisco Bay Regional Water Quality Control Board, 1999). The area is densely populated and highly urbanized and is characterized by industrial, commercial, and residential land uses. Although agriculture was important in the past, there is little agricultural land use in the study area at the present time (Izbicki and others, 2003).

Hydrogeologic Framework

The study area is located in a structural depression underlying San Francisco Bay that is bounded by the San Andreas fault to the west and the Hayward fault to the east (Trask and Rolston, 1951; Sedlock, 1995; Marlow and others, 1999). The thickest deposits in the study area are near San Leandro, along the margin of San Francisco Bay (Rogers and Figuers, 1991; Marlow and others, 1999), and deposits thin to the north. Deeper deposits within this structural depression have been compressed and folded as a result of movement along the faults (Marlow and others, 1999). During the last 130,000 years or more, the areal extent of the San Francisco Bay has been controlled by sea-level changes, geologic movement along faults, and sedimentation from upland streams. These processes produced a complex sequence of coarse-grained aquifers and fine-grained confining layers (Koltermann and Gorelick, 1992).

The study area is on part of the East Bay Plain that is composed of the alluvial fan of San Lorenzo Creek (*fig. 1*), which is underlain by a complex inter-fingering sequence

of late Pleistocene to Holocene unconsolidated marine and continental deposits (Brown and Caldwell, Inc., 1986; CH2M-Hill, Inc., 2000). The marine deposits primarily consist of estuarine mud and salt-marsh deposits that include the Young Bay Mud; the Old Bay Mud, also known as the Yerba Buena Mud (Sloan, 1992); and several other units (Trask and Rolston, 1951; Ross, 1977; Atwater and others, 1981; Rogers and Figuers, 1991; Sloan, 1992; CH2M-Hill Inc., 2000). The continental deposits consist of coarse-grained stream-channel deposits and finer-grained flood-plain deposits (Koltermann and Gorelick, 1992; Sloan, 1992), which compose the coalescing alluvial fans of San Leandro and San Lorenzo Creeks and other drainages along the east side of San Francisco Bay. Partly consolidated sedimentary rocks and deposits probably underlie the late Pleistocene continental and marine deposits (Marlow and others, 1999; Izbicki and others, 2003). Basement rocks are assumed to be the same as those found in the neighboring mountain ranges, which consist largely of Mesozoic "Great Valley" and "Franciscan" complexes and overlying Tertiary and younger rocks (Howard, 1979; Graymer, 2000).

The four primary aquifers in the study area consist of aeolian sand, alluvial sand, and gravel deposits separated by estuarine mud or fine-grained, alluvial flood-plain deposits. In many areas, the aquifers are discontinuous, and it is difficult to correlate sand and gravel layers over great distances between wells. In the study area, the aquifers are named (from shallowest to deepest) the Newark, Centerville, Freemont, and Deep aquifers (Izbicki and others, 2003). The aquifers in this study are the "time-equivilent" counterparts of aquifers in the alluvial fans of Alameda Creek, originally named by Brown and Caldwell (1986) and Maslonkowski (1988) and commonly known as the Niles Cone basin. It is not known if they are hydraulically connected to aquifers in the Niles Cone basin, which is approximately 15 miles to the south.

The Newark aquifer is present to a depth of 30 to 130 feet below land surface (fbls) throughout the study area (CH2M-Hill Inc., 2000). Water in the Newark aquifer is generally confined, except near recharge areas along the mountain front. The underlying Centerville aquifer is about 100-ft thick and extends to depths of about 220 fbls (Maslonkowski, 1984). In the Niles Cone basin, the Freemont aquifer is a generic name for discontinuous sand and gravel deposits between 240 and 400 fbls. In the study area, the name has been applied to sand and gravel deposits as deep as 500 ft by CH2M-Hill, Inc. (2000). The Deep aquifer occurs between 500 and 650 fbls, and in some areas it is as much as 140-ft thick. The Deep aquifer is thickest and most continuous south of San Leandro (Maslonkowski, 1988) and thins, eventually disappearing, to the north (CH2M-Hill, Inc., 2000). In this area, aquifers are underlain by partly consolidated deposits (Marlow and others, 1999) that have low values of porosity and permeability.

Methods

Design of Monitoring Sites

A total of 14 piezometers and 2 extensometers were constructed among six boreholes distributed among four sites: Bayside (EBAY, EXT1, EXT2), East Bay MUD Yard (EBMY), Kipp Academy (EBKA), and Stenzel Park (EBSP; *fig. 1*, *table 1*). Boreholes were drilled by using a hydraulic mud rotary rig operated by the USGS Western Region Research Drilling Unit. The four piezometer boreholes (EBAY, EBMY, EBKA, EBSP) are telescoping-diameter designs, where diameters range from 22 to 7.875 in., with the largest drilled diameter at the land surface and smallest drilled diameter at final depth. Borehole depths ranged from 460 to 1,040 fbls. At the Bayside site, 15-in. surface conductor casing was installed in the EBAY borehole to 100 fbls, and 14-in. surface conductor casing was installed in the EXT1 and EXT2 boreholes to 79 fbls. A summary of sites, boreholes, and types of data collected from each can be found in *table 1*.

Piezometer Construction and Instrumentation

The 14 piezometers at the 4 sites were constructed as nested, 2-in. or 2.5-in. diameter, schedule 80 polyvinyl chloride (PVC) casings, with 10- to 60-ft slotted-screen intervals; slot size was 1.2 by 0.02 inches, width by height, respectively. Screened intervals were sand packed by using a tremmie pipe with #3 Monterey sand; all other intervals were grouted with a 30-percent-solids bentonite grout to hydraulically isolate the sand packs and seal the boreholes from surface infiltration. The uppermost parts of the piezometers were encased in protective underground vaults fitted with locking lids for security purposes. The piezometers were developed by using an air-lifting and surging technique until no drilling mud was visible in the discharge and several water-quality parameters (specific conductance, pH, temperature) had stabilized. Construction diagrams for the piezometers are shown in *figure 2*. Although six piezometers were constructed in the EBAY borehole, the deepest piezometer (EBAY1) was not developed sufficiently and, therefore, was not responsive. Upon completion of EBAY1 piezometer construction, test equipment could not be lowered past a depth of 1,000 ft into the 2.5-in. PVC piezometer casing. Repeated attempts were made to clear the 1,000 to 1,010 ft interval by using airlifting techniques; however, by January 2008, silt filled the bottom 60 ft of the piezometer, including the screened interval, which, therefore, was not well-connected to the aquifer system. As a result of this malfunction, results of analyses from piezometer EBAY1 are not discussed.

A

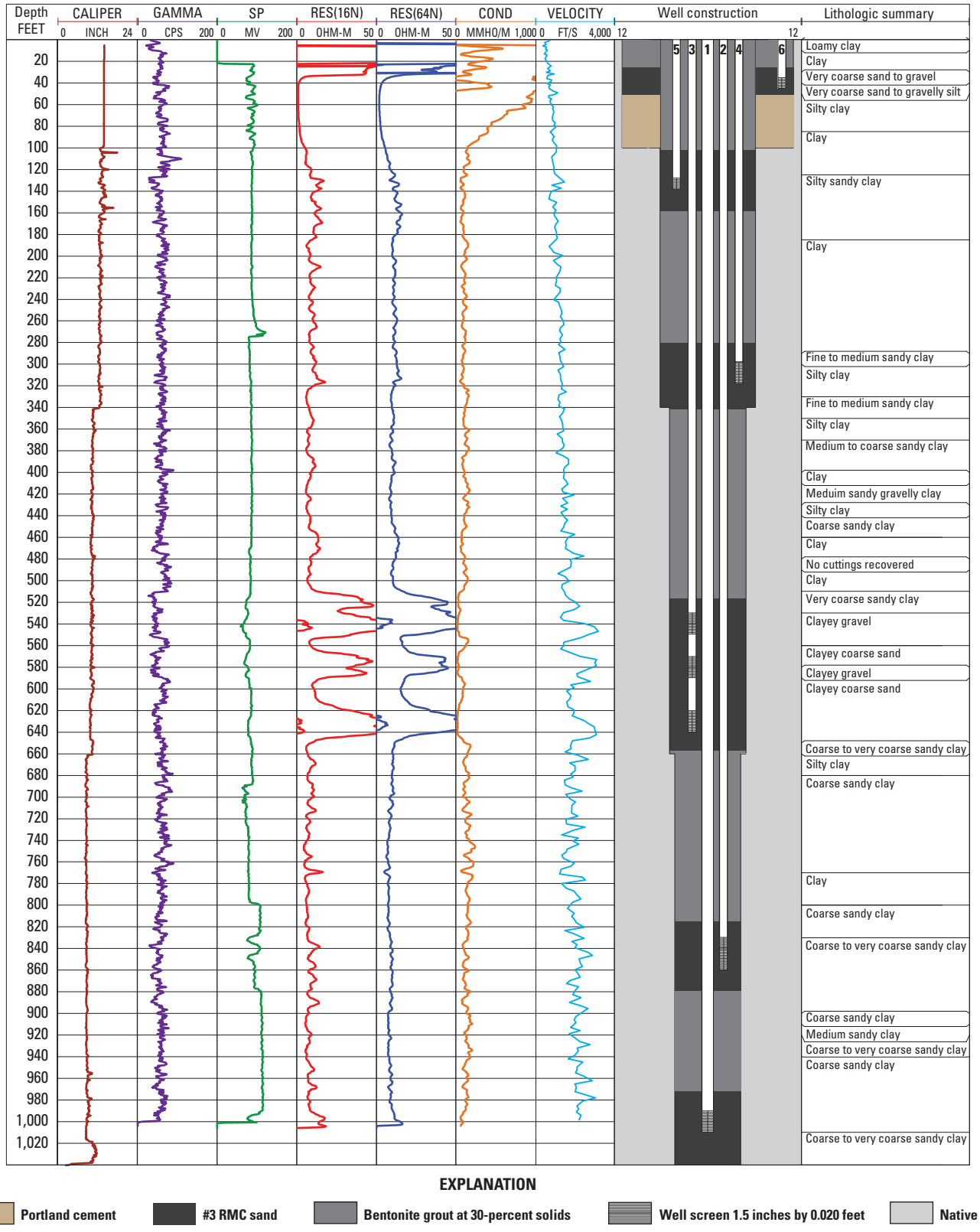

[Abbreviations: CPS, counts per second; MV, millivolts; OHM-M, ohm-meter; MMMHO/M, millimho per meter; FT/S, feet per second; SP, spontaneous potential]

Figure 2. Graphs showing wWell construction and lithological, geophysical, and velocity logs for East Bay monitoring sites: *A*, East Bay Bayside Monitoring Site (EBAY); *B*, East Bay Extensometer-1 Monitoring Site (EXT1) at Bayside; *C*, East Bay Extensometer-2 Monitoring Site (EXT2) at Bayside; *D*, East Bay Municipal Utility District Yard (EBMY); *E*, Kipp Academy (EBKA); and *F*, Stenzel Park (EBSP).

B

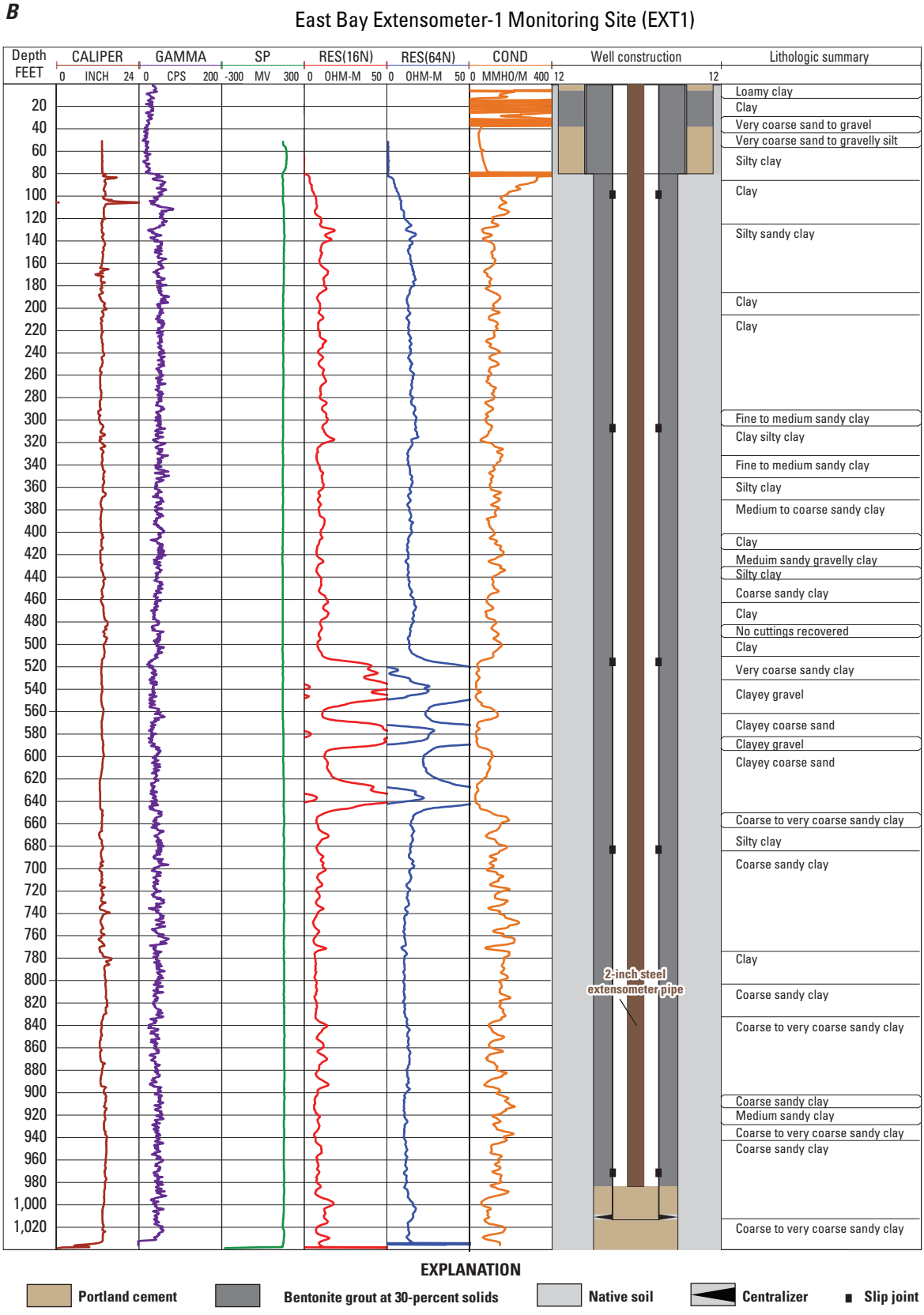

[Abbreviations: CPS, counts per second; MV, millivolts; OHM-M, ohm-meter; MMMHO/M, millimho per meter; FT/S, feet per second; SP, spontaneous potential]

Figure 2. —Continued

C

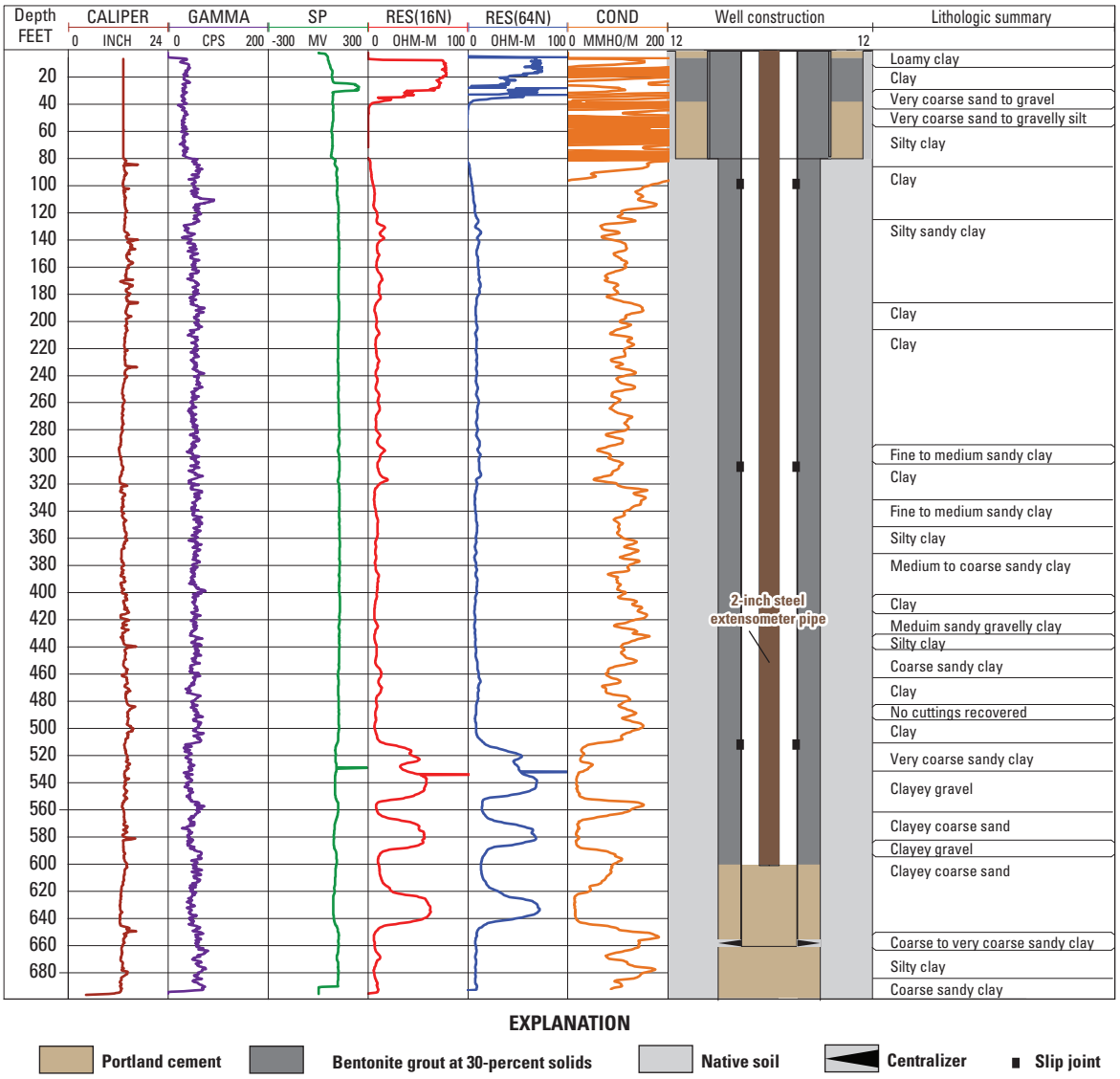

[Abbreviations: CPS, counts per second; MV, millivolts; OHM-M, ohm-meter; MMMHO/M, millimho per meter; FT/S, feet per second; SP, spontaneous potential]

Figure 2. —Continued

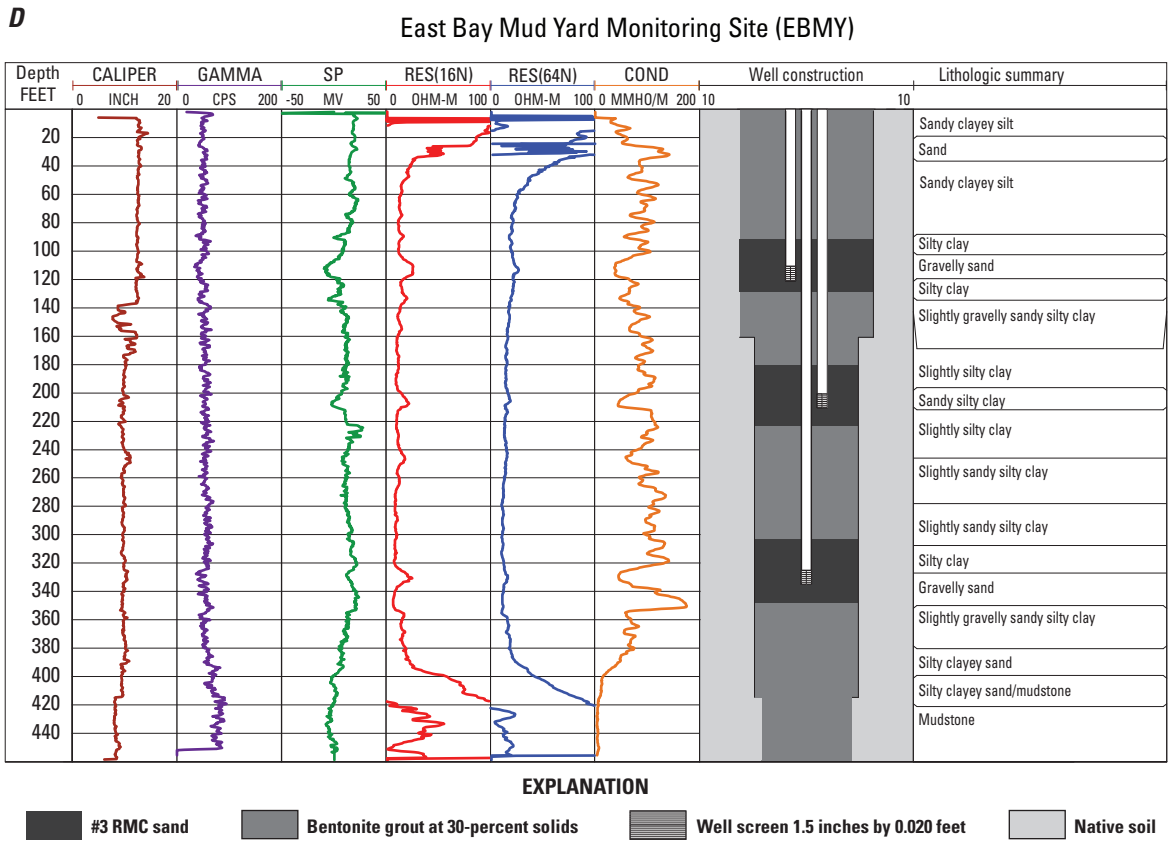

[Abbreviations: CPS, counts per second; MV, millivolts; OHM-M, ohm-meter; MMMHO/M, millimho per meter; FT/S, feet per second; SP, spontaneous potential]

Figure 2. —Continued

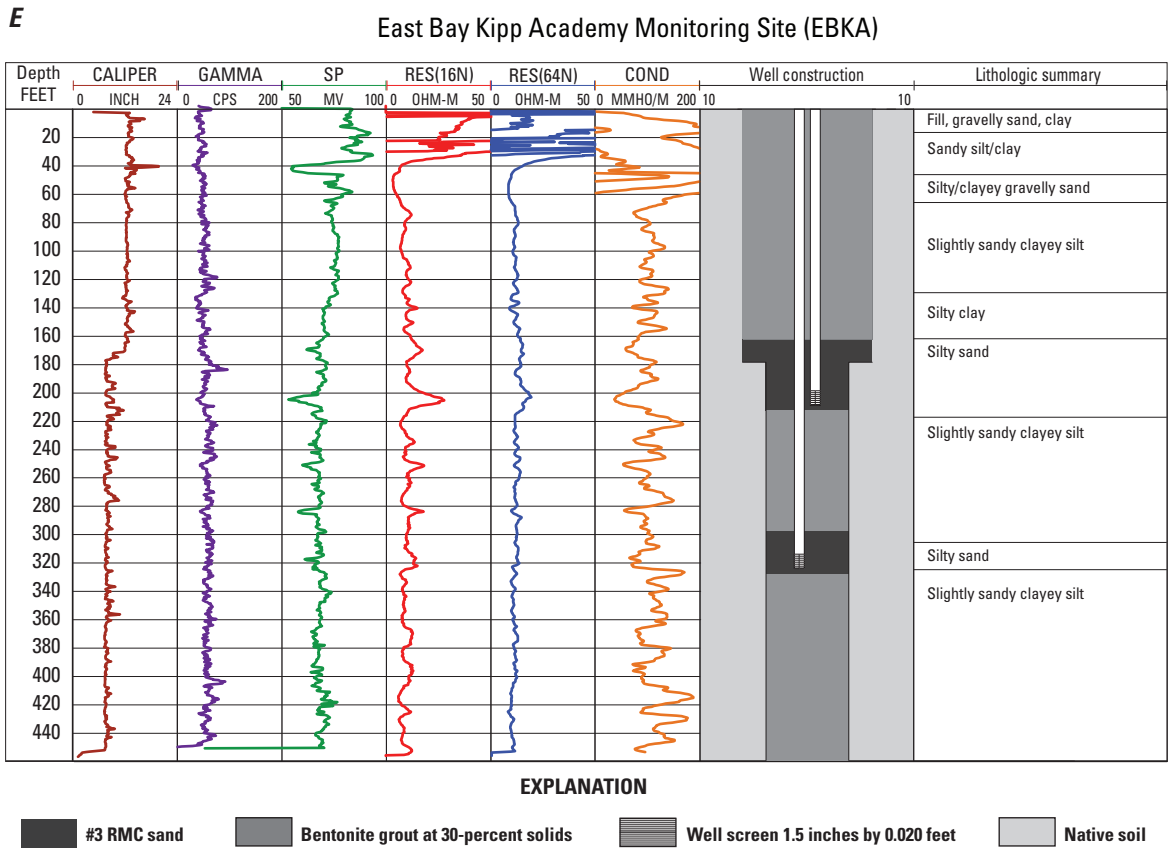

[Abbreviations: CPS, counts per second; MV, millivolts; OHM-M, ohm-meter; MMMHO/M, millimho per meter; FT/S, feet per second; SP, spontaneous potential]

Figure 2. —Continued

F

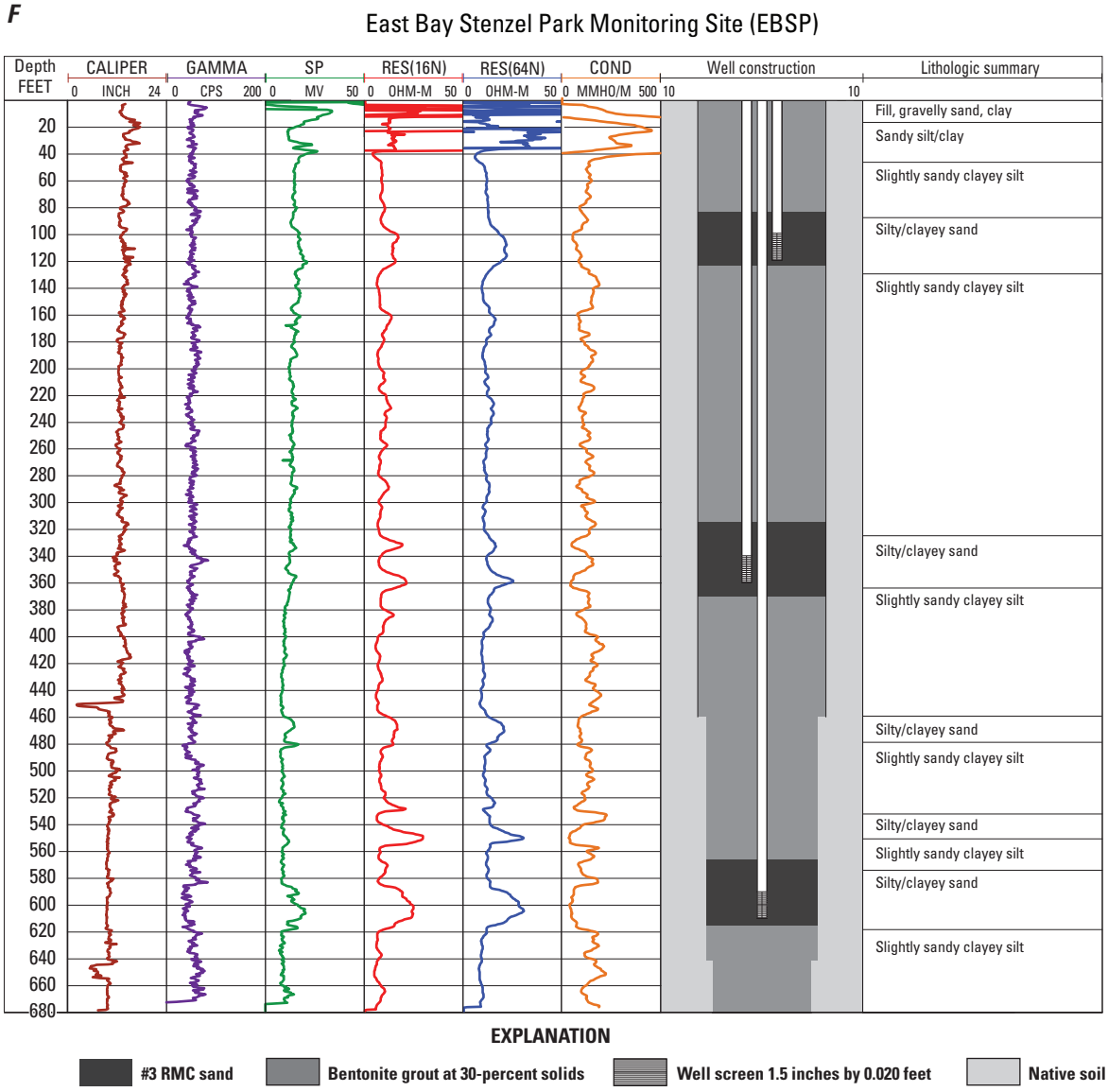

[Abbreviations: CPS, counts per second; MV, millivolts; OHM-M, ohm-meter; MMMHO/M, millimho per meter; FT/S, feet per second; SP, spontaneous potential]

Figure 2. —Continued

Submersible, vented, 10-pound per square inch (psi) pressure transducers and data loggers were installed to continuously measure and record water levels in the six EBAY piezometers. EBMY, EBSP, and EBKA data are managed by EBMUD and were not instrumented by the USGS. To prevent moisture from condensing in the vent tubes and affecting the measurements or potentially damaging the sensitive electronics of the transducers, the open (land-surface) ends of the transducer vent tubes were placed in vented canisters filled with desiccant. The transducers were calibrated at the time of installation to derive a relation to convert transducer output in millivolts (mV) to depth to water below land surface.

Extensometer Construction and Instrumentation

The dual-stage, counterweighted pipe extensometer was constructed at the Bayside study site, about 400 ft east-southeast of the ASR site. An extensometer, which is used, in this case, to measure the change in distance between the bottom of each borehole and the ground surface for two boreholes, provides a measure of aquifer-system compaction within a specified depth interval of sediments. A detailed description of borehole extensometric methods commonly used by the USGS can be found in Riley (1984). The borehole for the shallow extensometer (EXT2) was drilled to 696 fbls, and the borehole for the deep extensometer (EXT1) was drilled to 1,040 fbls (*fig. 3*). Inclinometer measurements made during drilling indicated that the boreholes deviated from vertical by less than 1.0 degree. Riley (1984) noted that extensometer boreholes should be vertically aligned to prevent friction between the measuring element and the casing because excessive friction can degrade extensometer measurements.

Construction of the extensometer involved several components (*fig. 3*). A 6-in.-diameter steel casing was anchored in cement at the bottom of each extensometer borehole. Three and five slip joints were installed along the well casing string in the shallow and deep extensometers, respectively, to allow the casing string to change length. Each slip joint has 30 in. of throw, and the bottom joint of each extensometer casing was compressed by 1 ft to allow vertical displacement in either direction. The slip joints were used to minimize skin friction. Negative skin friction (or downdrag) occurs between the casing and sediments adjacent to the borehole and can cause the extensometer instruments to under-record compaction or expansion by redistributing vertical stresses near the borehole. To further reduce negative skin friction, the annular space between the casing and the borehole was grouted with low-friction bentonite. A 2-in.-diameter steel extensometer pipe (the measuring element), with three 0.25-in. holes spaced 5-ft apart near the bottom of the pipe, was placed inside each 6-in. casing. The 2-in.-diameter steel extensometer pipe rests on a 0.75 in.-thick, 3.5-in.-diameter steel plate situated on top of flat cement in each borehole. The bottom of the extensometer pipe is about 980 fbls in EXT1(below the base of the Deep aquifer) and about 598 fbls in EXT2 (above the bottom of the Deep aquifer).

A wood-framed shelter was constructed over the dual-stage extensometer. An instrument table (*fig. 3*) was positioned over both extensometers. The table was mounted on three 4-in.-diameter steel legs that were cemented in holes bored to a depth of 30 fbls. To minimize the effect of shallow sediment movement on the extensometer measurements, each table leg was cemented in a 6-in.-PVC casing, which was inside gravel-filled cardboard forms that were placed around the table legs and the 14-in.-diameter extensometer surface casings to decouple them from the concrete pad constructed for the shelter foundation. Because the instrument table legs were anchored 30 fbls, the extensometers measure vertical deformation between about 30 fbls and the bottom of the borehole—696 fbls for EXT2 and 1,040 fbls for EXT1.

The extensometer pipe was supported above ground by a fulcrum assembly consisting of a fulcrum arm positioned on an arm support welded to a half-inch steel plate atop the 14-in. casing, and it was balanced with counterweights. Following the guidelines of Riley (1984), about 80 to 90 percent of the weight of the extensometer pipe was counterbalanced to minimize flexing of the extensometer pipe, which prevents the pipe from having contact with the well casing. The asymmetrical positioning of the fulcrum arm afforded the arm a mechanical advantage of about 10:1, reducing the required counterweights (1,160 pounds for the shallow and and 2,900 pounds for the deep extensometers, without using the fulcrum arm) by an order of magnitude.

Vertical deformation (compaction and expansion) of the aquifer system was measured by recording the movement of the instrument table relative to the top of the extensometer pipe by using digital and analog instruments. A Penny and Giles SLS190 linear displacement sensor, with a resolution of about 0.00001 ft and a travel range of 0.41010 ft, was the primary instrument for each extensometer. The top of the linear potentiometer was secured to the instrument table, and the bottom was secured to the extensometer pipe. As the instrument table moved relative to the extensometer pipe, the linear potentiometer output a voltage proportional to the displacement. The output voltage was recorded on an electronic data logger inside the shelter.

Analog dial gages also were used to measure vertical deformation. The dial gages were attached to pieces of angled metal affixed to the instrument table. A spring-controlled stem protruding from the bottom of the dial gage rested on a fixed reference surface attached to the extensometer pipe. The stem compressed or expanded as the instrument table moved relative to the fixed reference surface. The analog dial gage can be read to a precision of 0.0001 in. The dial-gage readings were not recorded electronically, but were read during each of the site visits, which took place every other month. These readings were used to check linear-displacement sensor performance.

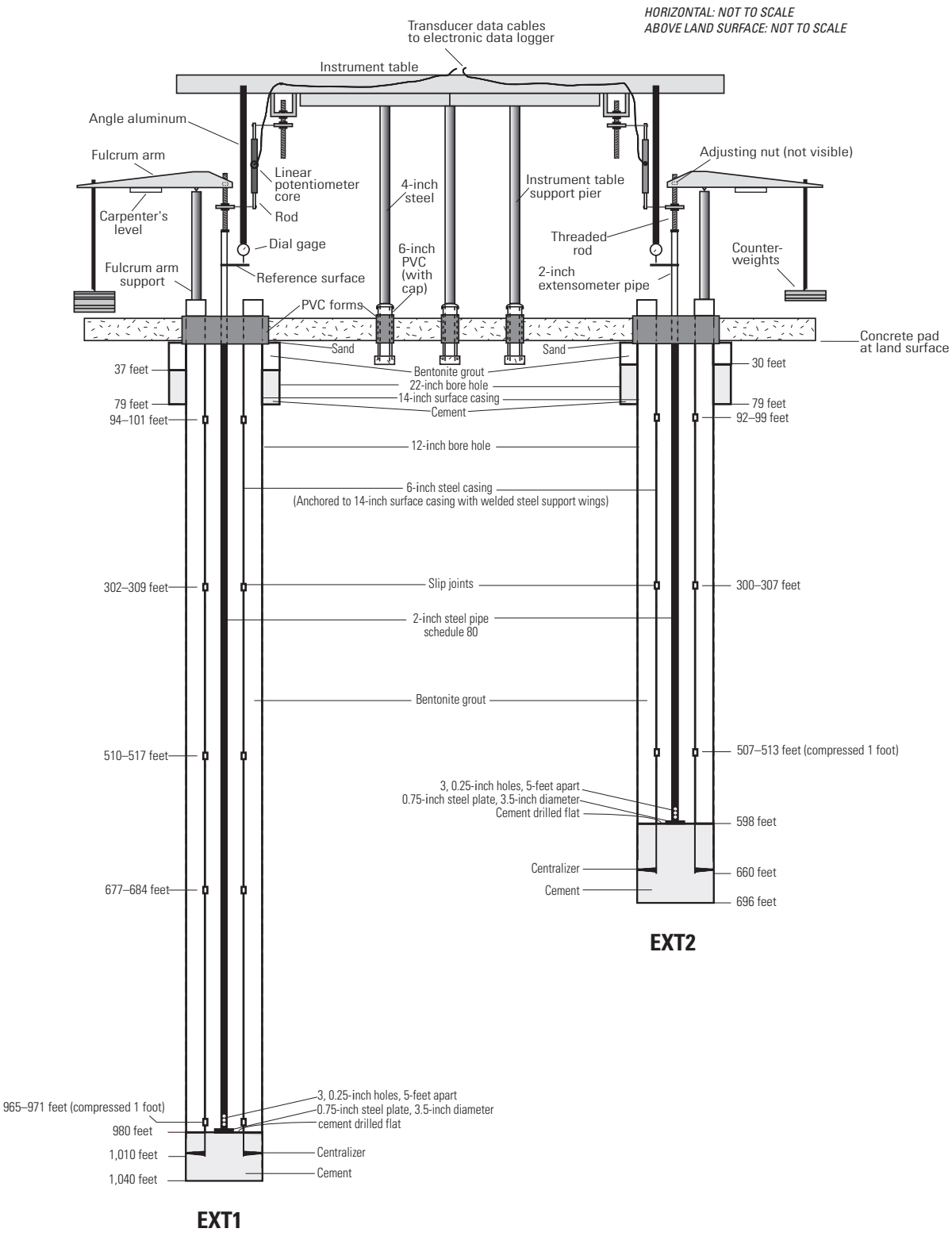

Figure 3. Diagram showing the cConstruction of the dual-stage extensometer at Bayside.

Lithologic and Geophysical Logging

Drill cuttings were collected at 5- and 10-ft intervals during drilling by using a number 60 to 120 mesh sieve and were placed in compartmentalized boxes for later detailed description and archiving. The lithology of drill cuttings was initially described in the field, then refined in the office, for grain size and any other noticeable features, such as wood or shell fragments. Particle-size descriptions followed the National Research Council (1947) classification. This classification allows for the correlation of general grain-size terms (such as "sand"), which have size limits determined in millimeters or inches. The cataloged drill cuttings were then compiled and simplified to construct a lithologic summary (*fig. 2*).

Upon completion of drilling the deepest borehole at each site, a suite of borehole geophysical logs was made in the uncased borehole by the USGS. The logs (*fig. 2*) generally included spontaneous potential, 16-in. and 64-in. normal resistivity, guard resistivity, natural gamma, and caliper logs. Interpretation of data derived from these logs were used to identify the depths of contacts between hydrogeologic units and to plan the length and location of the piezometer screen intervals for completion of construction of the piezometers in the borehole.

Water-Level and Aquifer-System-Compaction Measurements

Periodic water-level measurements were taken every other month in the EBAY piezometers by using either calibrated electric tape or steel tape; water levels were measured continuously by General Electric® Druck 10-psi gauged submersible pressure transducers and were recorded at the beginning of each hour by data loggers. The periodic and continuous measurements were compared; differences were attributed to electronic drift in the output signal of the transducers that was not a function of a change of the groundwater level (Rosenberry, 1990). The periodic and continuous groundwater-level data from the transducers were processed and stored in the USGS National Water Information System (NWIS) database. Computer programs in the NWIS database were used to convert the transducer outputs in mV to values of depth to groundwater in fbls by using an equation derived from the transducer calibration data. A datum correction was applied to the converted data to account for transducer drift. Gaps in the recorded data were caused by transducer failure.

Periodic aquifer-system compaction measurements were made at the EXT1 and EXT2 extensometers by using analog dial gages, and continuous aquifer-system compaction measurements were made hourly by using linear potentiometers and recording data loggers. The periodic and continuous measurements were compared, and the differences were attributed to electronic drift, which was negligible, or to downhole friction, which occurred in EXT1. The continuous aquifer-system compaction data from the linear potentiometers were processed and stored in the NWIS database. Computer programs in the NWIS database were used to convert the linear potentiometer output (in mV) to displacement (in ft) by using an equation derived from the linear potentiometer specifications. Datum corrections were applied to the converted data to account for linear potentiometer adjustments. Gaps in the recorded data were caused by disturbances to the extensometers during field-site maintainance visits.

Slug Tests

Slug tests were performed within the six EBAY piezometers and nine nearby wells between July 30 and August 3, 2007, to estimate hydraulic conductivity of the hydrogeologic units next to the screened zones (*fig. 1*). The slug tests were done in monitoring wells varying in diameter, depth, screen length, and construction method. For the nine wells not constructed by the USGS, construction information was limited. Key construction information about each well is summarized in *table 2*, and well construction diagrams for the EBAY piezometers are presented in *figure 2A*.

Four different sizes of slugs—two for each well diameter—were used to create the displacement of water in the well. The slugs were constructed of PVC pipe capped at both ends and filled with sand for weight. The slug was connected to parachute cord at one end, which allowed for quick and easy insertion and removal of the slug. The large slug used in the 2-inch-diameter wells measured 1.315 inches in diameter by 63.2-inches long (0.0497 cubic feet, or ft^3) and produced 2.42 ft of displacement. The small slug used in the 2-inch-diameter wells measured 1.05 inches in diameter by 61.25-inches long (0.0307 ft^3) and produced 1.50 ft of displacement. The large slug used in the 4-inch-diameter wells measured 2.375 inches in diameter by 66.75-inches long (0.1711 ft^3) and produced 1.94 ft of displacement. The small slug used in the 4-inch-diameter wells measured 1.66 inches in diameter by 68.5-inches long (0.0858 ft^3) and produced 0.98 ft of displacement.

Data for these tests were collected and recorded by using In-Situ® Inc., LevelTroll-500 10-psi- gauged pressure transducers. The transducers were calibrated at the factory prior to being used, and the calibrations were verified before the slug tests were performed.

Table 2. Well-identification and construction information for slug test and water-quality data collection sites, Alameda County, California.

[**Abbreviations**: ft, feet; fbls, feet below land surface; in., inches; USGS, U.S. Geological Survey; —, not available]

Well identification number	USGS site number	Altitude of land surface (ft)[1]	Depth (fbls)	Top of screen (fbls)	Bottom of screen (fbls)	Casing diameter (in.)
EBAY1	374004122092101	7.0	1,010	990	1,010	2.32
EBAY2	374004122092102	7.0	860	830	860	1.94
[2]EBAY3	374004122092103	7.0	640	530	550	1.94
[2]EBAY3	374004122092103	7.0	640	570	590	1.94
[2]EBAY3	374004122092103	7.0	640	620	640	1.94
EBAY4	374004122092104	7.0	318	298	318	1.94
EBAY5	374004122092105	7.0	138	128	138	1.94
EBAY6	374004122092106	7.0	45	35	45	1.94
EBKA1	374034122090701	15.0	325	315	325	1.94
EBKA2	374034122090702	15.0	210	200	210	1.94
EBMY1	374111122064601	52.0	335	325	335	1.94
EBMY2	374111122064602	52.0	210	200	210	1.94
EBMY3	374111122064603	52.0	120	110	120	1.94
EBSP1	374119122094301	5.0	610	590	610	1.94
EBSP2	374119122094302	5.0	360	340	360	1.94
EBSP3	374119122094303	5.0	120	100	120	1.94
MW-FH	374107122075301	34.7	540	500	530	1.94
[2]MW-1	374005122092502	5.9	650	520	550	1.94
[2]MW-1	374005122092502	5.9	650	570	590	1.94
[2]MW-1	374005122092502	5.9	650	620	640	1.94
MW-2D	374005122092202	6.1	200	160	190	1.94
[2]OW3	374005122092601	6.7	660	525	565	1.94
[2]OW3	374005122092601	6.7	660	575	595	1.94
[2]OW3	374005122092601	6.7	660	625	655	1.94
MW-3	374005122092501	7.5	660	520	650	1.94
MW-4	374011122093001	8.6	650	520	650	1.94
MW-5D	374034122090601	13.3	640	500	630	4.03
MW-6	374007122090401	9.2	655	480	650	4.03
MW-7	373956122084401	6.8	640	510	630	4.03

[1]The altitude of land surface is described in feet above the National Geodetic Vertical Datum (NGVD) 1929.

[2]This piezometer was constructed with 3 separate screened intervals.

Water levels for each well were measured before testing began by using a calibrated electric tape. The transducers were set at depths ranging from 20.0 to 21.4 ft below the water level, and the slug was lowered to approximately 5 ft above the water. Sufficient time, 30 minutes for most wells, was allowed to determine if water levels were static. The data logger was set to record the depth to water every second, and the slug was rapidly lowered into the water. Sufficient time was allowed for recovery of the water level. The slug was then quickly removed. Sufficient time was again allowed for recovery to static levels. This process was repeated four to nine times per well, depending on the recovery conditions. A second slug with a smaller volume was used to complete an additional five tests at each well.

Computations were performed by using a Microsoft® Excel spreadsheet created by Keith Halford (Halford and Kuniansky, 2002) of the USGS by using methods developed by James Butler of the Kansas Geological Survey (Butler and Garnett, 2000). The following assumptions were made for the computation of the data: the volume of water is injected into, or is discharged from, the well instantaneously, and the well is of finite diameter and fully penetrates the aquifer. The aquifers were assumed to be confined, homogeneous, isotropic, and of uniform thickness. It was assumed also that flow within the aquifer is horizontal and radially symmetric and that the response is evenly distributed over the entire screened interval. Accordingly, for these calculations, the aquifer thickness was assumed to be equal to the length of the screened interval of the monitoring well. For wells containing multiple screened intervals, the bottom of the screen was calculated by adding the effective screen length to the top of the screen; for example, a screened interval of 100–120 ft and 160–180 ft had an effective screened interval of 40 ft and was analyzed as a screen interval of 100–140 ft.

Water Quality

Sample Collection and Analysis

Water-quality samples were collected from all 14 piezometers constructed as part of this study. Piezometers are identified by borehole designation, numbered deepest to shallowest, and were sampled during two events. The six piezometers in the EBAY borehole were sampled in June of 2007 by USGS GAMA program personnel. The eight piezometers in the boreholes EBKA, EBMY, and EBSP were sampled in December 2008 by USGS National Water Quality Assessment (NAWQA) program personnel. All samples were collected and processed in accordance with protocols outlined by the USGS NAWQA program (Koterba and others, 1995) and the USGS National Field Manual (U.S. Geological Survey, variously dated).

Piezometers were pumped to purge at least three casing volumes of water from the piezometer (Wilde and others, 2006), except for EBAY1, which had a hydraulic conductivity too low to permit recovery in the time allotted for the sampling event. All piezometers, except the EBKA piezometers, were sampled by using a Grundfos® Redi-Flo2 submersible pump. Because piezometer instrumentation caused diameter restrictions, the EBKA piezometers were sampled by using a Waterra® inertial pumping system. Temperature, dissolved oxygen, pH, and specific conductance were measured by pumping groundwater through a flow-through chamber fitted with a YSI® 556 MPS (multiprobe system) multiparameter meter, which was calibrated daily. Turbidity was measured with a Hach M 2100P turbidimeter. Field measurements were recorded at 5-minute intervals for at least 30 minutes to determine parameter stability. Samples were collected after these measurements remained stable for 20 minutes.

Samples collected for nutrients, major and minor ions, and trace elements were analyzed by the USGS National Water Quality Laboratory (NWQL) in Denver, Colorado. The USGS Stable Isotope Laboratory in Reston, Virginia, analyzed samples for isotopic ratios of hydrogen and oxygen in water. Samples for activities of carbon-14 collected prior to November 2008 (EBAY 1–6) were analyzed by the University of Waterloo, Environmental Isotope Lab (CAN-UWIL) and the University of Arizona Accelerator Mass Spectrometry Lab (AZ-UAMSL). Samples for activities of carbon-14 collected after November 2008 were analyzed by the National Ocean Sciences AMS Facility (NOSAMS). The USGS Stable Isotope and Tritium Laboratory in Menlo Park, California, analyzed samples for tritium.

Quality Assurance

All quality-assurance methods followed protocols outlined by the USGS NAWQA program (Koterba and others, 1995), which are described in the USGS National Field Manual (U.S. Geological Survey, variously dated). A field blank was collected during the December 2008 sampling event to evaluate the potential of contamination in the field. Quality-control samples collected by the GAMA program for the June 2007 sampling are explained in detail by Ray and others (2009).

Core Collection, Processing, and Subsampling

Results of the cuttings descriptions and geophysical logs from EXT1 (deep extensometer borehole) were used to select intervals to be cored in the other Bayside site boreholes. Core samples, 2.3-in. diameter by 5-ft long, were taken from two boreholes at Bayside. In total, 284 ft of core was collected during August 2006—274 ft from EBAY (piezometer borehole) and 10 ft from EXT2 (shallow extensometer borehole)—to augment zones of poor core recovery in EBAY (*table 3*). Additional core was collected in 2007 at the Bayside site from borehole ALC085 by the USGS Earthquake Hazards Team to augment zones of poor core recovery (20–35 ft below land surface) from the EBAY borehole (Bennett and others, 2009).

Table 3. Core recovery for each 5-foot interval from the East Bay Bayside Monitoring Site (EBAY) and East Bay Extensometer-2 Monitoring Site (EXT2) boreholes.

[The "shoe" sample is taken from the detachable end of the inner core barrel. As the core is collected, the shoe acts as a drive point by funneling the soil into the core liner. This sample stuck inside the shoe is saved as core material but labeled as "shoe" because it is not in a liner and may be highly disturbed by the process of removing the material from the shoe.]

Core number	Core interval (feet)		Recovery (feet)		Total recovery (feet)	Recovery (percent)
	Top	Bottom	Core	Shoe		
EBAY_1	0	5	3.12	0.26	3.38	69
EBAY_2	5	10	4.33	0.30	4.63	94
EBAY_3	10	15	3.56	0.25	3.81	77
EBAY_4	15	20	3.64	0.28	3.92	80
EBAY_5	20	25	0.79	0.33	1.12	23
EBAY_6	25	30	1.03	0.26	1.30	26
EBAY_7	30	35	0.52	0.52	1.05	21
EBAY_8	35	40	2.81	0.30	3.10	63
EBAY_9	40	45	2.38	0.28	2.66	54
EBAY_10	45	50	3.58	0.36	3.94	80
EBAY_11	50	55	4.40	0.26	4.66	95
EBAY_12	55	60	4.13	0.30	4.43	90
EBAY_13	60	65	3.30	0.30	3.59	73
EBAY_14	65	70	3.46	0.28	3.74	76
EBAY_15	70	75	4.92	0.25	5.17	105
EBAY_16	75	80	4.92	0.26	5.18	105
EBAY_17	80	85	3.45	0.30	3.74	76
EBAY_18	85	90	4.35	0.31	4.66	95
EBAY_19	90	95	4.92	0.33	5.25	107
EBAY_20	95	100	4.92	0.26	5.18	105
EBAY_21	100	105	4.92	0.33	5.25	107
EBAY_22	105	110	4.92	0.31	5.23	106
EBAY_23	110	115	4.92	0.30	5.22	106
EBAY_24	115	120	2.44	0.26	2.71	55
EBAY_25	120	125	3.90	0.38	4.28	87
EBAY_26	125	130	4.66	0.30	4.95	101
EBAY_27	130	135	4.92	0.30	5.22	106
EBAY_28	135	140	3.89	0.30	4.18	85
EBAY_29	140	145	4.92	0.26	5.18	105
EBAY_30	145	150	4.43	0.23	4.66	95
EBAY_31	150	155	4.92	0.34	5.27	107
EBAY_32	155	160	2.99	0.28	3.26	66
EBAY_33	160	165	4.92	0.28	5.20	106
EBAY_34	165	170	4.89	0.30	5.18	105
EBAY_35	170	175	3.61	0.31	3.92	80
EBAY_36	175	180	4.92	0.33	5.25	107
EBAY_37	310	315	4.56	0.34	4.91	100
EBAY_38	315	320	2.44	0.25	2.69	55
EBAY_39	320	325	4.45	0.28	4.72	96
EBAY_40	325	330	2.13	0.23	2.36	48
EBAY_41	410	415	4.51	0.34	4.86	99
EBAY_42	415	420	2.21	0.31	2.53	51
EBAY_43	490	495	0.00	0.00	0.00	0
EBAY_44	495	500	4.92	0.30	5.22	106
EBAY_45	540	545	1.28	0.33	1.61	33
EBAY_46	545	550	2.66	0.26	2.92	59
EBAY_47	550	555	2.46	0.26	2.72	55
EBAY_48	555	560	4.92	0.28	5.20	106
EBAY_49	585	590	0.00	0.00	0.00	0
EBAY_50	590	595	4.89	0.36	5.25	107
EBAY_51	595	600	4.92	0.30	5.22	106
EBAY_52	640	645	0.00	0.00	0.00	0
EBAY_53	645	647.5	0.00	0.00	0.00	0
EBAY_54	647.5	650	1.89	0.25	2.13	87
EBAY_55	650	655	0.00	0.00	0.00	0
EBAY_56	655	660	3.25	0.61	3.86	78
EBAY_57	755	760	0.26	0.30	0.56	11
EBAY_58	760	765	2.92	0.20	3.12	63
EBAY_59	765	770	2.74	0.25	2.99	61
EBAY_60	770	775	4.86	0.26	5.12	104
EBAY_61	775	780	4.92	0.30	5.22	106
EBAY_62	820	825	1.51	0.31	1.82	37
EBAY_63	825	830	2.69	0.31	3.00	61
EBAY_64	830	835	3.77	0.31	4.08	83
EBAY_65	835	840	4.22	0.00	4.22	86
EBAY_66	910	915	4.28	0.26	4.54	92
EBAY_67	915	920	4.59	0.38	4.97	101
EBAY_68	985	990	3.35	0.30	3.64	74
EBAY_69	990	995	2.07	0.43	2.49	51
EBAY_70	995	1,000	3.12	0.36	3.48	71
EBAY_71	1,010	1,015	4.18	0.31	4.49	91
EBAY_72	1,015	1,020	4.43	0.79	5.22	106
EBAY_73	1,030	1,035	4.53	0.49	5.02	102
EBAY_74	1,035	1,040	4.04	0.28	4.31	88

Attempted feet of core			Total core (feet)	Total shoe (feet)	Total recovery (feet)	Final (percent)
359.27			252.67	21.28	273.95	76
EXT2_1	35	40	4.41	0.20	4.61	94
EXT2_2	40	45	4.92	0.25	5.17	105

Attempted feet of core			Total core (feet)	Total shoe (feet)	Total recovery (feet)	Final (percent)
9.84			9.33	0.44	9.78	99

Sediment cores were processed at the USGS labs at Menlo Park, California, between August 8 and September 9, 2006. Between August 8 and 18, 2006, the USGS Heat-Flow-Studies Group measured thermal conductivity of core material at three places on each 5-ft-core section. The cores were scanned by using the GEOTEK™ Multi-Sensor Core Logger (MSCL) system to non-destructively test the whole core for compressional wave velocity, gamma bulk density, magnetic susceptibility, and electrical resistivity, which provided an indication of sediment lithology without disturbing the cores. The compressional wave-velocity sensor measures the compressional wave velocity as a function of distance over time by transmitting an ultrasonic compressional pulse through the core between a piezoelectric transmitter-receiver transducer pair. The gamma bulk-density sensor passes gamma rays through the core sample, which are detected on the other side. The density is determined by measuring the number of gamma photons that pass through the core unattenuated. The magnetic-susceptibility sensor produces an alternating magnetic field, which is influenced by the magnetic susceptibility of the material being analyzed. The resulting changes detected in the oscillator frequency are converted into magnetic-susceptibility values. The electrical-resistivity sensor operates by inducing a high-frequency magnetic field in the core sample from a transmitter coil. A receiver coil measures the resulting electrical currents in the core sample, which are inversely proportional to the resistivity. A more detailed description of the MSCL system sensors can be found on the GEOTEK website (*http://www.geotek.co.uk/products/sensors,* accessed September 12, 2012). The MSCL logs were used to select core intervals for physical testing (consolidation and permeability) and absolute-age determination. These cores were split; half of the core was digitally photographed, scanned with the MSCL system, and archived in a 'D' tube, which was capped and taped, at the USGS refrigerated storage facility in Menlo Park, California. USGS staff described sedimentological features in the other half of the core and collected subsamples for the determination of chemical, physical, and mechanical properties, mineralogy, age-dating, and depositional environment. A sedimentological database was created to document the physical description of each of the cores, subsample depths, and MSCL data. A summary of analyses performed on the cores is presented in *table 4*.

Physical and Mechanical Determinations

Physical and mechanical charactersitics of the sediment cores were determined in the laboratory to better understand how the aquifer system reacts to applied stress, such as ASR injection. These determinations included estimations of bulk density, porosity, volumetric water content, saturation values, vertical hydraulic conductivity, and consolidation potential.

Bulk-density, porosity, volumetric water-content, and saturation values were calculated by heating the samples in an oven set to a 105ºC. As soon as possible after a core was split, a small, round plug of core was removed and weighed. If a sedimentological change was noted within a length of core, then more than one plug of core was removed to represent each section. These sediment plugs were dried for at least 18 hours in a drying oven at 102–107°C. After drying, the plugs were weighed again, and moisture content by mass was calculated as the amount of mass loss due to evaporation. A relative-humidity oven was used to estimate residual water content, effective porosity, and effective saturation of these sediment cores. Each method was performed in accordance with Yucca Mountain Project Branch (YMPB-USGS-HP-229, R3-M3) protocols.

Vertical hydraulic-conductivity values were determined by USGS scientists in the California Water Science Center in Sacramento for 20 selected cores by using measurements from a Tri-Flex 2 Permeability Test System (ELE International, Loveland, Colo.) in accordance with ASTM Standard D5084 (American Society for Testing and Materials, 2003). Saturated vertical hydraulic conductivity values were corrected to 20°C. Specific water chemistry for use in the vertical hydraulic-conductivity measurements was synthesized on the basis of the results of the pore-water chemistry analyses to mimic chemical conditions in the aquifer system. Changes in water chemistry could cause expansion and contraction of clays, which would affect the hydraulic conductivity (Lambe and Whitman, 1969; Hille, 1980). The 20 pore-water chemical determinations were compared and categorized into five water types. Each core sample was assigned a water type according to depth similarity between the pore-water determination and core sample. Synthetic water flowed through core samples under gradients ranging from 21 to 400 kilopascal (kPa). Most samples were tested twice by using two different gradients, but three samples (EBAY_2, EXT2_2, and EBAY_60) were analyzed twice with the same test gradient.

A computerized and fully automated, uniaxial load frame (Geocomp Corporation, Boxborough, Mass.) was used to perform incremental-consolidation (non-back-pressured) tests by using the traditional incremental-loading method of Casagrande (1936). Samples were provided with double-drainage within a water-filled cell. The breaks in slope in the consolidation curves generated were interpreted, in part, by using the methods of Schmertmann (1954), which primarily attempt to overcome the effects of sample disturbance. Results from the consolidation tests were used to calculate elastic and inelastic specific storages. These calculations were derived by Sneed (2001).

Table 4. Summary of analyses conducted on sediment cores from the East Bay Bayside Monitoring Site (EBAY) and East Bay Extensometer-2 Monitoring Site (EXT2) boreholes.

[**Abbreviations:** ICP-MS, inductively coupled plasma-mass spectroscopy; INAA, instrumental neutron activation by abbreviated count; IRSL, infrared stimulated luminescence; OSL, optically stimulated luminescence; SEM-EDS, scanning electron microscopy-energy dispersive spectroscopy; XRD, X-ray diffraction; —, no analysis]

Core number	Analysis type (table number)										
	Moisture content (11)	Vertical hydraulic conductivity (12)	Physical properties (13)	Consolidation (14)	Quartz blue-light OSL and feldspar IRSL ages (15)	Depositional environment (16)	XRD mineralogy (17)	SEM-EDS mineralogy (18)	ICP-MS solids (21)	INAA solids (22)	Pore-water water quality (24–27)
EXT2_1	—	—	—	—	x	—	—	—	—	x	—
EXT2_2	—	x	x	—	—	—	—	—	—	—	—
EBAY_1	x	—	—	—	—	—	—	—	—	—	—
EBAY_2	x	x	x	x	—	x	—	—	—	—	x
EBAY_3	x	—	—	—	—	x	—	—	—	—	—
EBAY_4	x	—	—	—	—	x	—	—	—	—	—
EBAY_6	x	—	—	—	—	—	—	—	—	—	—
EBAY_8	—	—	—	—	x	—	—	—	—	x	—
EBAY_9	—	—	—	—	x	—	—	—	—	x	—
EBAY_10	—	—	—	—	x	x	x	x	x	x	—
EBAY_11	x	—	—	—	—	—	—	—	—	—	—
EBAY_12	x	x	x	x	—	x	—	—	—	—	x
EBAY_13	x	—	—	—	—	—	—	—	—	—	—
EBAY_14	x	—	—	—	—	—	—	—	—	—	x
EBAY_15	x	x	x	x	—	x	—	—	—	—	—
EBAY_16	x	—	—	—	—	x	—	—	—	—	—
EBAY_17	x	—	—	—	x	x	x	x	x	x	—
EBAY_18	—	x	x	x	—	x	—	—	—	—	—
EBAY_19	x	—	—	—	—	x	—	—	—	—	x
EBAY_20	x	x	x	x	—	—	—	—	—	—	—
EBAY_21	x	—	—	—	—	—	—	—	—	—	—
EBAY_22	x	x	x	x	—	x	—	—	—	—	—
EBAY_23	x	—	—	—	—	—	—	—	—	—	—
EBAY_24	x	—	—	—	—	—	—	—	—	—	—
EBAY_25	x	—	—	—	x	—	x	x	x	x	—
EBAY_26	x	—	—	—	—	x	—	—	—	—	—
EBAY_27	—	—	—	—	—	x	—	—	—	—	—
EBAY_28	x	x	x	x	—	x	—	—	—	—	—
EBAY_29	x	x	x	x	—	x	x	x	x	—	
EBAY_30	x	—	—	—	—	—	—	—	—	—	x
EBAY_31	x	—	—	—	—	—	—	—	—	—	—
EBAY_32	x	—	—	—	—	—	—	—	—	—	—
EBAY_33	x	—	—	—	x	—	x	x	x	x	—
EBAY_34	x	—	—	—	—	—	—	—	—	—	—
EBAY_35	x	—	—	—	x	—	x	x	x	x	—
EBAY_36	x	x	x	x	—	x	—	—	—	—	—
EBAY_37	x	—	—	—	x	—	x	x	x	x	—
EBAY_39	x	x	x	x	—	—	—	—	—	—	x
EBAY_40	x	—	—	—	—	x	—	—	—	—	—
EBAY_41	x	x	x	x	—	x	x	x	x	—	x
EBAY_44	x	x	x	x	—	x	x	x	x	—	x
EBAY_46	—	—	—		—	—	x	x	x	—	—
EBAY_48	x	x	x	x	—	x	x	x	x	—	x
EBAY_50	x	x	x	x	—	x	x	x	x	—	—
EBAY_51	x	—	—	—	—	—	—	—	—	—	x
EBAY_54	x	—	—	—	—	x	—	—	—	—	x
EBAY_56	x	—	—	—	—	x	—	—	—	—	x
EBAY_58	x	—	—	—	—	x	—	—	—	—	x
EBAY_59	x	—	—	—	—	x	x	x	x	—	—
EBAY_60	x	x	x	—	—	—	x	x	x	—	x
EBAY_61	x	—	—	—	—	—	—	—	—	—	—
EBAY_62	—	—	—	—	—	—	—	—	—	—	x
EBAY_63	x	x	x	—	—	—	—	—	—	—	—
EBAY_64	x	—	—	—	—	x	—	—	—	—	—
EBAY_65	—	—	—	—	—	—	—	x	x	—	—
EBAY_66	x	—	—	—	—	x	—	—	—	—	x
EBAY_67	x	x	x	x	—	—	—	—	—	—	
EBAY_68	x	—	—	—	—	x	—	—	—	—	x
EBAY_70	x	—	—	—	—	—	x	x	x	—	—
EBAY_71	x	—	—	—	—	—	—	—	—	—	x
EBAY_72	x	x	x	x	—	x	—	—	—	—	—
EBAY_73	x	x	x	—	—	—	x	x	x	—	—
EBAY_74	x	—	—	x	—	x	—	—	—	—	x

Age Determinations

Most minerals react to ionizing radiation by essentially gaining energy at the electron level, which accumulates through time if that energy is not released (as light) by some outside stimuli (sunlight or intense heat over 200°C). Thus, sediment grains can record their exposure history to ionizing radiation, which can then be "read" in the laboratory and used much like a clock. This procedure is referred to as luminescence geochronology (Aitken, 1998), the goal of which is to establish the timing of the burial of mineral grains in sedimentary deposits. In terrestrial environments, exposure to sunlight during sediment transport resets the clock, which is why a luminescence age is considered a burial age. In the laboratory, the sediment sample is stimulated to emit light by exposing it to light of specific wavelengths in prescribed manners. The intensity of emitted light measured in the laboratory is proportional to the trapped charge population, which is proportional to the total absorbed radiation dose that the sedimentary deposit experienced, and that relation is proportional to the time elapsed since burial (Murray and others, 1995; Olley and others, 1998; Galbraith and others, 1999; Lepper, 2001; Lepper and McKeever, 2002).

Quartz blue-light optically stimulated luminescence (OSL) and feldspar infrared-stimulated luminescence (IRSL) methods were applied to nine core samples to determine deposition or burial ages (*table 4*). The quartz blue-light OSL method was chosen as the preferred method of age determination, but was not applicable to the two deepest, oldest samples; therefore, these two samples were analyzed by using only the feldspar IRSL method. Three of the seven samples analyzed by using quartz blue-light OSL were also analyzed by using the feldspar IRSL method.

Determination of Depositional Environment

Cores were inspected for the presence of foraminifera and diatom fossils to establish the depositional environment and age. Thirty-one 4-centimeter (cm) long sections from thirty sediment core samples were analyzed for foraminifera (*table 4*). These sediment samples were wet-sieved through nested 63-micrometer (µm), 150-µm, and 1.0-millimeter (mm) screens to segregate the size fractions. Sediment remaining on the screens was transferred to filter paper and air dried. Foraminifera were extracted from the greater than 63-µm fraction. Samples containing abundant benthic foraminifera were split with the aid of a microsplitter into an aliquot containing at least 300 specimens, which were then picked and identified. Specimens from samples containing very rare foraminifera or other biological constituents were removed from the sediment and placed on faunal slides for archival purposes. The foraminiferal slides and residues were filed at the U.S. Geological Survey, Menlo Park, California. One sample was floated with sodium polytungstate to concentrate the foraminifera before picking.

Relative foraminiferal species abundances of benthic taxa for the two samples with more than 300 foraminifera were computed by using a sum of total benthic foraminifera for that sample. The remaining samples were considered to be statistically invalid, and the species therein were listed only as present.

Four samples, 1-cm in length, were processed for diatom analysis by using hydrogen peroxide, hydrochloric acid, and nitric acid to remove carbonate and organic matter, and sodium pyrophosphate to deflocculate the remaining clay (Battarbee, 1986). Approximately 50 microliters (µl) of the resulting suspension was dried on a 22- by 30-mm coverslip and permanently mounted by using Naphrax®. At least 300 frustules were enumerated by following the method of Schrader and Gersonde (1978) and using an Olympus BH-2 microscope at magnifications of 500X or 1,000X. Diatom identification was based on Lowe (1974), Gasse (1986), Krammer and Lange-Bertalot (1986, 1988, 1991a, 1991b), Lange-Bertalot and Krammer (1987, 1989), Cumming and others (1995), Round and Bukhtiyarova (1996), Krammer (1997a, 1997b, 2000, 2002), and Lange-Bertalot (2001).

Mineralogy of Cores

The mineralogical composition of 16 core samples was determined by X-ray diffraction (XRD; *table 4*). The XRD method of analysis involves a focused X-ray beam directed at a pulverized mineral. Components of the beam are transmitted through the sample then absorbed, refracted and scattered, and diffracted. Each mineral lattice produces a distinct pattern when an X-ray beam is transmitted through it. The mineralogy of the cores was determined to establish a chemical baseline for better understanding of the potential chemical reactions that could occur between ASR water and the substrate.

Scanning electron microscopy (SEM) and energy dispersive spectroscopy (EDS) were used to analyze 17 samples to (1) identify any secondary minerals, (2) determine the relative abundance of secondary precipitates from the detrital material, (3) determine the presence or absence of organic carbon, (4) determine and document the presence or absence of ferric oxyhydroxide coatings on mineral grains, (5) determine the occurrence of clay minerals, and (6) characterize the morphology of the sediment (*table 4*).

Three preparations were made for each sample: (1) a bulk sample was placed on an SEM stub to determine the relationship of the secondary mineral precipitate to the detrital grains, (2) a carbon-coated grain mount was made to determine the area fraction of each phase, and (3) a gold-coated grain mount was made to determine the area fraction of organic material.

Bulk samples were placed on a SEM sample stub and coated with carbon for conductivity. Approximately 0.2 grams (g) of ground sample was placed in approximately 1 milliliter (mL) of isopropanol and shaken to disperse the particles. A 20-µl aliquot was taken from the top, middle, and bottom of the mixture, and these were filtered onto a gold coated polycarbonate filter by using a Millipore® setup. The loaded filters were gold coated in preparation for determination of organic content and grain-size analysis.

Samples were analyzed by using a JEOL 5800LV scanning electron microscope operated at 15 kilovolts (kV) and 0.5 to 1.0 nanoamp (nA) beam current. Representative areas of the unground bulk samples were analyzed to determine mineralogy, particle morphology, and possible pore-filling minerals. Backscattered electron imaging was used to search for higher average atomic-number accessory minerals, such as apatite, zircon, and sphene and iron oxide coatings.

Binary backscattered images of the grain mounts were thresholded so that the grains were black and the background filter was white. Automated size analyses were acquired with the Noran System Six Feature Sizing software. Grain-size data were then acquired until over 100 particles were analyzed.

Elemental Composition of Cores

The elemental composition of 17 core samples extracted from between 48 and 1,034 fbls was determined by using inductively coupled plasma-mass spectroscopy (ICP-MS solids; *table 4*). This method uses a high-temperature inductively coupled plasma source to convert the atoms into ions, which are then separated and detected by the mass spectrometer (Wolf, 2005; Garbarino and others, 2006).

Instrumental neutron activation by abbreviated count (INAA) also was used to determine the elemental composition of nine core samples extracted from between 37 and 312 fbls (*table 4*). This is a non-destructive, highly precise, and accurate analytical technique capable of determining up to 48 elements in almost all types of sample matrices. The INAA procedure involves irradiating the samples and appropriate standard reference materials with neutrons in the USGS TRIGA (Training, Research, Isotopes, General Atomics) reactor to produce unstable radioactive nuclides. Many of these radionuclides emit gamma rays with characteristic energies that can be measured by utilizing high-resolution semiconductor detectors (Budahn and Wandless, 1996). The rate at which gamma rays are emitted from an element in the sample is directly proportional to its concentration. Samples as small as 1 milligram (mg) can be quantitatively measured by INAA. Detection limits are in the parts per million to parts per billion range depending on the element and sample matrix (*http://geology.usgs.gov/usgs/capabilities/chema/inst_neutron_anal.shtml#tech*; accessed April 15, 2009).

Pore-Water Chemistry

Twenty pore-water samples were collected from nineteen sections of core from sediment cores take from the EBAY site (*table 4*). Two of the samples were collected from different depths of the EBAY_2 core to assess variation within a single core. The pore water was extracted by using a hydraulic press and stainless steel capsule system, as described by Manheim and others (1994). A section of core was taken from one half of each of the 19 sections of split-core. The pore water was extracted by gradually applying 3,000–8,000 psi of pressure to approximately 50 g of sediment from the core in the capsule system; 2–11 mL of pore water was collected by syringe and filtered through a 0.45-mm polyethersulfone disk filter. Salinity (as percent sodium chloride) and pH were measured, and then the samples were prepared for the analysis of major ions, trace metals, stable-isotope ratios of hydrogen and oxygen in water, dissolved inorganic carbon (DIC), and alkalinity.

The USGS California Water Science Center Water-Quality Laboratory in San Diego analyzed the samples for the following dissolved anions: chloride, nitrite, bromide, nitrate, orthophosphate, and sulfate. Samples were analyzed by using a non-suppressed ion-chromatographic method (Waters Corporation, 1992), which was adapted for small-volume, complex-matrix samples, or both (Michael Land, U.S. Geological Survey, written commun., 2009).

Cation and trace-element concentrations were determined by collision/reaction cell inductively coupled plasma-mass spectrometry (cICP-MS) at the USGS National Water Quality Laboratory (NWQL) in Denver, Colorado (Garbarino and others, 2006).

Samples for DIC were analyzed at the USGS California Water Science Center Water-Quality Laboratory in Sacramento. Samples were diluted, and DIC was measured by using a Shimadzu TOC 5000A total organic carbon analyzer. Alkalinity was calculated from DIC, given pH, partial pressure (or the concentration of carbon dioxide in the atmosphere), and the three equilibrium constants for the carbonate system. This calculation assumes that the samples and, therefore, the aquifer are in equilibrium with atmospheric carbon dioxide (Miranda Fram, U.S. Geological Survey, written commun., 2006).

Samples were analyzed for stable-isotope ratios of hydrogen and oxygen in water by gaseous hydrogen and carbon dioxide-water equilibration and stable-isotope mass spectrometry (Coplen and others, 1991) at the USGS Stable Isotope Laboratory in Reston, Virginia.

In addition, 53 cores were sampled for percent-water content. These samples were cut from the split core, weighed, then placed in a drying oven for 18–130 hours. After drying, samples were weighed again, and the percent-water content calculated. This analysis was done at the time the core was processed at the USGS labs in Menlo Park, California.

Results

Lithologic and Geophysical Logs

The lithologic and geophysical logs from the Bayside boreholes indicated unconsolidated to partly consolidated continental and marine alluvial deposits consisting mostly of silt and clay, with the exception of three coarse-sand and gravel beds totaling nearly 98 ft between 508 and 650 fbls (*figs. 2A*, *B*, and *C*). Shear-wave borehole velocity log values, measured at the EBAY site, ranged from 686 feet per second (ft/s), in the upper 100 ft, to 906 ft/s, in the upper 330 ft, which is about 656 ft/s slower than values reported for several 1,000-ft-deep boreholes in the Santa Clara Valley (Brocher and others, 2007). The USGS Earthquake Hazards Program designates shear-wave velocities in the upper 100 ft from 656 to 1,148 ft/s as class D (stiff soil) on a scale from A (4,921 ft/s) to E (less than 656 ft/s), where shaking is amplified in low-velocity soil and rock types (U.S. Geological Survey, 2012). Boreholes in the Santa Clara Valley penetrated coarser sediments than the clay and silt that were penetrated at the Bayside Site (Brocher and others, 2007). In addition, the shear-wave velocities were slightly slower than predicted by empirical relations between the shear-wave velocity of P waves (V_p) and of S waves (V_s; Castagna and others, 1985). The pronounced seismic-velocity highs at 541, 571, and 633 fbls corresponded to several-feet-thick stringers of coarse sand and gravel. These stringers produce strong, coherent seismic reflectors traceable in nearby seismic-reflection lines at least 1.2 miles (mi) away from the borehole (Catchings and others, 2006). The seismic cone-penetration test (SCPT), performed at the ALCO85 borehole, included determinations of stratification, soil type, shear-wave velocity, density, consistency, penetration resistance, grain size, strength, plasticity, and liquidity, which are described in detail in Bennett and others (2009). According to their study, two stratigraphic intervals, the Holocene bay mud (3.3–11.5 ft) and an interval referred to as the sensitive zone (26.2–28.9 ft), stood out in this 35-ft boring. Similarities between these intervals included relatively high values of water content and liquidity index, as well as low values for shear-wave velocities and friction. Grain size and stratigraphic sequence distinguish these intervals from each other. The Holocene bay mud has an average median grain size of 0.005 mm, with an average of 3-percent sand, and the sensitive zone has an average median grain size of 0.030 mm, with an average of 24-percent sand (Bennet and others, 2009). The Holocene bay mud has a fining-upward stratigraphic sequence, and the sensitive zone has a coarsening-upward stratigraphic sequence (Bennet and others, 2009).

Soil-index properties can be used to determine if a soil is susceptible to liquefaction. Bennett and others (2009) identified two intervals, the sensitive zone at 26-ft deep and the dense sand between 33 and 43-ft deep, as having a low liquefaction potential. A more detailed analysis of liquefaction potential is described in their report.

The lithologic and geophysical logs from the EBMY borehole indicated unconsolidated to partly consolidated continental and marine alluvial deposits consisting mostly of silt and clay (*fig. 2D*). Mudstone was encountered at about 410 fbls.

The lithologic and geophysical logs from the EBKA borehole indicated unconsolidated to partly consolidated continental and marine alluvial deposits consisting mostly of silt and clay, with the exception of two depth intervals of silty sand, at 160–220 fbls and 310–330 fbls, and one depth interval of gravelly sand, at 50–60 fbls (*fig. 2E*).

The lithologic and geophysical logs from the EBSP borehole indicated unconsolidated to partly consolidated continental and marine alluvial deposits consisting of clay, silt, and sand (*fig. 2F*).

Water Levels and Aquifer-System Compaction

At Bayside, periodic and continuous water-level and aquifer-system-compaction measurements were made beginning in April 2008 and July 2008, respectively (*figs. 4A, B*). Continuous barometric pressure and air temperature also were measured beginning in July 2008 at Bayside (*fig. 4C*). Water-level differences in piezometers EBAY2 through EBAY6 showed decreasing hydraulic head with decreasing depth, except for EBAY5, which exhibited the highest hydraulic head (*fig. 4A*).

The water-level data showed that all of the piezometers fluctuate diurnally. The diurnal response of the piezometers is caused, in part, by pressure changes induced by tides in the San Francisco Bay—the shoreline is only about 1,500 ft from the Bayside site (*fig. 1*). EBAY3 had the largest magnitude of response; EBAY6 exhibited the smallest response; the other three piezometers exhibited intermediate responses to tide cycles (*fig. 4A*).

The water-level data showed that some of the water levels in the piezometers fluctuate seasonally. EBAY2 did not exhibit water-level fluctuations at seasonal frequencies, but, instead, showed water level rising at a fairly constant rate for the period of record (*fig. 4A*). EBAY3 and EBAY4 exhibited water-level fluctuations at seasonal frequencies. Water levels were higher in the winter and spring, with the highest levels in March 2009, and water levels were lower in the summer and fall, with the lowest water levels in September 2008. Water levels in EBAY3 ranged from about 7.7 to 13.8 fbls, whereas water levels in EBAY4 ranged from about 6.5 to 10.3 fbls. Similar to EBAY3 and EBAY4, water levels in EBAY5 were higher in the winter and spring and lower in the summer and fall; EBAY5 water levels ranged from about 0.3 to 1.7 fbls. Seasonal water-level highs and lows in EBAY5 were in April and October—2 to 3 weeks after EBAY3 and EBAY4 reached their respective maxima and minima.

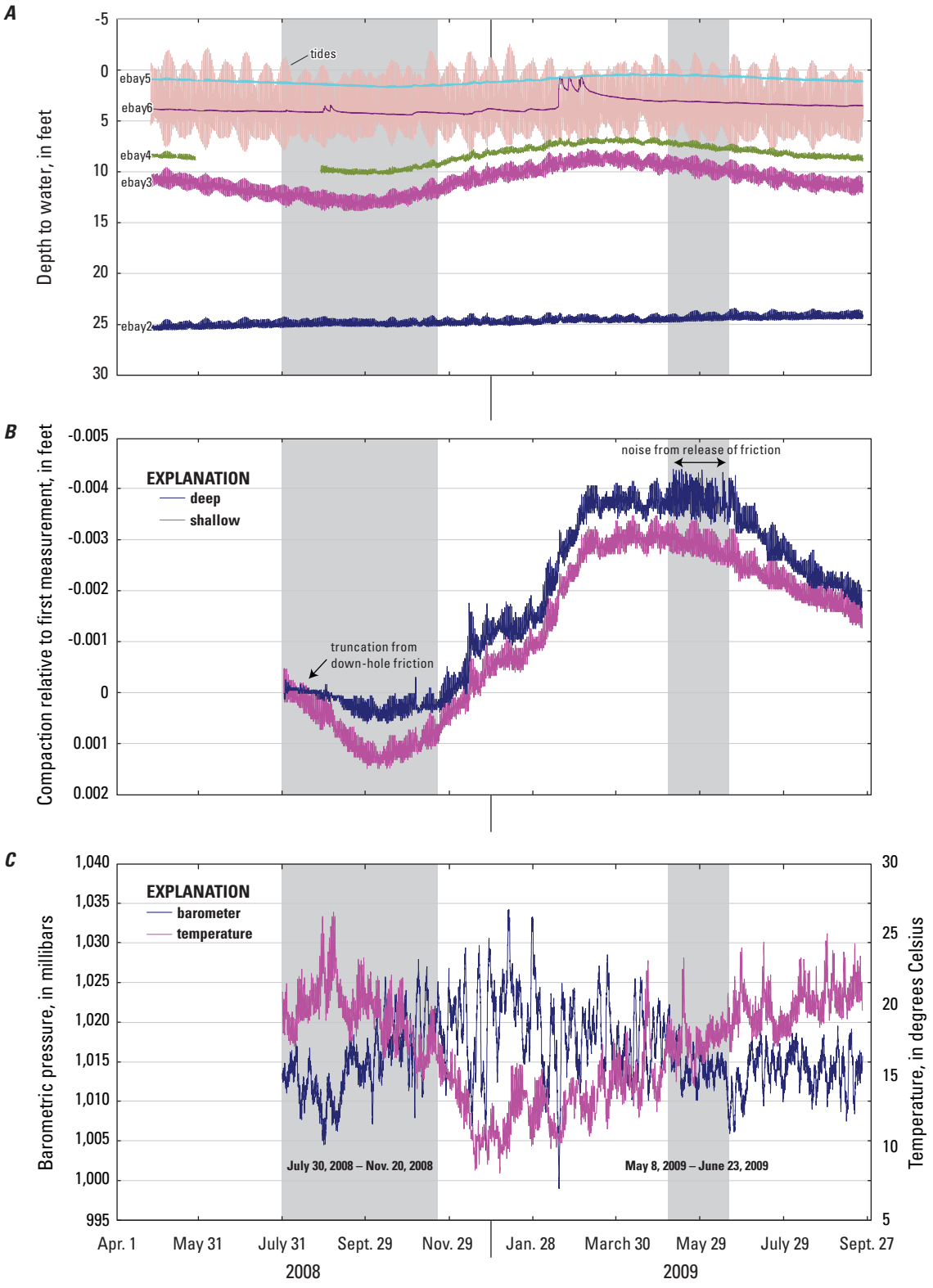

Figure 4. Graphs showing *A,* Periodic and continuous water levels in East Bay Bayside Monitoring site (EBAY) piezometers, including nearby tide cycles. *B,* Aquifer-system compaction measurements in Bayside extensometers, grey areas indicated periods of friction. *C,* Surface barometric pressure and shelter temperature for Bayside extensometers.

EBAY6 did not exhibit a seasonal water-level fluctuation but, instead, showed a general monotonic decline periodically interrupted by quickly rising water levels, which corresponded to rainfall events. EBAY6 responded with a water-level rise to pile-driving during construction in August and September 2008 at the neighboring water treatment plant. In February 2009, large, abrupt water-level rises were caused by a series of rainfall events that caused water to flood the subterranean piezometer housing vault and EBAY6, which had the shortest distance from the bottom of the vault to the top of the 2-in. casing of the six piezometers in the vault. The distance was extended to reduce potential for water to enter the casing in EBAY6 during future rainfall events.

The aquifer-system compaction data for both the deep and shallow extensometers showed seasonal as well as diurnal fluctuations (*fig. 4B*). The downward trends indicate compaction of the aquifer system, and the upward trends indicate vertical expansion of the aquifer system. Positive values indicate net compaction, and negative values indicate net expansion relative to the first measurement. Aquifer-system deformation occurs in response to short-term (daily) tidal cycles, which are superimposed on the seasonal responses to water-level changes in the Deep aquifer and reflected in water levels measured in EBAY3. Compaction is related to water-level drawdown in the Deep aquifer, and expansion is related to water-level recovery.

Other factors that potentially can affect the compaction of the aquifer system and compaction measurements include atmospheric loading caused by changes in barometric pressure at land surface, and diurnal fluctuations of shelter and equipment temperatures. The effects of atmospheric pressure variations on compaction measurements were observed to be fairly insignificant at other extensometer installations (Pavelko, 2000; Sneed and Galloway, 2000) and likely had little influence on compaction measurements at the bayside extensometers. The effects of temperature variations on compaction measurements were observed to be significant at an uninsulated extensometer shelter in Las Vegas, Nevada, but were insignificant at an insulated extensometer shelter in Antelope Valley, California (Pavelko, 2000; Sneed and Galloway, 2000). The extensometer shelter at Bayside is insulated, and diurnal temperature fluctuations were fairly small compared to the desert climates of Las Vegas and Antelope Valley, indicating temperature variations likely did not significantly influence compaction measurements.

At times, the deep extensometer data were degraded by downhole friction. The friction likely is caused by contact of the 2-in.-extensometer pipe with the 6-in.-casing. This contact could be a result of a non-plumb 2-in.-pipe, 6-in.-pipe, the borehole, some, or all of these things. When downhole friction occurred, the deep extensometer was adjusted until the friction was eliminated. The extensometer record indicated degradation by friction from July 30, 2008, to November 20, 2008. During this period, the deep extensometer record was truncated, indicating that the friction was great enough to restrict the extensometer pipe from moving through the full range. Another instance of downhole friction occurred between May 8, 2009, and June 23, 2009. During this period, the deep extensometer record was noisy, indicating that the friction restricted movement of the extensometer pipe for short periods before the stress threshold was reached, releasing the pipe and causing the large swing in values shown in the record (*fig. 4B*).

During periods when data from the deep extensometer were not degraded by downhole friction (for example, November 20, 2008–May 7, 2009), the data from the shallow and deep extensometers showed similar timing and magnitude of deformation. This similarity between data indicates that, for the range of stress occurring since the extensometers were instrumented, nearly all of the deformation at the Bayside site took place from 30 to 696 fbls, and that there was only a small amount of deformation from 696 to 1,040 fbls.

Slug Tests

Slug tests were performed to estimate hydraulic conductivity of the hydrogeologic units next to the screened zones. Water levels were measured in each piezometer before and after the slug tests. The number of tests analyzed, dampening coefficient (which accounts for the oscillation in the water level), estimated hydraulic conductivity, and the root-mean-square error, in addition to water levels for each piezometer, are presented in *table 5*. The hydraulic conductivity of the sediments surrounding piezometer EBAY3 within the Deep aquifer zone was estimated to be 32 feet per day (ft/d). Hydraulic conductivities of the sediments surrounding the remaining piezometers ranged from 0.34 to 120 ft/d. The slug-test time-series data sets and the computations of estimated hydraulic conductivities are on file at the USGS California Water Science Center, Sacramento, California.

Groundwater Quality

Results from the analyses of groundwater samples collected from the four piezometer sites are presented by constituent group in *tables 6 through 10*. Groundwater-quality results from the EBAY piezometers, including some constituents not reported here, have previously been published by Ray and others (2009). Some of these results are presented again here for convenience and comparison to pore-water quality from the same location.

Field and laboratory measurements of water-quality indicators in groundwater, such as turbidity, dissolved oxygen, water temperature, pH, specific conductance, and alkalinity, are presented in *table 6*. Turbidity is caused by suspended and dissolved matter, such as clay or silt, and can make water appear cloudy or muddy (Anderson, 2005). Natural turbidity concentrations in groundwater are typically less than 5 nephelometric turbidity ratio units (NTRU), although values

Table 5. Results of slug tests from monitoring wells, Alameda County, California.

[**Abbreviations**: fbls, feet below land surface; ft, feet; ft/day, feet per day; mm/dd/yyyy, month/day/year; 1/sec, per second]

Well identification number	Date (mm/dd/yyyy)	Depth to water prior to test (fbls)	Depth to water after test (fbls)	Number of tests	Dampening coefficient (1/sec)	Hydraulic conductivity (ft/day)	Squared error (ft)	Top of screen (fbls)	Bottom of screen (fbls)
EBAY2	07/30/2007	25.85	25.56	12	2.68	9.6	0.09	830	860
[1]EBAY3	07/30/2007	14.56	14.97	9	4.14	32	0.18	530	550
[1]EBAY3	07/30/2007	14.56	14.97	9	4.14	32	0.18	570	590
[1]EBAY3	07/30/2007	14.56	14.97	9	4.14	32	0.18	620	640
EBAY4	07/31/2007	10.31	10.27	12	0.54	14	0.06	298	318
EBAY5	07/31/2007	2.07	1.93	16	0.01	4.2	0.06	128	138
EBAY6	07/31/2007	3.86	3.89	15	0.01	5.6	0.08	35	45
MW-FH	08/03/2007	45.73	45.85	12	4.10	51	0.16	500	530
[1]MW-1	08/01/2007	17.53	17.40	14	4.07	31	0.20	520	550
[1]MW-1	08/01/2007	17.53	17.40	14	4.07	31	0.20	570	590
[1]MW-1	08/01/2007	17.53	17.40	14	4.07	31	0.20	620	640
MW-2D	08/01/2007	10.52	10.44	13	0.01	0.34	0.06	160	190
[1]OW3	08/01/2007	19.13	18.85	14	4.10	24	0.28	525	565
[1]OW3	08/01/2007	19.13	18.85	14	4.10	24	0.28	575	595
[1]OW3	08/01/2007	19.13	18.85	14	4.10	24	0.28	625	655
MW-3	08/01/2007	19.69	19.02	15	4.06	8.7	0.26	520	650
MW-4	08/01/2007	17.21	17.70	13	4.02	14	0.21	520	650
MW-5D	08/02/2007	22.72	22.79	18	4.13	120	0.14	500	630
MW-6	08/02/2007	18.44	18.50	18	3.84	27	0.09	480	650
MW-7	08/02/2007	15.45	15.33	18	3.64	19	0.09	510	630

[1] Monitoring wells with multiple screened intervals.

of up to 19 NTRU have been reported in natural systems (Nightingale and Bianchi, 1977; Strausberg, 1983; Puls and Powell, 1992). At Bayside, turbidity ranged from 0.1 to 17 NTRU and had a mean and median of 4.5 and 0.25 NTRU, respectively. EBAY6, at 17 NTRU, had a markedly higher turbidity than the other EBAY piezometers. Turbidity results for EBKA1, EBKA2, and EBSP3 were high, at 206, 28, and 50 NTRU, respectively, and are not indicative of NTRU values representing environmental conditions. Turbidity results for all other piezometers were less than 5 NTRU (*table 6*).

Specific conductance and pH were measured in the field and in the laboratory for most groundwater samples. Laboratory values for pH and specific conductance can differ from field values because of exposure to the atmosphere. Field pH values were not collected from piezometers at the Stenzel Park site because of equipment failure. The pH values measured in the field at the other three locations ranged from 6.5 to 8.2 pH units (*table 6*).

Dissolved oxygen and specific conductance are used as indicators of natural processes that control water chemistry. All piezometers had dissolved oxygen readings of less than 1 milligram per liter (mg/L), with the exception of the deep piezometer EBKA1, where it was 2.3 mg/L. Dissolved oxygen was not detected in two piezometers at the Bayside site (EBAY2 and EBAY3). Specific conductance measured in the field ranged from 517 to 98,900 microsiemens per centimeter (µS/cm). Piezometers at the Bayside site had both the lowest (EBAY3) and the highest (EBAY6) values. Piezometer EBAY6, the shallowest of the pizeometers, had a specific conductance of 98,900 µS/cm, which was much greater than any of the other piezometers at all of the sites (*table 6*) and is consistent with the conductance log shown in *figure 2A*.

Alkalinity, which measures the ability of a sample to neutralize strong acid, was measured in the field for the EBAY piezometers only, but samples from all piezometers were sent to the NWQL for alkalinity analysis. Field alkalinity, averaged from two replicate measurements, from the five EBAY piezometers ranged from 148 to 389 mg/L. These results were consistently lower, yet comparable to lab results of alkalinity analysis from the same piezometers, which ranged from 156 to 402 mg/L. The entire suite of results from lab analyses of alkalinity was within the previously reported range. The lowest observed alkalinity values were from EBAY3, and the highest were from EBAY6. Results from field and laboratory alkalinity analyses are presented in *table 6*.

Table 6. Water-quality indicators in groundwater samples collected in June 2007 and in December 2008.

[The five digit number in parentheses below the constituent name is the U.S. Geological Survey (USGS) parameter code used to uniquely identify a specific constituent or property. **Abbreviations**: A, average value of two replicate measurements; $CaCO_3$, calcium carbonate; E, estimated value; fbls, feet below land surface; hh:mm, hour:minute; mg/L, milligrams per liter; mm/dd/yyyy, month/day/year; NTRU, nephelometric turbidity ratio units; µS/cm, microsiemens per centimeter; °C, degrees Celsius; <, less than; —, sample not collected]

Well identification number	Date/Time (mm/dd/yyyy hh:mm)	Depth to water (fbls)	Turbidity, field (NTRU) (63676)	Dissolved oxygen, field (mg/L) (00300)	Water temperature, field (°C) (00010)	pH, field (standard units) (00400)	pH, lab[1] (standard units) (00403)	Specific conductance, field (µS/cm at 25°C) (00095)	Specific conductance, lab[1] (µS/cm at 25°C) (90095)	Alkalinity, field (mg/L as $CaCO_3$) (29802)	Alkalinity, lab[1] (mg/L as $CaCO_3$) (29801)
EBAY2	06/19/2007 11:40	—	0.2	<0.2	20.0	8.2	8.2	985	1,000	A249	261
EBAY3	06/18/2007 15:00	—	0.1	<0.2	20.5	7.6	7.8	517	518	A148	156
EBAY4	06/18/2007 11:00	—	0.1	0.2	19.5	7.7	7.9	789	796	A249	260
EBAY5	06/20/2007 10:00	—	0.3	0.2	18.5	7.8	8.0	771	803	A284	289
EBAY6	06/20/2007 14:00	—	17	0.5	19.0	6.5	6.7	98,900	E101,000	A389	402
EBKA1	12/15/2008 14:50	8.25	206	2.3	19.0	7.9	8.0	769	773	—	234
EBKA2	12/15/2008 17:10	2.36	[2]28	0.6	17.5	7.5	7.7	770	777	—	282
EBMY1	12/17/2008 10:00	44.36	1.0	0.3	20.5	7.7	7.8	779	785	—	269
EBMY2	12/17/2008 11:30	34.18	0.1	0.2	20.0	7.5	7.6	721	731	—	272
EBMY3	12/17/2008 13:00	23.76	[2]0.2	0.3	20.0	7.2	7.3	1,001	1,010	—	369
EBSP1	12/16/2008 10:20	15.96	0.5	0.3	20.0	—	7.6	929	938	—	241
EBSP2	12/16/2008 13:00	7.87	0.4	0.3	18.5	—	7.8	753	755	—	269
EBSP3	12/16/2008 14:30	4.23	50	0.3	18.0	—	8.0	643	673	—	243

[1]USGS National Water Quality Laboratory, Denver, Colorado.

[2]Represents a median value.

Nutrient samples were collected only from the EBAY piezometers 2–6. Results are presented in *table 7* for reference and comparison to pore-water results later in the report. For a more detailed discussion of these results see Ray and others (2009). Ammonia (as nitrogen) was detected in four of the five groundwater samples—EBAY3 was the exception—and concentrations ranged from 0.167 to 2.46 mg/L. Nitrate plus nitrite (as nitrogen) was detected only in piezometer EBAY3. Nitrite (as nitrogen) was not detected in the samples. Orthophospate (as phosphorus) was detected in all groundwater samples, with concentrations ranging from 0.146 to 1.27 mg/L. Total nitrogen (nitrate, nitrite, ammonia, and organic nitrogen), as nitrogen, was detected in all piezometers, with concentrations ranging from 0.19 to 2.17 mg/L. EBAY6 showed noticeably higher concentrations for detected constituents than any of the deeper piezometers (*table 7*).

Samples from 13 piezometers were analyzed for 10 different ions and total dissolved solids (TDS; *table 8*). Groundwater samples from EBAY6, the shallowest of the 14 piezometers, showed the highest concentrations of all of the ion constituents (*table 8*), except fluoride, iodide, and silica. Groundwater samples from EBAY3 exhibited the lowest concentrations of calcium, magnesium, potassium, bromide, chloride, sulfate, and total dissolved solids.

In samples collected from 13 piezometers, 24 trace elements were analyzed (*table 9*). Ten of the elements were detected in all piezometers: arsenic, barium, boron, lithium, manganese, molybdenum, nickel, strontium, uranium, and vanadium. Four of the elements—antimony, cadmium, cobalt and tungsten—had a detection frequency of 92 percent, whereas chromium and iron had slightly lower detection frequencies, at 85 and 69 percent, respectively. Aluminum, copper, selenium, and zinc had detection frequencies of less than 50 percent, whereas beryllium, lead, silver, and thallium were not detected in any of the piezometer samples. Similar to results of constituent concentrations, samples from EBAY6 showed the highest concentrations for most of the elements. The samples from EBAY6 also had nine elements that were not detected at the standard limits, but detection limits were raised because of dilution of the sample for analysis (*table 9*). Groundwater samples from EBAY3 exhibited the lowest concentrations for aluminum, arsenic, barium, cadmium, copper, lithium, strontium, and uranium.

The isotopic ratios of oxygen and hydrogen in water, as well as tritium and carbon-14 activities, were determined for most piezometer samples (*table 10*). The isotopic ratios of oxygen and hydrogen in water help infer the source of the groundwater recharge. These stable-isotopic ratios fall along the global meteoric water line. Generally, the stable-isotopic analyses of groundwater and pore-water showed similar deuterium and oxygen-18 values at similar depths (*fig. 5*). The groundwater sample from EBAY3 (585 fbls) contained less deuterium and oxygen than the other samples, however, indicating a recharge source from a higher elevation or an inland location. Tritium is a naturally occurring radioisotope of hydrogen that decays to helium-3. As tritium decays, its detectable concentration decreases. In this way, tritium can be used to distinguish between groundwater that was recently recharged and older groundwater (Michel, 1989). Tritium concentrations in groundwater from piezometers sampled in this study ranged from undetectable to 10.6 picocuries per liter (pCi/L; *table 10*), with the highest concentration found at EBMY3. Tritium concentrations from samples collected at EBAY3 were among the upper range measured in this study (4.2 pCi/L), indicating more recent recharge. Carbon-14 is a naturally occurring, unstable isotope of carbon that can be used to estimate groundwater age from the time of recharge. Carbon-14 data are reported as percent modern carbon (*table 10*). Results for carbon-14 from these piezometers ranged from 2.24 to 93.49 percent modern carbon.

Table 7. Nutrients in groundwater samples collected in June 2007 and analyzed by the U.S. Geological Survey (USGS) National Water Quality Laboratory, Denver, Colorado.

[The five digit number in parentheses below the constituent name is the USGS parameter code used to uniquely identify a specific constituent or property. **Abbreviations**: ID, identification; mg/L, milligrams per liter; <, less than]

Well ID number	Ammonia, as nitrogen (mg/L) (00608)	Nitrate plus nitrite, as nitrogen (mg/L) (00631)	Nitrite, as nitrogen (mg/L) (00613)	Orthophosphate, as phosphorus (mg/L) (00671)	Total nitrogen (nitrate + nitrite + ammonia + organic-nitrogen), as nitrogen (mg/L) (62854)
EBAY2	0.167	<0.06	<0.002	0.239	0.19
EBAY3	<0.020	0.36	<0.002	0.146	0.40
EBAY4	0.183	<0.06	<0.002	0.428	0.23
EBAY5	0.728	<0.06	<0.002	0.990	0.68
EBAY6	2.46	<0.06	<0.002	1.27	2.17

Table 8. Major and minor ions, and total dissolved solids detected in filtered groundwater samples collected in June 2007 and in December 2008 and analyzed by the U.S. Geological Survey (USGS) National Water Quality Laboratory, Denver, Colorado.

[The five digit number in parentheses below the constituent name is the USGS parameter code used to uniquely identify a specific constituent or property. **Abbreviation**: mg/L, milligrams per liter]

Well identification number	Calcium (mg/L) (00915)	Magnesium (mg/L) (00925)	Potassium (mg/L) (00935)	Sodium (mg/L) (00930)	Bromide (mg/L) (71870)	Chloride (mg/L) (00940)	Fluoride (mg/L) (00950)	Iodide (mg/L) (71865)	Silica (mg/L) (00955)	Sulfate (mg/L) (00945)	Total dissolved solids (mg/L) (70300)
EBAY2	15.7	6.08	1.53	190	0.64	138	0.33	1.75	21.2	37.2	568
EBAY3	15.6	4.56	1.16	92.1	0.14	47.1	0.28	0.357	22.7	33.1	302
EBAY4	32.9	11.4	1.53	127	0.20	68.1	0.20	0.310	31.3	50.7	487
EBAY5	34.0	17.5	5.22	121	0.22	62.3	0.27	0.258	35.1	37.5	488
EBAY6	1,350	2,910	376	22,700	140	44,200	0.13	1.29	22.5	5,540	77,800
EBKA1	32.5	10.2	1.87	120	0.24	63.4	0.16	0.331	21.1	67.3	454
EBKA2	55.3	24.0	2.42	83.1	0.17	56.4	0.24	0.103	32.2	44.5	459
EBMY1	44.3	11.9	2.34	116	0.21	52.6	0.33	0.232	26.4	61.0	474
EBMY2	60.0	19.7	2.52	68.7	0.14	47.2	0.23	0.039	27.6	42.8	428
EBMY3	107	37.3	1.86	59.3	0.50	51.9	0.21	0.004	31.2	65.0	614
EBSP1	35.0	11.7	1.85	150	0.37	123	0.28	0.582	23.6	48.2	528
EBSP2	38.3	14.8	1.88	111	0.18	53.4	0.21	0.238	31.7	49.5	465
EBSP3	40.4	18.3	2.88	79.8	0.16	42.9	0.28	0.054	28.8	36.2	390

Table 9. Trace metals in groundwater samples collected in June 2007 and in December 2008 and analyzed by the U.S. Geological Survey (USGS) National Water Quality Laboratory, Denver, Colorado.

[The five digit number in parentheses below the constituent name is the USGS parameter code used to uniquely identify a specific constituent or property. **Abbreviations**: E, estimated; V, result affected by contamination; µg/L, micrograms per liter; <, less than]

Well identification number	Aluminum (µg/L) (01106)	Antimony (µg/L) (01095)	Arsenic (µg/L) (01000)	Barium (µg/L) (01005)	Beryllium (µg/L) (01010)	Boron (µg/L) (01020)	Cadmium (µg/L) (01025)	Chromium (µg/L) (01030)	Cobalt (µg/L) (01035)	Copper (µg/L) (01040)	Iron (µg/L) (01046)	Lead (µg/L) (01049)
EBAY2	2.6	0.13	6.4	69	<0.06	549	0.04	E0.07	<0.04	<0.40	E5	<0.12
EBAY3	E1.4	E0.05	0.71	31	<0.06	344	E0.02	0.12	0.08	<0.40	<6	<0.12
EBAY4	E1.5	0.08	6.3	49	<0.06	449	E0.02	0.31	E0.02	<0.40	E5	<0.12
EBAY5	<8.0	0.09	13.5	36	<0.06	451	<0.04	0.15	0.04	0.47	<6	<0.12
EBAY6	<80.0	<3.00	8.5	98	<3.00	5,720	10.0	6.5	43.0	E16.0	<300	<6.00
EBKA1	<4.0	0.09	18.7	47	<0.02	488	0.05	<0.12	0.06	<1.0	<4	<0.06
EBKA2	<4.0	0.07	3.4	69	<0.02	393	E0.02	<0.12	0.14	<1.0	7	<0.06
EBMY1	4.0	0.07	3.2	42	<0.02	394	0.05	E0.08	0.11	<1.0	5	<0.06
EBMY2	E2.1	0.09	2.2	62	<0.02	305	0.03	E0.07	0.23	<1.0	E4	<0.06
EBMY3	<4.0	0.08	1.5	220	<0.02	410	0.02	0.81	0.14	<1.0	E2	<0.06
EBSP1	<4.0	E0.04	1.9	90	<0.02	400	0.03	E0.07	0.09	<1.0	14	<0.06
EBSP2	E2.4	0.06	6.0	59	<0.02	468	0.03	E0.09	0.06	<1.0	E4	<0.06
EBSP3	<4.0	0.09	6.0	69	<0.02	313	0.03	E0.08	0.10	<1.0	10	<0.06

Well identification number	Lithium (µg/L) (01130)	Manganese (µg/L) (01056)	Molybdenum (µg/L) (01060)	Nickel (µg/L) (01065)	Selenium (µg/L) (01145)	Silver (µg/L) (01075)	Strontium (µg/L) (01080)	Thallium (µg/L) (01057)	Tungsten (µg/L) (01155)	Uranium (µg/L) (22703)	Vanadium (µg/L) (01085)	Zinc (µg/L) (01090)
EBAY2	11.6	25.4	33.8	0.13	E0.04	<0.2	260	<0.04	0.49	0.73	5.4	<0.60
EBAY3	10.5	55.1	10.6	0.17	<0.08	<0.1	187	<0.04	0.18	0.34	1.8	<0.60
EBAY4	11.2	152	9.5	0.38	<0.08	<0.1	544	<0.04	0.31	1.36	1.1	<0.60
EBAY5	15.2	90.3	5.9	0.31	<0.08	<0.1	401	<0.04	0.32	0.77	1.3	<0.60
EBAY6	412	37,000	20.0	46.5	7.5	<5.0	23,600	<2.00	<3.0	9.50	9.5	<30.0
EBKA1	10.5	78.4	16.5	0.70	<0.06	<0.008	535	<0.04	0.35	2.25	0.43	E1.2
EBKA2	18.6	238	7.0	0.60	<0.06	<0.008	713	<0.04	0.21	2.01	3.6	<2.0
EBMY1	11.0	192	13.7	V0.54	<0.06	<0.008	517	<0.04	0.75	3.04	6.0	<2.0
EBMY2	13.5	406	7.7	V0.82	<0.06	<0.008	622	<0.04	1.4	2.50	1.8	2.1
EBMY3	17.1	17.8	2.1	V1.3	0.80	<0.008	794	<0.04	0.13	2.21	3.4	<2.0
EBSP1	20.0	118	8.6	V0.44	<0.06	<0.008	392	<0.04	0.43	1.18	1.4	<2.0
EBSP2	19.4	88.5	10.2	V0.49	<0.06	<0.008	632	<0.04	0.15	1.75	3.5	E1.1
EBSP3	13.3	131	9.0	V0.65	0.15	<0.008	428	<0.04	1.1	0.91	1.7	E1.0

Table 10. Stable isotope ratios, tritium, and carbon-14 activities in groundwater.

[The five digit number in parentheses below the constituent name is the U.S. Geological Survey (USGS) parameter code used to uniquely identify a specific constituent or property. Stable isotope ratios are reported in the standard delta notation (δ), the ratio of a heavier isotope to the more common lighter isotope of that element, relative to a standard reference material. **Abbreviations**: C, carbon; H, hydrogen; nc, sample not collected; O, oxygen; pCi/L, picocuries per liter; —, not detected]

Well identification number	δ^2H of water (per mil) (82082)[1]	δ^{18}O of water (per mil) (82085)[1]	Tritium (pCi/L) (07000)[2]	δ^{13}C of dissolved carbonates (per mil) (82081)	Carbon-14 (percent modern) (49933)
EBAY2	–50.4	–7.46	—	[3]–11.46	[3]2.24
EBAY3	–67.8	–9.66	4.2	[3]–14.33	[3]14.93
EBAY4	–43.3	–6.37	—	[3]–15.49	[3]16.93
EBAY5	–40.8	–6.01	0.3	[3]–14.65	[3]31.14
EBAY6	–20.5	–2.38	0.6	[3]–14.95	[3]73.75
EBKA1	–43.9	–6.63	1.8	[4]–13.93	[4]7.48
EBKA2	nc	nc	0.6	[4]–15.28	[4]45.11
EBMY1	–43.6	–6.66	1.1	[4]–15.82	[4]12.87
EBMY2	–38.7	–6.11	—	[4]–14.15	[4]70.36
EBMY3	–43.6	–6.50	10.6	[4]–16.58	[4]93.49
EBSP1	–53.5	–7.70	1.2	[4]–15.25	[4]6.34
EBSP2	–40.5	–6.21	—	[4]–14.44	[4]13.84
EBSP3	nc	nc	0.5	[4]–15.26	[4]59.31

[1]USGS-National Research Program, Stable Isotope Laboratory, Reston, Virginia.

[2]USGS Tritium Laboratory, Menlo Park, California.

[3]University of Waterloo, Environmental Isotope Lab (CAN-UWIL); University of Arizona Accelerator Mass Spectrometry Lab (AZ-UAMSL).

[4]National Ocean Sciences Accelerator Mass Spectrometry Facility (NOSAMS).

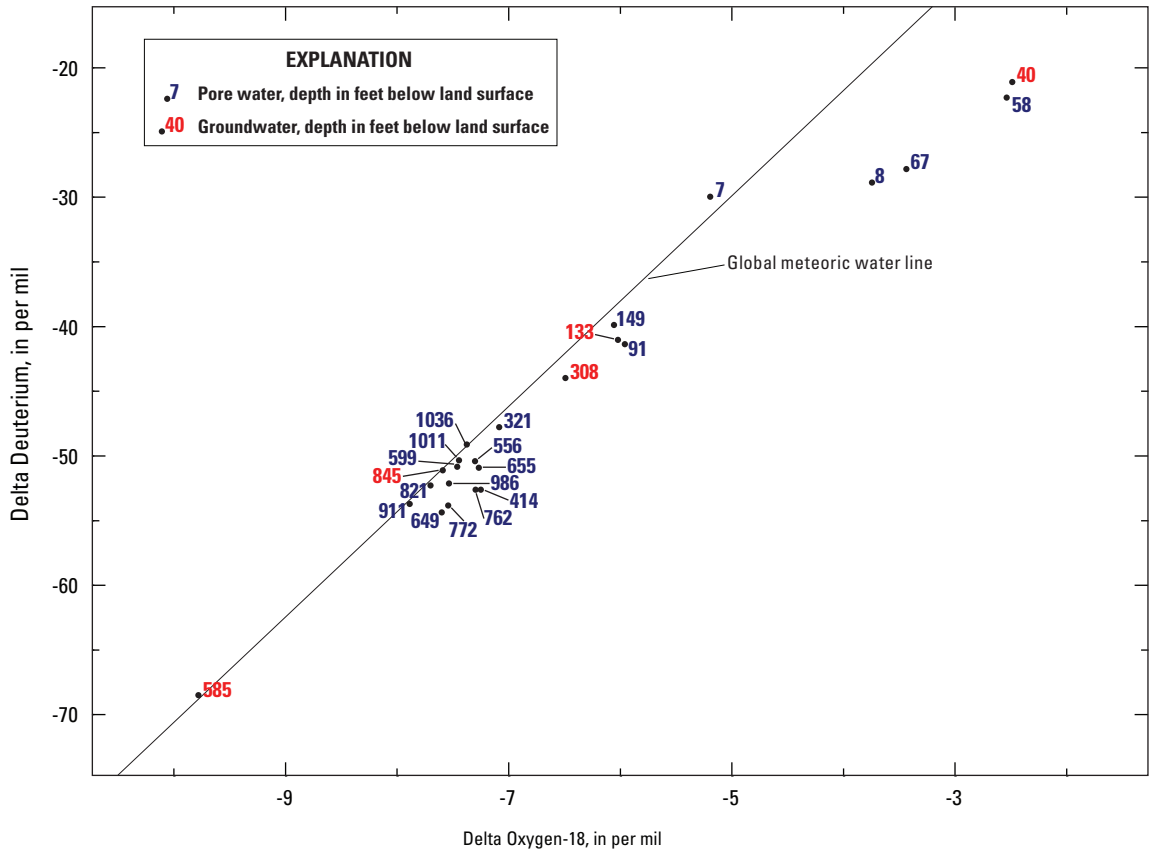

Figure 5. Graph showing cComparison of isotopic ratios of hydrogen and oxygen between pore-water and groundwater at similar depths from the East Bay Bayside Monitoring Site (EBAY) core and EBAY piezometers, respectively.

Quality-Control Sample Results

Quality-control samples collected by the GAMA program for the June 2007 sampling event at Bayside were explained in detail by Ray and others (2009). Assessment of an additional field blank that was collected by the NAWQA program during the December 2008 sampling event at Kipp Academy, East Bay Mud Yard, and Stenzel Park revealed no detections in the blank sample, with the exception of nickel. We infer that the same process that caused the detection of nickel in the field blank (0.34 µg/L) could have contributed to the corresponding environmental samples. Because of this, a "V" code was applied to the trace nickel data from the December 2008 sampling event, indicating that the results could have been affected by contamination (*table 9*).

Core Analyses

Physical and Mechanical Determinations

Moisture content of the EBAY core is summarized in *table 11*. Moisture content is expressed both as water mass in cubic centimeters and as a percentage of weight in grams.

Saturated vertical hydraulic-conductivity tests for 20 samples ranged from 0.0004 to 23.7 centimeters per day (cm/d), with a geometric mean of 0.04 cm/d (*table 12*). The test gradient varied according to sample material and ranged from 21 to 400 kPa.

Table 11. Moisture content by mass and percent for core samples from the East Bay Bayside Monitoring Site (EBAY) borehole.

[**Abbreviations**: cc, cubic centimeters; ft, feet; g, grams; hr, hours; LSD, land surface datum]

Core number	Sample depth (ft below LSD)	Wet weight (g)	Dry weight (g)	Drying time (hr)	Moisture content by mass (cc)	Moisture content (percent)
EBAY_1	3.0	34.93	26.19	49	8.74	25.0
EBAY_2	6.3	25.02	15.1	42	9.92	39.6
EBAY_3	10.7	37.23	27.06	40	10.17	27.3
EBAY_3	13.3	31.50	26.23	40	5.27	16.7
EBAY_4	17.5	28.44	23.82	38	4.62	16.2
EBAY_6	26.2	38.52	32.6	49	5.92	15.4
EBAY_11	51.1	28.66	22.86	40	5.80	20.2
EBAY_12	58.0	30.43	25.27	47	5.16	17.0
EBAY_13	62.4	30.90	25.49	44	5.41	17.5
EBAY_14	67.2	30.77	26.49	44	4.28	13.9
EBAY_15	71.3	42.89	35.96	40	6.93	16.2
EBAY_16	77.0	33.82	27.3	40	6.52	19.3
EBAY_17	81.9	40.15	32.49	39	7.66	19.1
EBAY_19	94.1	32.50	26.54	49	5.96	18.3
EBAY_19	90.8	42.34	34.69	48	7.65	18.1
EBAY_20	95.5	37.99	28.44	48	9.55	25.1
EBAY_21	102.1	33.30	27.19	45	6.11	18.3
EBAY_22	109.6	39.04	30.37	44	8.67	22.2
EBAY_23	112.1	41.75	34.29	43	7.46	17.9
EBAY_24	116.5	36.24	28.79	42	7.45	20.6
EBAY_25	122.3	32.83	28.86	41	3.97	12.1
EBAY_26	128.2	28.13	22.43	105	5.70	20.3
EBAY_28	136.7	32.94	22.52	101	10.42	31.6
EBAY_29	141.0	37.07	26.15	99	10.92	29.5
EBAY_30	146.3	27.90	20.17	98	7.73	27.7
EBAY_31	150.5	33.28	27.93	97	5.35	16.1
EBAY_32	157.4	37.04	31.06	80	5.98	16.1
EBAY_33	161.9	40.72	33.84	79	6.88	16.9
EBAY_34	168.4	37.49	30.64	77	6.85	18.3
EBAY_35	172.1	38.02	30.86	75	7.16	18.8
EBAY_36	178.4	35.25	28.61	74	6.64	18.8
EBAY_37	313.5	43.06	36.74	72	6.32	14.7
EBAY_39	320.6	35.18	28.06	72	7.12	20.2
EBAY_40	325.9	42.60	34.38	55	8.22	19.3
EBAY_41	414.0	44.52	36.2	54	8.32	18.7
EBAY_44	498.0	35.18	29.6	51	5.58	15.9
EBAY_48	556.0	39.03	31.82	122	7.21	18.5
EBAY_50	594.2	69.55	60.35	118	9.20	13.2
EBAY_51	597.2	26.81	23.14	130	3.67	13.7
EBAY_54	648.9	31.30	25.71	115	5.59	17.9
EBAY_56	656.0	32.45	27.06	113	5.39	16.6
EBAY_58	762.0	38.62	30.13	97	8.49	22.0
EBAY_59	765.3	38.08	29.61	95	8.47	22.2
EBAY_60	771.0	33.97	27.49	95	6.48	19.1
EBAY_60	773.9	25.20	20.53	107	4.67	18.5
EBAY_61	778.4	34.35	28.9	92	5.45	15.9
EBAY_63	826.8	35.62	29.5	90	6.12	17.2
EBAY_64	831.5	41.48	34.36	91	7.12	17.2
EBAY_66	910.4	31.67	26.02	25	5.65	17.8
EBAY_67	915.7	36.68	30.93	23	5.75	15.7
EBAY_68	987.6	32.37	27.99	20	4.38	13.5
EBAY_70	998.3	43.02	38.67	18	4.35	10.1
EBAY_71	1,014.0	32.03	26.81	40	5.22	16.3
EBAY_72	1,015.8	53.67	44.43	38	9.24	17.2
EBAY_73	1,032.0	42.80	36.16	43	6.64	15.5
EBAY_74	1,035.7	57.36	48.44	41	8.92	15.6

Table 12. Vertical hydraulic conductivity of selected cores from the East Bay Bayside Monitoring Site (EBAY) and East Bay Extensometer-2 Monitoring Site (EXT2) boreholes.

[**Abbreviations**: ft, feet; LSD, land surface datum; cm/d, centimeters per day; kPa, kilopascals]

Core number	Sample depth (ft below LSD)	Saturated hydraulic conductivity (cm/d)	Test gradient (kPa)
EBAY_2	8.8	0.3062	200
EBAY_2	8.8	0.2223	200
EXT2_2	42.5	0.0448	200
EXT2_2	42.5	0.0655	200
EBAY_12	58.3	1.5065	119
EBAY_12	58.3	2.3704	200
EBAY_15	73.4	0.4801	200
EBAY_15	73.4	0.4287	300
EBAY_18	88.2	0.0016	282
EBAY_20	99.1	21.2827	21
EBAY_20	99.1	23.7224	28
EBAY_22	108.3	0.0554	84
EBAY_28	135.8	0.0098	42
EBAY_28	135.8	0.0099	210
EBAY_29	142.5	0.0035	42
EBAY_29	142.5	0.0031	210
EBAY_36	179.0	0.0006	210
EBAY_39	321.6	0.0230	182
EBAY_39	321.6	0.0151	100
EBAY_41	412.9	0.0088	182
EBAY_41	412.9	0.0077	250
EBAY_44	499.1	0.0017	182
EBAY_44	499.1	0.0006	300
EBAY_48	557.1	0.0013	305
EBAY_50	591.1	0.0004	200
EBAY_50	591.1	0.0009	400
EBAY_60	772.6	0.0100	300
EBAY_60	772.6	0.0063	300
EBAY_63	827.6	0.4219	126
EBAY_63	827.6	0.3740	35
EBAY_67	916.8	5.4168	35
EBAY_67	916.8	5.0799	49
EBAY_72	1,017.9	0.0125	210
EBAY_72	1,017.9	0.0066	300
EBAY_73	1,034.4	0.0273	300
EBAY_73	1,034.4	0.0231	318

For the 20 samples for which vertical hydraulic conductivity was measured, bulk density ranged from 0.76 to 1.79 grams per cubic centimeter (g/cm^3) and had a geometric mean of 1.50 g/cm^3 (*table 13*). Porosity and volumetric water content ranged from 34.6 to 70.6 percent and had geometric means of 44 and 43 percent, respectively. Effective porosity ranged from 28.2 to 62.1 percent and had a geometric mean of 36 percent; saturation and effective saturation ranged from about 89 to 100 percent and had geometric means of 97 and 96 percent, respectively (*table 13*). Grain size, strength, density, and results of Atterberg tests performed on selected cores are described in detail in Bennett and others (2009).

The results of the consolidation tests on 17 samples are shown in *table 14*. Analysis of 1 of the 17 samples was aborted prior to completion; therefore, no coefficient of elastic consolidation (C_r) was determined for that sample (EBAY_22). The fairly small ratios of past maximum stress to calculated effective stress indicated that, normally, the sediments are consolidated below about 135 ft. Shallow depths showed evidence of bioturbation and subaerial exposure (Robert Kayen, USGS, written commun., 2007). The sample EBAY_2 was determined to be disturbed because of its shallow depth and, therefore, was excluded from the calculations of minimums, maximums, and geometric means of the samples shown in *table 14* and discussed here.

Elastic and inelastic specific-storage values, calculated from consolidation test results, generally decreased with depth. Elastic specific storage values ranged from 5.5×10^{-6} to 5.8×10^{-5} per foot (ft^{-1}), and inelastic specific storage values ranged from 7.7×10^{-5} to 8.6×10^{-4} ft^{-1}. The geometric mean of elastic specific storage for the clay samples was 1.6×10^{-5} ft^{-1}, which is greater than values reported by Sneed (2001) for samples collected from the San Joaquin Valley. Conversely, the geometric mean of inelastic specific-storage values for the clay samples was 1.9×10^{-4} ft^{-1}, which is less than values reported by Sneed (2001).

Age Dating

Luminescence geochronology results for nine samples, ranging in depth from about 39 to 312 fbls, are shown in *table 15*. Quartz blue-light OSL methods applied to seven of the samples indicated that ages ranged from about 27,800 (±2,260) to 169,000 (±36,100) years old. The two deepest samples (173 and 312 fbls) were tested by using only feldspar infrared stimulated luminescence and yielded only minimum ages, which ranged from greater than 86,600 to greater than 119,000 years old, because the advanced age of these samples was beyond the capability of the Quartz blue-light OSL method (*table 15*).

Table 13. Physical properties of selected cores from the East Bay Bayside Monitoring Site (EBAY) and East Bay Extensometer-2 Monitoring Site (EXT2) boreholes.

[**Abbreviations**: ft, feet; LSD, land surface datum; g/cm^3, grams per cubic centimeter; °C, degrees Celsius]

Core number	Sample depth (ft below LSD)	105°C oven calculations				Relative humidity oven calculations		
		Bulk density (g/cm^3)	Porosity (percent)	Volumetric water content (percent)	Saturation (percent)	Residual water content (percent)	Effective porosity (percent)	Effective saturation (percent)
EBAY_2	8.8	0.76	70.6	70.6	100.0	8.5	62.1	100.0
EXT2_2	42.5	1.43	47.8	47.8	100.0	11.8	36.0	100.0
EBAY_12	58.3	1.63	40.3	39.0	96.7	7.8	32.5	96.0
EBAY_15	73.4	1.60	39.8	39.2	98.4	6.6	33.3	98.1
EBAY_18	88.2	1.48	45.5	45.2	99.4	10.1	35.4	99.2
EBAY_20	99.1	1.74	35.9	35.0	97.4	7.0	28.9	96.7
EBAY_22	108.3	1.43	49.2	46.7	94.9	7.6	41.7	94.0
EBAY_28	135.8	1.19	60.2	54.4	90.3	6.1	54.1	89.2
EBAY_29	142.5	1.19	56.4	55.6	98.5	6.2	50.3	98.3
EBAY_36	179.0	1.70	40.0	39.1	97.6	5.5	34.5	97.2
EBAY_39	321.6	1.65	39.6	39.6	100.0	8.9	30.7	100.0
EBAY_41	412.9	1.64	40.1	40.1	100.0	7.7	32.3	100.0
EBAY_44	499.1	1.64	40.8	40.8	100.0	9.5	31.3	100.0
EBAY_48	557.1	1.53	44.8	44.7	99.8	12.2	32.5	99.7
EBAY_50	591.1	1.64	40.6	39.6	97.6	7.5	33.1	97.1
EBAY_60	772.6	1.50	46.0	44.5	96.8	13.3	32.7	95.6
EBAY_63	827.6	1.62	41.3	39.4	95.5	8.6	32.7	94.3
EBAY_67	916.8	1.61	41.3	39.1	94.6	9.3	32.1	93.1
EBAY_72	1,017.9	1.61	44.5	41.2	92.5	10.9	33.7	90.1
EBAY_73	1,034.4	1.79	37.1	34.6	93.3	8.9	28.2	91.3

Table 14. Consolidation test results of selected cores from the East Bay Bayside Monitoring Site (EBAY) borehole.

[**Abbreviations**: ft, feet; ft^{-1}, per foot; kPa, kilopascals; LSD, land surface datum; —, no data]

Core number	Sample depth (ft below LSD)	Maximum past stress (kPa)	Calculated effective stress (kPa)	Coefficient of inelastic consolidation (C_c)	Coefficient of elastic consolidation (C_r)	Initial void ratio (e_0)	Inelastic specific storage (ft^{-1})	Elastic specific storage (ft^{-1})
[1]EBAY_2	8.3	60	21	1.31	0.105	2.69	7.7E-03	6.2E-04
EBAY_12	58.8	725	167	0.265	0.014	0.66	2.9E-04	1.5E-05
EBAY_15	73.9	1,100	218	0.276	0.01	0.69	1.9E-04	7.0E-06
[1]EBAY_18	88.6	520	266	0.34	0.041	0.77	4.8E-04	5.8E-05
EBAY_20	99.6	725	303	0.25	0.01	0.60	2.8E-04	1.1E-05
[1]EBAY_22	108.5	810	332	0.48	—	0.86	4.1E-04	—
[1]EBAY_28	136.3	700	413	1.30	0.08	1.8	8.6E-04	5.3E-05
[1]EBAY_29	144.1	700	433	0.94	0.067	1.31	7.5E-04	5.4E-05
[1]EBAY_36	179.5	1,000	546	0.29	0.03	0.64	2.3E-04	2.4E-05
[1]EBAY_39	321.2	2,300	1,080	0.44	0.036	0.67	1.5E-04	1.2E-05
[1]EBAY_41	411.9	2,100	1,393	0.45	0.035	0.68	1.7E-04	1.3E-05
[1]EBAY_44	498.6	3,250	1,680	0.33	0.035	0.55	8.5E-05	9.0E-06
[1]EBAY_48	557.6	3,050	1,919	0.48	0.052	0.73	1.2E-04	1.3E-05
[1]EBAY_50	591.6	2,100	2,038	0.29	0.033	0.56	1.1E-04	1.3E-05
[1]EBAY_67	917.1	3,600	3,185	0.37	0.028	0.58	8.4E-05	6.4E-06
[1]EBAY_72	1,018.2	3,800	3,551	0.35	0.042	0.56	7.7E-05	9.2E-06
[1]EBAY_74	1,036.6	4,000	3,610	0.36	0.026	0.52	7.7E-05	5.5E-06
						min[2]	7.7E-05	5.5E-06
						max[2]	8.6E-04	5.8E-05
						geometric mean[2]	2.0E-04	1.5E-05
						geometric mean of clay samples[2]	1.9E-04	1.6E-05

[1]Clay sample.

[2]Calculation excludes EBAY_2.

Table 15. Quartz blue-light optically stimulated luminescence (OSL) and feldspar infrared stimulated luminescence (IRSL) ages of selected cores from the East Bay Bayside Monitoring Site (EBAY) and East Bay Extensometer-2 Monitoring Site (EXT2) boreholes.

[**Abbreviations:** ft, feet; Gy, absorbed radiation energy per unit mass (Gray); Gy/ka, absorbed radiation energy per unit mass per thousand years; ka, thousand years; LSD, land surface datum; ppm, parts per million; %, percent; n, number of replicated equivalent dose (De) estimates used to calculate the mean.]

Core number	Sample depth (ft below LSD)	Water content[1] (%)	Potassium[2] (%)	Thorium[2] (ppm)	Uranium[2] (ppm)	Cosmic dose additions[3] (Gy/ka)	Total dose rate (D_r) (Gy/ka)	Equivalent dose (D_e) (Gy)	n[4]	Age (ka)[5]	Age (ka)[6]
EXT2_1	38.9	13 (27)	0.97 ± 0.05	3.58 ± 0.25	1.33 ± 0.11	0.053 ± 0.001	1.42 ± 0.06	39.5 ± 2.77	21 (21)	27.8 ± 2.26	—
EBAY_8	37.4	10 (40)	1.53 ± 0.10	5.15 ± 0.29	1.78 ± 0.18	0.055 ± 0.001	2.17 ± 0.08	66.9 ± 4.93	26 (28)	30.8 ± 2.54	34.5 ± 2.68
											33.0 ± 2.94
EBAY_9	42.3	17 (42)	1.62 ± 0.07	5.18 ± 0.27	1.79 ± 0.17	0.048 ± 0.001	2.10 ± 0.07	68.0 ± 4.40	21 (24)	32.4 ± 2.35	—
EBAY_10	48.2	14 (19)	1.14 ± 0.04	7.32 ± 0.29	1.94 ± 0.13	0.042 ± 0.001	1.90 ± 0.05	63.9 ± 3.38	19 (20)	33.7 ± 2.04	—
EBAY_17	83.2	17 (22)	1.79 ± 0.05	7.12 ± 0.24	2.13 ± 0.11	0.022 ± 0.001	2.41 ± 0.05	99.2 ± 5.65	19 (20)	41.2 ± 2.53	—
EBAY_25	125.3	18 (46)	1.81 ± 0.07	7.76 ± 0.36	2.30 ± 0.16	0.018 ± 0.001	2.12 ± 0.07	166 ± 29.3	23 (23)	78.5 ± 14.0	>49.5 ± 9.38
											61.2 ± 6.28
EBAY_33	163.1	18 (44)	1.69 ± 0.05	5.65 ± 0.23	1.26 ± 0.10	0.011 ± 0.001	1.76 ± 0.05	298 ± 6.25	23 (25)	169 ± 36.1	181 ± 24.2
EBAY_35	172.7	18 (53)	1.81 ± 0.06	6.69 ± 0.24	1.56 ± 0.10	0.009 ± 0.001	1.86 ± 0.04	—	—	—	>87.6 ± 23.5
								—	—	—	>86.6 ± 38.2
EBAY_37	311.7	16 (17)	1.20 ± 0.07	4.77 ± 0.35	1.40 ± 0.08	0.003 ± 0.001	1.61 ± 0.07	—	—	—	>119 ± 15.3

[1]Field moisture, with figures in parentheses indicating the complete sample saturation percentage. Ages calculated using 75–80% of saturation values.

[2]Analyses obtained using laboratory Gamma Spectrometry (low resolution sodium iodide detector).

[3]Cosmic doses and attenuation with depth were calculated using the methods of Prescott and Hutton (1994).

[4]Figures in parentheses indicate total number of measurements made including failed runs with unusable data.

[5]Dose rate and age for fine-grained 180–90 micrometer quartz sand. Linear + exponential fit used on age, errors to one sigma.

[6]Feldspar from fine-grains of 4 to 11 microns, due to extremely old ages obtained on quartz. Exponential fit used for equivalent dose. Errors one sigma. Fade tests indicate no correction.

Depositional Environment

Core samples were inspected for foraminifera, which were quantified and identified, whereas ostracods, diatoms, and shell fragments were noted for presence only. Foraminifera specimens were found in EBAY_2, EBAY_28, and EBAY_29 and enumerated in only EBAY_28 and EBAY_29. A combination of diatoms, ostracods, and shell fragments was observed in EBAY_2, EBAY_22, EBAY_28, EBAY_29, and EBAY_36. The abundance of foraminifera in two core samples and the presence of foraminifera, diatoms, ostracods, and shell fragments in these five core samples are presented in *table 16*.

Eight species of benthic foraminifera, including two varieties of *Elphidium excavatum*, were identified in the EBAY core samples. Of these species, only two were abundant specimens (greater than 16 percent; *table 16*): *Elphidiella hannai* and *Elphidium excavatum* var. *selseyensis*. Common species (greater than 5 percent) included *Ammonia beccarii*, *Buccella frigida*, and *Elphidium excavatum* var. *clavatum*. Only rare specimens (less than 3 percent) of the other four species were encountered: *Bolivina vaughani*, *Elphidium gunteri*, *Trochammina inflata,*and *Trochammina macrescens*. Other biologic constituents recovered during the foraminifera analysis included diatoms, ostracods, and shell fragments.

Both arenaceous and calcareous foraminiferal species were represented in the EBAY core. All of these species are common today in shallow embayments and estuaries along the Pacific Coast of North America (Phleger, 1967; Scott and others, 1976; Jennings and Nelson, 1992; McCormick and others, 1994; McGann, 2007).

The two deepest samples containing foraminifera in the EBAY core were between 145 and 135 fbls. Sample EBAY_29 (*tables 3* and *16*) was characterized by dominant *Elphidiella hannai* (56 percent) and abundant *Elphidium excavatum* var. *selseyensis* (31 percent), as well as common *Ammonia beccarii* (6 percent). Species dominance was reversed in Sample EBAY_28, with higher percentages of *Elphidium excavatum* var. *selseyensis* (64 percent), abundant *Elphidiella hannai* (17 percent), and common *Buccella frigida* (7 percent), *Elphidium excavatum* var. *clavatum* (6 percent), and *Ammonia beccarii* (5 percent). These are typical modern deep to shallow subtidal estuarine foraminiferal assemblages found in areas of the San Francisco Bay estuary, such as San Pablo, Richardson, Central, and South bays (Means, 1965; Slater, 1965; Quinterno, 1968; Locke, 1971; Arnal and others, 1980). Similar assemblages also have been reported in late Pleistocene and Holocene estuarine deposits in San Francisco Bay along the San Francisco–Oakland Bay Bridge transect (McGann and others, 2002) and about 3.7 mi south of the bridge along the proposed, but never built, Southern Crossing transect (Sloan, 1992). Of the three biofacies identified in these older sediments, an assemblage dominated by *Elphidiella hannai* (Sample EBAY_29) would be assigned to Biofacies C, representing deep subtidal regions of about 39 to 72 ft water depth and salinity of about 15 to 32 practical salinity units (psu). Sample EBAY_28, dominated by *Elphidium excavatum* (inclusive of both varieties, *Elphidium excavatum* var. *selseyensis* and *Elphidium excavatum* var. *clavatum*), would be referable to Biofacies B, indicative of shallow subtidal environments of water depths from about 7 to 49 ft and salinity of about 10 to 30 psu (Sloan, 1992; McGann and others, 2002).

Table 16. Percentage abundance of the benthic foraminifera in core from the East Bay Bayside Monitoring Site (EBAY) borehole.

[**Abbreviations:** ft, feet; LSD, land surface datum; X, presence of benthic foraminifera and other biological constituents in a non-statistical count; —, non-detect]

Species/ samples	Sample depth (ft below LSD)				
	7.00	109	137	141	179
	Core number				
	EBAY_2	EBAY_22	EBAY_28	EBAY_29	EBAY_36
Ammonia beccarii	—	—	5.2	6.4	—
Bolivina vaughani	—	—	—	0.5	—
Buccella frigida	—	—	6.9	3.4	—
Elphidiella hannai	—	—	16.7	55.6	—
Elphidium excavatum clavatum	—	—	5.9	1.1	—
Elphidium excavatum selseyensis	—	—	64.1	30.6	—
Elphidium gunteri	—	—	1.3	2.3	—
Trochammina inflata	X	—	—	—	—
Trochammina macrescens	X	—	—	—	—
Total count	—	—	306	435	—
Other constituents					
Diatoms	X	—	—	X	—
Ostracods	—	X	—	X	X
Shell fragments	—	—	X	—	X

The shallowest sediment-core sample containing foraminifera was EBAY_2 (*tables 3* and *16*). Two arenaceous species, *Trochammina inflata* and *Trochammina macrescens*, were present, and they were not observed elsewhere in the core. Recent assemblages with these two species have been reported from the mudflat, marsh, and brackish waters regions in Suisun, Richardson, and San Pablo bays in the San Francisco Bay estuary (Means, 1965; Slater, 1965; Locke, 1971; Connor, 1975). In the late Pleistocene and Holocene deposits under the bay, an assemblage dominated by *Trochammina inflata* would be assigned to Biofaces A, indicative of intertidal mudflat and marsh conditions, water depths from about 0 to 7 ft, and a maximum salinity of about 10 psu. These relatively wide ranges in water temperature and salinity, in addition to a high organic input, contribute to making the mudflats, marshes, and brackish regions stressful environments, and foraminiferal faunas are typically characterized by low faunal diversity (Phleger, 1970; Murray, 1973). Commonly, calcareous taxa are absent in these marginal environments because they dissolve in the unfavorable physical and chemical conditions (e.g., low pH) within the sediments (Parker and Athern, 1959; Phleger, 1967; Scott and Medioli, 1980; Scott and Leckie, 1990; Jennings and Nelson, 1992).

Selection of samples for diatom analysis was guided by the results of the foraminifera analysis. Nearly all of the 31 core samples analyzed for foraminifera were taken from similar locations in the core that were selected for diatom analysis and were found barren of microfossils. Of the two samples where diatoms were observed, only one sample (EBAY_29) had diatoms in any abundance, and all were fragmented. The assemblage indicated marine to brackish conditions (Scott Starratt, U.S. Geological Survey, written commun., 2007).

Mineralogy

X-ray diffraction results for 16 samples revealed clay and non-clay minerals composed an average of 40.8 and 59.2 percent of the core-sample mineralogy, respectively (*table 17*). Of the seven clay minerals identified by XRD, illite and smectite occur most frequently, at an average of 13 percent each, followed by chlorite, muscovite, biotite, kaolanite, and gibbsite (*table 17*). The relative abundances of clay minerals are greatest (greater than 50 percent) at depths of 142, 499, 547, 557, and 772 fbls, and are least at a depth of 767 fbls (*fig. 6*). Two of the segments, at depths of 547 and 557 fbls, that contained a relatively high abundance of clay lie within the Deep aquifer zone consisting of three coarse-sand and gravel beds. This is consistent with the resistivity logs from *figure 2A* showing decreased resistivity at these depths, where clay is present, and increased resistivity at depths where sand and gravel are present.

Table 17. Relative abundance of minerals determined from x-ray defraction analyses of core samples collected from the EBAY borehole, San Lorenzo, California.

[**Abbreviations:** LSD, land surface datum]

Core number	Sample depth (feet below LSD)	Non-clay									Total non-clay (percent)
		Quartz (percent)	Potassium feldspar (percent)	Plagioclase (percent)	Calcite (percent)	Aragonite (percent)	Ankerite (percent)	Goethite (percent)	Maghemite (percent)	Apatite (percent)	
EBAY_10	48.2	38.6	9.7	24.8	1.4	1.0	0.2	0.6	0.0	0.7	76.0
EBAY_17	83.2	30.2	9.8	26.3	3.4	1.5	0.4	0.6	0.5	0.2	71.5
EBAY_25	123.8	31.7	10.4	22.8	1.9	1.5	0.1	0.6	0.8	0.1	68.5
EBAY_29	142.5	22.0	4.4	19.8	1.2	0.4	0.3	0.3	0.0	0.9	48.9
EBAY_33	163.1	35.1	9.2	22.7	1.9	1.3	0.0	0.5	1.0	0.7	71.1
EBAY_35	172.7	27.3	7.8	23.4	1.7	1.2	0.0	0.4	0.4	0.6	61.7
EBAY_37	311.6	35.3	9.2	23.6	2.2	1.5	0.2	0.7	0.1	1.0	72.3
EBAY_41	412.9	25.0	6.2	21.2	1.0	0.2	0.0	0.4	0.0	0.5	54.3
EBAY_44	499.1	20.1	3.2	16.2	1.0	0.4	0.2	0.6	0.0	0.3	41.5
EBAY_46	547.4	23.1	4.1	14.7	1.5	1.4	0.2	0.7	0.2	0.6	45.0
EBAY_48	557.1	17.6	3.6	11.6	1.1	0.5	0.5	0.4	0.0	0.3	35.1
EBAY_50	594.4	34.4	3.7	20.4	1.3	1.3	0.1	0.9	0.0	0.3	61.0
EBAY_59	767.6	38.8	10.2	25.8	9.2	1.5	2.5	0.4	0.6	0.2	87.8
EBAY_60	772.6	17.4	3.6	8.2	6.1	0.0	0.9	0.2	0.3	0.1	36.8
EBAY_70	996.2	40.3	2.2	4.7	2.3	1.9	1.2	2.0	4.9	0.7	58.3
EBAY_73	1,034.4	34.5	2.4	17.8	0.8	0.4	0.2	1.4	0.0	0.9	57.9

Table 17. Relative abundance of minerals determined from X-ray defraction analyses of core samples collected from the East Bay Bayside Monitoring Site (EBAY) borehole, San Lorenzo, California.—Continued

[**Abbreviations:** LSD, land surface datum]

Core number	Sample depth (feet below LSD)	Clay								Total clay (percent)
		Gibbsite (percent)	Kaolinite (percent)	Smectite		Illite (percent)	Muscovite (percent)	Biotite (percent)	Chlorite (percent)	
				Sodium-smectite (percent)	Ferruginous smectite (percent)					
EBAY_10	48.2	0.0	0.1	6.8	3.6	6.9	2.0	1.8	2.8	24.0
EBAY_17	83.2	0.0	0.8	6.7	3.5	7.0	3.3	2.0	5.1	28.5
EBAY_25	123.8	0.0	1.4	11.4	3.9	4.9	3.3	2.5	4.3	31.5
EBAY_29	142.5	0.0	5.9	5.5	13.7	14.0	2.2	2.5	7.4	51.1
EBAY_33	163.1	0.0	0.7	3.6	6.3	7.8	4.7	1.8	4.0	28.9
EBAY_35	172.7	0.0	0.9	6.0	6.4	11.6	5.2	2.9	5.4	38.3
EBAY_37	311.6	0.0	0.9	7.4	4.7	8.1	2.0	2.2	2.4	27.7
EBAY_41	412.9	0.1	2.2	3.2	8.4	15.8	4.2	3.5	8.3	45.7
EBAY_44	499.1	0.3	4.5	0.0	16.5	19.3	6.1	4.6	7.2	58.5
EBAY_46	547.4	0.0	2.6	2.6	15.9	18.9	6.5	4.0	4.3	55.0
EBAY_48	557.1	0.5	5.1	0.0	17.5	24.1	8.5	4.1	5.1	64.9
EBAY_50	594.4	0.1	1.9	0.0	8.0	17.3	4.4	4.6	2.8	39.0
EBAY_59	767.6	0.0	0.0	0.5	1.6	5.9	0.0	0.3	3.8	12.2
EBAY_60	772.6	0.0	9.6	5.8	18.4	21.0	0.7	3.7	4.1	63.2
EBAY_70	996.2	1.7	1.7	0.0	7.5	14.3	5.1	9.9	1.4	41.7
EBAY_73	1,034.4	0.2	4.6	0.0	12.7	18.1	0.6	4.0	1.9	42.1

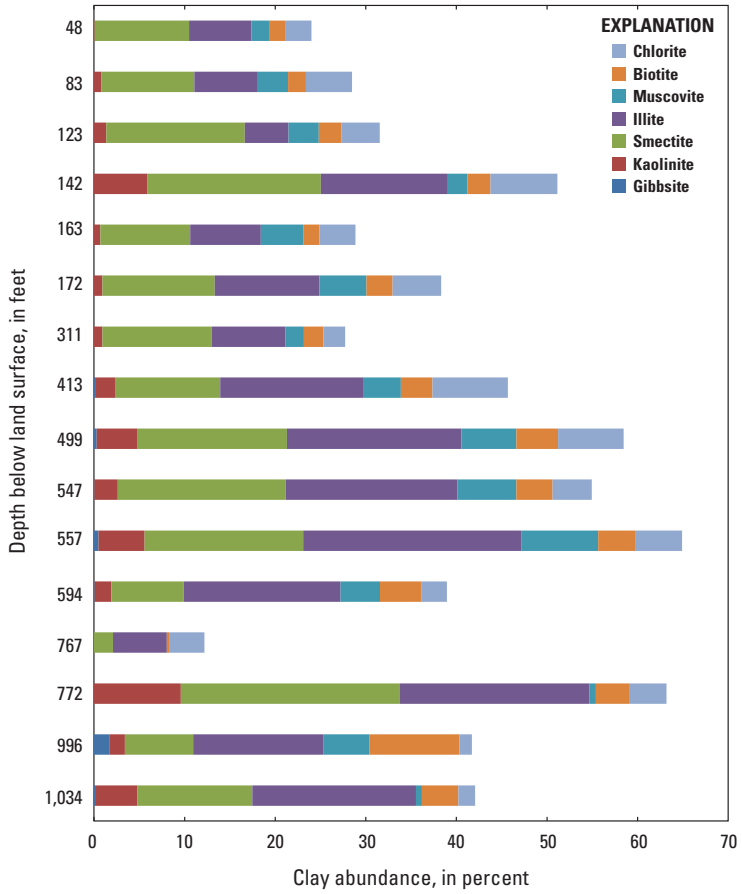

Figure 6. Graph showing rRelative clay abundance versus depth of core samples from East Bay Bayside monitoring site in San Lorenzo, California.

The clay mineral, smectite, has low-layer charge and cations in only about a third of interlayer sites, which allows water to move in and out of the inter-clay layers, causing it to swell with the addition of water and shrink with the subtraction of water (Nesse, 2000). In addition, the swelling potential of smectite increases when monovalent cations sorb to the double layer (Hille, 1980). Compression and swell indexes from Lambe and Whitman (1969) describe the shrink-swell potential of smectite, illite, and kaolinite, depending upon the exchangeable cation between the tetrahedral–octahedral–tetrahedral layers. In general, divalent cations, such as calcium, magnesium, and iron, in the exchange complex reduce the swelling potential of montmorillonite, illite, and kaolanite (Lambe and Whitman, 1969; Hille, 1980). Trivalent aluminum at a low pH also reduces swelling potential, as does high salinity. If a salt-rich soil matrix is flushed with freshwater in the absence of calcium ions, however, the potential for swelling is high (Hille, 1980). Two types of smectite (sodium smectite and ferruginous smectite) were identified in the core samples; sodium smectite has a greater compression index than ferruginous smectite by a factor of 1.6 (Lambe and Whitman, 1969). The relative concentration of sodium smectite decreases with depth as ferruginous smectite increases in a one-to-one relation. The average percent weight of sodium smectite within the total weight percent of smectite was 29.2 percent, and ferruginous smectite composed 70.8 percent of the total smectite in all of the samples. Illite, because of its relatively high layer charge and the abundance of cations in the interlayer sites, does not have a great potential to swell when moistened (Nesse, 2000). Kaolanite has a low shrink-swell potential because weak electrostatic bonds yield a low cation exchange capacity; therefore, water molecules are not commonly found in the interlayer positions (Nesse, 2000). Amounts of illite and kaolanite did not follow a trend with depth.

Of the nine non-clay minerals identified by XRD, quartz and plagioclase were the most abundant, followed by lesser amounts of potassium feldspar, calcite, aragonite, goethite, maghemite, apatite, and ankerite (*table 17*). Clay percentages were inversely related to percentages of non-clay minerals.

The mineralogical composition of 17 core samples was determined by SEM/EDS (*table 18*). The SEM/EDS and XRD analyses identified 10 of the same minerals, the SEM/EDS analysis exclusively identified 10 minerals, and the XRD analysis exclusively identified 4 minerals (*table 19*). The SEM/EDS analysis encountered difficulty identifying carbonate minerals because they occur as a fine intergrowth with clay minerals.

Framboidal pyrite, detected in EBAY_29, was the only secondary mineral observed by the SEM analysis. The presence of framboidal pyrite indicates that this sample was extracted from reducing conditions. In addition to framboidal pyrite, EBAY_29 contained the only organic matter observed (diatoms) in these core samples (*table 18*). The lack of organic matter in the other samples could be due to oxidation processes.

Iron oxide was observed on five samples, and manganese oxide possibly observed on one sample. It is unclear, however, if the presence of iron oxide was as a result of improper sample collection and storage techniques that allowed oxidation of the samples after collection.

The clay minerals primarily were composed of a mixture of illite and smectite. In addition to illite and smectite, distinct grains of biotite, chlorite, kaolanite, and muscovite were observed in the samples. The texture and morphologies of material in EBAY_65 indicated detrital origin.

Quartz and feldspar in the samples exhibited angular to sub-rounded morphology. These larger detrital grains also showed evidence of dissolution pitting.

The relative abundance of coarse or fine particles in samples identified by the XRD analysis were compared to SEM analysis results (*table 20*). Particle size from 7 of 17 samples was determined by using SEM. The relative abundance of coarse or fine particles, as measured by the XRD analysis, were not reflected in 57 percent of the grain-size analyses determined by using SEM. The inaccuracy of particle-size determination by SEM is attributed to flocculated clays and larger particles falling out of suspension during the grain-size analysis.

Table 18. Scanning electron microscopy/energy dispersive spectroscopy (SEM/EDS) results showing the presence or absence of minerals from core samples collected from the East Bay Bayside Monitoring Site (EBAY) borehole, San Lorenzo, California.

[**Abbreviations**: LSD, land surface datum; X, mineral detected by SEM/EDS; —, not detected]

Core number	Sample depth (feet below LSD)	Albite	Amphibole	Apatite	Biotite	Calcite	Chlorite	Clay (Illite and smectite)	Diopside	Epidote	Kaolanite	Muscovite
EBAY_10	48.2	X	—	—	X	X[1]	X	X	—	—	—	—
EBAY_17	83.2	—	—	—	—	—	X	X	—	—	—	X
EBAY_25	123.8	X	—	—	X	—	X	X	—	—	X	—
EBAY_29	142.5	X	—	—	—	—	X	X	—	—	—	X
EBAY_33	163.1	X	—	—	—	—	—	X	—	—	—	X
EBAY_35	172.7	X	—	—	—	—	X	X	—	—	—	—
EBAY_37	311.6	X	—	—	X	—	X	X	—	—	X	—
EBAY_41	412.9	X	—	—	—	—	X	X	—	—	—	—
EBAY_44	499.1	X	—	—	—	—	X	X	—	—	—	—
EBAY_46	547.4	X	—	—	—	—	X	X	—	—	—	—
EBAY_48	557.1	X	—	—	—	X[1]	—	X	—	X	X	X
EBAY_50	594.4	X	—	—	—	—	—	X	—	—	—	—
EBAY_59	767.6	—	—	X	—	—	—	X	—	—	—	—
EBAY_60	772.6	X	—	—	—	—	—	X	—	—	—	—
EBAY_65	838.5	—	X	—	—	X	—	X	X	—	—	—
EBAY_70	996.2	—	—	—	—	—	—	X	—	X	—	X
EBAY_73	1,034.4	X	—	—	—	—	X	X	—	—	—	X

Core number	Sample depth (feet below LSD)	Plagioclase	Potassium feldspar	Pyrite	Quartz	Rutile	Sphene	Talc	Zircon	Iron oxide	Manganese oxide	Diatoms
EBAY_10	48.2	X	X	—	X	—	X	—	—	X	—	—
EBAY_17	83.2	X	—	—	X	—	—	—	—	—	—	—
EBAY_25	123.8	X	X	—	X	—	—	—	—	X	—	—
EBAY_29	142.5	X	—	X	X	—	—	—	—	—	—	X
EBAY_33	163.1	X	—	—	X	X	—	X[1]	—	—	—	—
EBAY_35	172.7	—	X[2]	—	X	—	—	—	—	—	—	—
EBAY_37	311.6	X	X	—	X	—	—	—	—	—	—	—
EBAY_41	412.9	X	—	—	X	—	—	—	—	X	—	—
EBAY_44	499.1	X	X[2]	—	X	X	—	—	—	—	X[1]	—
EBAY_46	547.4	—	X	—	X	—	—	—	—	—	—	—
EBAY_48	557.1	X	—	—	X	—	X	—	—	X[1]	—	—
EBAY_50	594.4	X	—	—	X	—	—	—	—	—	—	—
EBAY_59	767.6	X	X	—	X	—	—	—	—	—	—	—
EBAY_60	772.6	—	—	—	—	—	—	—	X	—	—	—
EBAY_65	838.5	X	X[2]	—	X	—	—	—	X	—	—	—
EBAY_70	996.2	—	—	—	—	—	—	—	—	X	—	—
EBAY_73	1,034.4	—	—	—	X	—	X	—	—	—	—	—

[1]Estimated.

[2]Reported as feldspar.

Table 19. Comparison between minerals detected by scanning electron microscope (SEM) and X-ray diffraction (XRD) from core samples collected from the East Bay Bayside Monitoring Site (EBAY) borehole, San Lorenzo, California.

[**Abbreviations**: X, detected; —, not detected]

Mineral	XRD	SEM
Clay		
Biotite	X	X
Chlorite	X	X
Clay (illite and smectite)	X	X
Gibbsite	X	—
Kaolanite	X	X
Muscovite	X	X
Talc	—	X
Non-clay		
Amphibole	—	X
Apatite	X	X
Ankerite	X	—
Calcite	X	X
Diopside	—	X
Epidote	—	X
Goethite	X	—
Maghemite	X	—
Plagioclase (includes Albite)	X	X
Potassium feldspar	X	X
Pyrite	—	X
Quartz	X	X
Rutile	—	X
Sphene	—	X
Zircon	—	X
Iron oxide	—	X
Manganese oxide	—	X

Table 20. Comparison between relative grain sizes detected by scanning electron microscope (SEM) and X-ray diffraction (XRD) analyses of core samples collected from the East Bay Bayside Monitoring Site (EBAY) borehole, San Lorenzo, California.

[**Abbreviations**: LSD, land surface datum; NA, information not available; X, indicates greater percentage of coarse or fine grains; *, not sufficiently determined by particle size analysis; >, greater than, —, no data]

Core number	Sample depth (ft below LSD)	SEM		XRD	
		Coarse (percent)	Fine (percent)	Coarse (>50 percent)	Fine (>50 percent)
EBAY_10	48.2	*	*	X	—
EBAY_17	83.2	*	*	X	—
EBAY_25	123.8	—	X	X	—
EBAY_29	142.5	—	X	—	X
EBAY_33	163.1	*	*	X	—
EBAY_35	172.7	*	*	X	—
EBAY_37	311.6	X	—	X	—
EBAY_41	412.9	*	*	X	—
EBAY_44	499.1	*	*	—	X
EBAY_46	547.4	X	—	—	X
EBAY_48	557.1	—	X	—	X
EBAY_50	594.4	*	*	X	—
EBAY_59	767.6	—	X	X	—
EBAY_60	772.6	*	*	—	X
EBAY_65	838.5	*	*	NA	NA
EBAY_70	996.2	*	*	X	—
EBAY_73	1034.4	—	X	X	—

Elemental Composition

Elemental composition of 17 cores samples was determined by using ICP-MS (*table 21*), and elemental composition of 9 core samples was determined by using INAA (*table 22*). Six samples (EBAY_10, EBAY _17, EBAY _25, EBAY _33, EBAY _35, and EBAY _37) were analyzed by using both methods; 19 element determinations were common to both analyses (*table 23*). The coefficient of determination (R^2), a measure of the agreement between the data and a linear regression, was used to compare the results from the ICP-MS and from the INAA analyses. The average R^2 value of 0.687 and median R^2 value of 0.799 indicated a relatively strong overall correlation for results derived from the two methods (*table 23*). R^2 values of 11 elements were equal to or greater than the median, indicating a strong correlation; 4 elements had R^2 values between the median and mean, indicating reasonable correlation; and 4 elements had low R^2 values, indicating a weak or poor correlation (*table 23*). Because the ICP-MS analysis was applied to more samples than the INAA analysis, the following discussion focuses on results from the ICP-MS analyses.

Comparison of major and trace elements to depth, revealed patterns common among the 37 elements analyzed by ICP-MS. Concentrations by depth showed a similar pattern in 26 of the 37 elements analyzed, which are *italicized* in *table 21*. Examples of this pattern are shown for zinc, scandium, and iron in *figure 7*. These 26 elements generally exhibited relatively high concentrations at the depths of 142, 499, 557, and 773 ft; had relatively low concentrations at depths of 48, 312, 768, and 838 ft; and showed a noticeable increase in concentration from 768 fbls to 773 fbls (*table 21*, *fig. 7*). Included in this group were cadmium and lead, which differed from this pattern in only the shallowest two samples. A different pattern emerged among calcium, sodium, strontium, and phosphorus, which showed a noticeable decrease in concentration from 768 fbls to 773 fbls. Calcium and phosphorous were similar, having higher concentrations at depths of 83 and 768 ft and lower concentrations at depths of 48, 124, 163, 594, and 1,034 ft.

Table 21. Element concentrations determined by inductively coupled plasma-mass spectroscopy (ICP-MS) analyses of core samples collected from the East Bay Bayside Monitoring Site (EBAY) borehole, San Lorenzo, California.

[The number in parentheses is the minimum detectable limit. *Italicized* elements show similar patterns to each other in changes in concentration with depth. **Abbreviations**: LSD, land surface datum; ppm, part per million; <, less than]

Core number	Sample depth (feet below LSD)	*Aluminium* (ppm) (50)	*Antimony* (ppm) (0.04)	Arsenic (ppm) (1)	Barium (ppm) (0.2)	*Beryllium* (ppm) (0.03)	Bismuth (ppm) (0.06)	*Cadmium* (ppm) (0.007)	*Caesium* (ppm) (0.003)	Calcium (ppm) (100)	*Cerium* (ppm) (0.1)
EBAY_10	48.2	61,400	0.87	6.4	649	1.1	0.10	0.69	2.2	12,200	30.9
EBAY_17	83.2	68,500	0.88	11.0	718	1.1	0.10	0.42	2.8	25,900	46.0
EBAY_25	123.8	71,000	0.97	7.6	736	1.3	0.10	0.10	2.8	12,100	39.8
EBAY_29	142.5	86,600	0.48	9.6	568	1.5	0.12	0.12	4.3	13,600	39.9
EBAY_33	163.1	68,200	0.82	7.2	707	1.1	0.09	0.08	2.7	11,000	37.7
EBAY_35	172.7	77,100	0.93	21.1	710	1.3	0.12	0.12	3.4	11,700	45.7
EBAY_37	311.6	67,900	0.69	6.7	639	0.94	0.06	0.16	2.2	13,400	38.7
EBAY_41	412.9	85,800	0.83	9.0	617	1.5	0.15	0.10	4.0	14,200	49.4
EBAY_44	499.1	91,800	0.96	10.0	632	1.8	0.18	0.16	4.7	12,600	56.1
EBAY_46	547.4	85,800	0.85	10.0	574	1.4	0.15	0.14	4.0	12,100	52.6
EBAY_48	557.1	98,200	0.89	10.0	653	1.9	0.19	0.18	5.3	13,100	51.9
EBAY_50	594.4	75,100	0.87	8.7	558	1.2	0.11	0.16	3.2	8,590	49.1
EBAY_59	767.6	50,800	0.40	1.3	582	0.72	<0.06	0.06	0.90	53,200	27.2
EBAY_60	772.6	91,300	0.70	3.8	583	1.6	0.15	0.18	4.3	26,500	45.4
EBAY_65	838.5	53,400	0.56	5.9	622	0.67	<0.06	0.15	1.3	9,360	22.8
EBAY_70	996.2	70,200	1.1	9.4	403	0.96	0.06	0.20	2.3	20,000	34.9
EBAY_73	1,034.4	82,900	0.88	9.0	430	1.5	0.08	0.08	3.2	10,400	44.0

Core number	Sample depth (feet below LSD)	*Chromium* (ppm) (0.5)	*Cobalt* (ppm) (0.03)	*Copper* (ppm) (2)	*Gallium* (ppm) (0.02)	*Iron* (ppm) (50)	*Lanthanum* (ppm) (0.05)	*Lead* (ppm) (0.4)	*Lithium* (ppm) (0.3)	*Magnesium* (ppm) (6)	*Manganese* (ppm) (0.7)
EBAY_10	48.2	76.0	8.6	20.8	11.5	20,900	16.5	23.4	22.0	8,010	326
EBAY_17	83.2	71.8	11.2	23.4	13.3	26,300	25.1	14.4	27.4	12,800	468
EBAY_25	123.8	77.7	11.4	23.8	13.4	26,900	22.1	12.6	30.2	9,670	291
EBAY_29	142.5	157	18.9	37.7	18.3	45,400	20.7	12.2	55.8	18,500	534
EBAY_33	163.1	80.1	9.5	21.2	13.2	25,200	19.8	10.8	25.2	9,140	331
EBAY_35	172.7	115	14.6	30.2	15.2	33,100	24.4	11.8	33.0	13,100	425
EBAY_37	311.6	91.4	12.6	19.3	12.4	25,400	21.6	8.74	21.5	8,930	471
EBAY_41	412.9	159	19.3	41.2	17.4	42,300	25.2	12.7	40.9	18,500	504
EBAY_44	499.1	183	23.2	50.8	19.4	51,100	29.2	14.3	46.0	20,600	804
EBAY_46	547.4	160	17.8	40.4	18.1	52,000	27.9	11.0	39.1	17,500	584
EBAY_48	557.1	190	24.8	53.7	21.3	55,200	28.1	13.7	47.4	22,600	826
EBAY_50	594.4	150	15.1	32.0	14.6	36,800	25.2	10.0	34.0	12,200	690
EBAY_59	767.6	52.8	4.4	9.3	7.0	6,990	14.0	5.35	13.6	12,000	549
EBAY_60	772.6	209	22.7	49.6	19.2	52,700	24.7	11.8	51.8	23,900	1,290
EBAY_65	838.5	156	14.8	39.8	10.0	29,600	12.0	5.99	23.9	12,600	396
EBAY_70	996.2	233	17.2	35.5	14.8	45,200	19.8	9.02	29.5	15,500	769
EBAY_73	1,034.4	207	19.6	49.7	16.0	43,500	25.4	8.44	31.6	12,200	610

Table 21. Element concentrations determined by inductively coupled plasma-mass spectroscopy (ICP-MS) analyses of core samples collected from the East Bay Bayside Monitoring Site (EBAY) borehole, San Lorenzo, California.—Continued

[The number in parentheses is the minimum detectable limit. *Italicized* elements show similar patterns to each other in changes in concentration with depth. **Abbreviations**: LSD, land surface datum; ppm, part per million; <, less than]

Core number	Sample depth (feet below LSD)	Molybdenum (ppm) (0.05)	*Nickel* (ppm) (0.3)	*Niobium* (ppm) (0.1)	Phosphorus (ppm) (5)	Potassium (ppm) (20)	*Rubidium* (ppm) (0.01)	*Scandium* (ppm) (0.04)	Silver (ppm) (0.01)	Sodium (ppm) (20)	Strontium (ppm) (0.8)
EBAY_10	48.2	0.96	40.1	7.5	474	15,500	53.8	8.5	0.216	21,300	272
EBAY_17	83.2	0.56	42.8	9.8	583	16,400	61.4	11.1	0.055	19,200	449
EBAY_25	123.8	0.42	52.4	8.9	407	18,300	67.4	10.4	0.078	17,800	294
EBAY_29	142.5	0.91	92.6	9.4	504	18,000	80.3	17.0	0.108	14,900	246
EBAY_33	163.1	0.35	43.1	9.3	263	17,500	63.4	10.0	0.055	18,000	276
EBAY_35	172.7	0.54	68.3	12	509	17,600	68.1	13.3	0.149	18,300	281
EBAY_37	311.6	0.58	48.7	11	514	15,100	54.0	9.5	0.075	19,900	307
EBAY_41	412.9	0.42	103	11	523	17,600	75.6	14.9	0.098	18,000	240
EBAY_44	499.1	0.59	142	11	632	17,500	79.9	17.9	0.098	14,500	177
EBAY_46	547.4	0.69	118	13	872	16,900	74.4	17.2	0.019	14,400	170
EBAY_48	557.1	0.65	143	11	742	21,400	91.4	20.3	0.282	10,900	170
EBAY_50	594.4	0.72	93.9	11	316	13,700	62.8	14.2	0.071	18,200	146
EBAY_59	767.6	0.20	28.2	2.6	958	11,900	34.3	3.8	0.074	20,800	394
EBAY_60	772.6	0.36	156	11	331	13,300	74.8	20.0	0.051	9,360	239
EBAY_65	838.5	1.3	127	3.8	529	7,970	27.3	11.4	0.103	15,500	145
EBAY_70	996.2	6.3	89.0	8.2	635	12,200	49.7	18.2	0.058	12,800	118
EBAY_73	1,034.4	0.72	141	10	249	12,400	60.4	16.0	0.054	18,600	143

Core number	Sample depth (feet below LSD)	*Thallium* (ppm) (0.08)	*Thorium* (ppm) (0.1)	*Titanium* (ppm) (40)	Uranium (ppm) (0.02)	*Vanadium* (ppm) (0.2)	*Ytterbium* (ppm) (0.05)	*Zinc* (ppm) (3)
EBAY_10	48.2	0.35	4.74	2,690	1.18	67.0	13.7	49.9
EBAY_17	83.2	0.42	6.88	3,100	1.94	79.6	25.0	55.8
EBAY_25	123.8	0.42	6.22	3,170	1.66	82.4	16.9	55.4
EBAY_29	142.5	0.43	7.21	4,170	2.23	145	21.3	98.7
EBAY_33	163.1	0.40	5.93	3,240	1.36	75.6	15.6	52.3
EBAY_35	172.7	0.42	7.22	3,980	1.62	106	20.9	72.4
EBAY_37	311.6	0.33	5.25	3,770	1.42	74.6	16.4	51.6
EBAY_41	412.9	0.46	7.89	4,160	2.07	128	22.3	92.6
EBAY_44	499.1	0.52	9.12	4,360	2.00	150	28.2	108
EBAY_46	547.4	0.45	8.72	4,600	2.22	139	22.7	98.1
EBAY_48	557.1	0.57	8.78	4,260	2.26	164	26.8	122
EBAY_50	594.4	0.39	7.21	3,870	1.93	110	23.4	68.8
EBAY_59	767.6	0.21	2.58	1,290	1.73	52.4	13.5	16.3
EBAY_60	772.6	0.51	7.51	4,810	1.55	127	22.2	102
EBAY_65	838.5	0.19	2.85	2,420	1.13	97.5	16.2	50.6
EBAY_70	996.2	0.30	4.68	5,290	1.71	135	25.4	77.4
EBAY_73	1,034.4	0.39	6.03	4,410	1.52	132	24.5	72.3

Table 22. Element concentrations determined by instrumental neutron activation by abbreviated count (INAA) analyses of core samples collected from the East Bay Bayside Monitoring Site (EBAY) borehole, San Lorenzo, California.

[**Abbreviations**: LSD, land surface datum; ppm, parts per million; ppb, parts per billion]

Core number	Sample depth (feet below LSD)	Iron (percent)	Calcium (percent)	Sodium (percent)	Potassium (percent)	Rubidium (ppm)	Strontium (ppm)	Cesium (ppm)	Barium (ppm)	Thorium (ppm)	Uranium (ppm)	Lantanum (ppm)
EBAY_8	37.4	1.31	0.81	1.64	1.08	35.00	179.00	1.18	495.00	3.56	1.32	13.50
EXT2_1	38.9	2.05	0.93	1.78	1.00	38.20	161.00	1.66	465.00	3.67	1.13	12.80
EBAY_9	42.3	1.22	0.87	1.82	1.31	37.30	222.00	1.33	486.00	3.58	1.05	12.20
EBAY_10	48.2	1.65	0.92	1.80	1.22	46.70	237.00	1.73	555.00	4.30	1.38	14.70
EBAY_17	83.2	2.37	1.39	1.80	1.51	59.10	335.00	2.65	678.00	5.95	1.74	17.30
EBAY_25	123.8	2.25	0.96	1.47	1.28	56.80	255.00	2.48	642.00	5.28	1.82	15.80
EBAY_33	163.1	2.08	0.80	1.47	1.34	53.50	233.00	2.35	620.00	4.71	1.36	14.80
EBAY_35	172.6	2.55	0.90	1.43	1.27	56.50	210.00	2.95	591.00	6.42	1.67	18.40
EBAY_37	311.6	2.13	1.08	1.35	1.23	42.70	205.00	1.96	493.00	5.23	1.38	14.80

Core number	Sample depth (feet below LSD)	Cerium (ppm)	Neodymium (ppm)	Samarium (ppm)	Europium (ppm)	Gadolinium (ppm)	Terbium (ppm)	Holmium (ppm)	Thulium (ppm)	Ytterbium (ppm)	Lutetium (ppm)	Zircronium (ppm)
EBAY_8	37.4	25.60	12.40	2.23	0.50	2.00	0.27	0.43	0.19	1.23	0.20	402.00
EXT2_1	38.9	24.30	13.40	2.56	0.63	2.69	0.36	0.48	0.20	1.31	0.19	101.00
EBAY_9	42.3	23.20	10.70	2.24	0.56	2.25	0.27	0.38	0.16	0.98	0.14	130.00
EBAY_10	48.2	28.40	13.80	2.69	0.67	2.68	0.35	0.50	0.21	1.31	0.21	147.00
EBAY_17	83.2	33.30	16.00	3.16	0.79	2.99	0.42	0.59	0.25	1.50	0.23	140.00
EBAY_25	123.8	31.70	15.60	3.30	0.77	3.10	0.43	0.62	0.26	1.54	0.24	147.00
EBAY_33	163.1	30.40	14.60	3.09	0.74	2.68	0.40	0.56	0.23	1.44	0.22	137.00
EBAY_35	172.6	36.10	17.20	3.67	0.82	2.95	0.48	0.67	0.27	1.64	0.26	110.00
EBAY_37	311.6	29.50	14.00	2.93	0.68	3.00	0.38	0.56	0.24	1.41	0.22	157.00

Core number	Sample depth (feet below LSD)	Hafnium (ppm)	Tantalum (ppm)	Tungsten (ppm)	Scandium (ppm)	Chromium (ppm)	Cobalt (ppm)	Nickel (ppm)	Zinc (ppm)	Arsenic (ppm)	Antimony (ppm)	Gold (ppb)
EBAY_8	37.4	9.88	0.53	0.70	4.43	385.00	15.00	23.90	25.50	3.86	0.60	2.33
EXT2_1	38.9	2.76	0.41	1.10	7.44	93.40	7.32	40.60	39.20	5.31	0.57	2.66
EBAY_9	42.3	3.10	0.36	0.71	4.69	106.00	4.89	22.70	22.80	3.50	0.46	1.42
EBAY_10	48.2	3.87	0.65	2.11	6.25	133.00	6.68	29.60	33.10	4.45	0.61	1.42
EBAY_17	83.2	3.62	0.62	1.33	8.83	112.00	9.91	40.80	46.00	9.56	0.95	2.36
EBAY_25	123.8	4.13	0.59	1.29	8.29	95.30	9.26	43.20	43.60	6.34	0.89	2.95
EBAY_33	163.1	3.43	0.51	1.06	7.74	97.90	7.70	34.20	39.90	6.53	0.79	1.46
EBAY_35	172.6	2.98	0.60	1.10	10.20	110.00	11.30	57.20	54.20	13.60	0.75	2.69
EBAY_37	311.6	4.00	0.52	1.10	7.53	142.00	10.50	42.10	38.70	5.20	0.68	13.20

Table 22. Element concentrations determined by instrumental neutron activation by abbreviated count (INAA) analyses of core samples collected from the East Bay Bayside Monitoring Site (EBAY) borehole, San Lorenzo, California.—Continued

[**Abbreviations**: LSD, land surface datum; ppm, parts per million; ppb, parts per billion]

Core number	Sample depth (feet below LSD)	Lanthanum (ppm)	Cerium (ppm)	Neodymium (ppm)	Samarium (ppm)	Europium (ppm)	Gadolinium (ppm)	Terbium (ppm)	Holmium (ppm)	Thulium (ppm)	Ytterbium (ppm)	Lutetium (ppm)
EBAY_8	37.4	43.41	31.49	20.53	11.38	6.81	7.69	5.74	5.96	5.74	5.86	6.19
EXT2_1	38.9	41.16	29.89	22.19	13.06	8.54	10.35	7.55	6.62	6.04	6.24	5.88
EBAY_9	42.3	39.23	28.54	17.72	11.43	7.51	8.65	5.77	5.29	4.75	4.68	4.37
EBAY_10	48.2	47.27	34.93	22.85	13.72	9.01	10.31	7.43	6.98	6.50	6.24	6.44
EBAY_17	83.2	55.63	40.96	26.49	16.12	10.65	11.50	8.91	8.18	7.73	7.14	7.24
EBAY_25	123.8	50.80	38.99	25.83	16.84	10.41	11.92	9.09	8.62	7.82	7.33	7.49
EBAY_33	163.1	47.59	37.39	24.17	15.77	10.01	10.31	8.49	7.86	7.09	6.86	6.75
EBAY_35	172.6	59.16	44.40	28.48	18.72	11.14	11.35	10.26	9.33	8.28	7.81	7.96
EBAY_37	311.6	47.59	36.29	23.18	14.95	9.23	11.54	7.98	7.73	7.21	6.71	6.81

Table 23. Summary statistics for inductively coupled plasma-mass spectroscopy (ICP-MS) and instrumental neutron activation by abbreviated count (INAA) analyses and method comparison from core samples from the East Bay Bayside Monitoring Site (EBAY) borehole, San Lorenzo, California.

[**Abbreviations**: ppm, parts per million; R^2; coefficient of determination]

Element	ICP-MS (ppm)					INAA (ppm)					R^2	Correlation coefficient
	Maximum	Minimum	Mean	Median	Standard deviation	Maximum	Minimum	Mean	Median	Standard deviation		
Arsenic	21.1	6.4	10.0	7.4	5.7	13.6	4.5	7.6	6.4	3.4	0.94	0.97
Barium	736.0	639.0	693.2	708.5	39.5	678.0	493.0	596.5	605.5	65.9	0.80	0.89
Calcium	25,900	11,000	14,383	12,150	5,696.1	13,900	7,970	10,078	9,380	2,082.4	0.90	0.95
Cerium	46.0	30.9	39.8	39.3	5.6	44.4	34.9	38.8	38.2	3.4	0.80	0.89
Cobalt	14.6	8.6	11.3	11.3	2.2	11.3	6.7	9.2	9.6	1.7	0.93	0.96
Chromium	115.0	71.8	85.3	78.9	16.0	142.0	95.3	115.0	111.0	18.8	0.01	0.09
Cesium	3.4	2.2	2.7	2.8	0.4	3.0	1.7	2.4	2.4	0.4	0.93	0.96
Iron	33,100	20,900	26,300	25,850	39,44.1	25,500	16,500	21,716	21,900	3,068.8	0.85	0.92
Potassium	18,300	15,100	16,733	16,950	1,272.3	15,100	12,200	13,083	12,750	1,075.9	0.03	0.17
Lanthanum	25.1	16.5	21.6	21.9	3.1	59.2	47.3	51.3	49.2	5.0	0.67	0.82
Sodium	21,300	17,800	19,083	18,750	1,343.8	18,000	13,500	15,533	14,700	1,960.3	0.29	0.53
Nickel	68.3	40.1	49.2	45.9	10.4	57.2	29.6	41.2	41.5	9.4	0.90	0.95
Rubidium	68.1	53.8	61.4	62.4	6.3	59.1	42.7	52.6	55.0	6.5	0.71	0.84
Antimony	1.0	0.7	0.9	0.9	0.1	0.9	0.6	0.8	0.8	0.1	0.21	0.45
Scandium	13.3	8.5	10.5	10.2	1.6	10.2	6.3	8.1	8.0	1.3	0.97	0.99
Strontium	449.0	272.0	313.2	287.5	67.8	335.0	205.0	245.8	235.0	47.4	0.78	0.88
Thorium	7.2	4.7	6.0	6.1	0.9	6.4	4.3	5.3	5.3	0.8	0.80	0.89
Uranium	1.9	1.2	1.5	1.5	0.3	1.8	1.4	1.6	1.5	0.2	0.71	0.84
Zinc	72.4	49.9	56.2	53.9	8.2	54.2	33.1	42.6	41.8	7.2	0.85	0.92

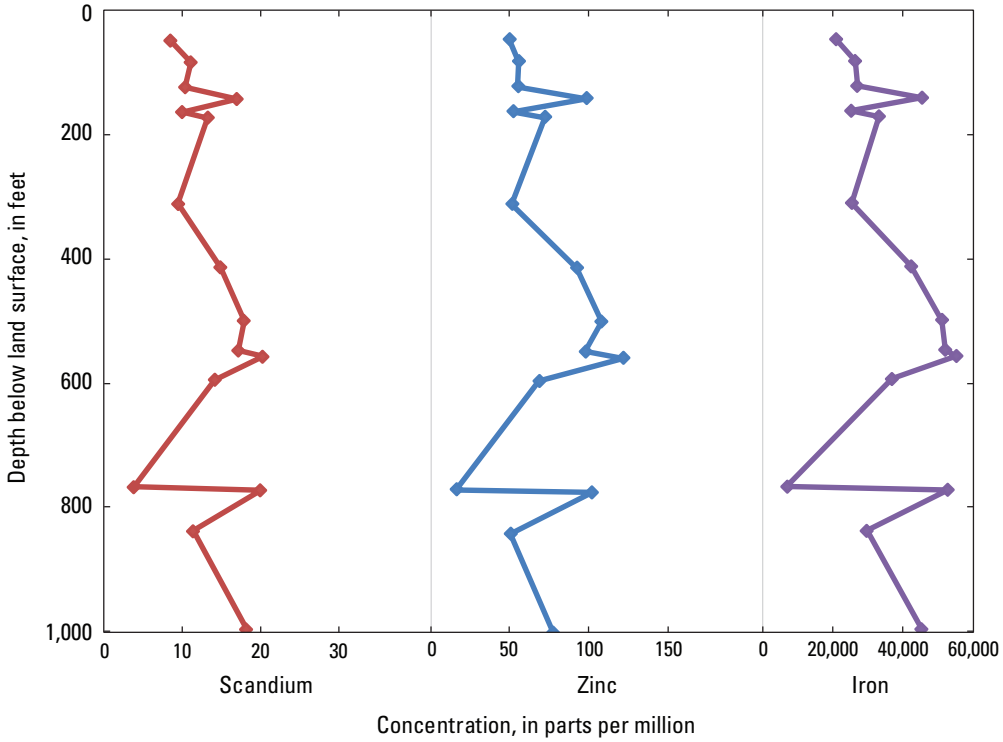

Figure 7. Example of elements, scandium, zinc, and iron, in core samples from the East Bay Bayside Monitoring Site (EBAY) borehole, showing similar patterns in concentration at depth below land surface in feet.

Sodium (with the exception of the decreasing relative concentrations between the depths of 767 and 772 ft) exhibited a pattern that mirrored that of calcium and phosphorus. There were relatively high concentrations of sodium at the same depths where calcium and phosphorus were in low concentrations. No depth-related patterns in concentration were apparent for 7 of the 37 elements, including silver, arsenic, barium, bismuth, potassium, molybdenum, and uranium.

Pore-Water Chemistry

The results from the analyses of 20 EBAY pore-water samples for pH, salinity, major ions, trace metals, stable isotopes of hydrogen and oxygen, DIC, and alkalinity are presented in *tables 24 through 27*. Comparisons between samples of the pore-water analyzed from the EBAY core and the groundwater analyzed from the EBAY piezometers showed similar concentrations for several constituents. Water-quality indicators, pH and alkalinity, are shown in *figure 8*; major ions and trace elements are shown in *figures 9* and *10*, respectively. In these figures, pore-water results are presented as points along a line, and groundwater results are represented as points corresponding to the center of the screened interval from which the sample was collected. Gaps in the graphical representation of pore-water represent missing data points. For example, pore-water samples were analyzed for bromide at depths of 655, 762, and 771 fbls, but calcium was not analyzed at 762 fbls and, therefore, has a missing datum point.

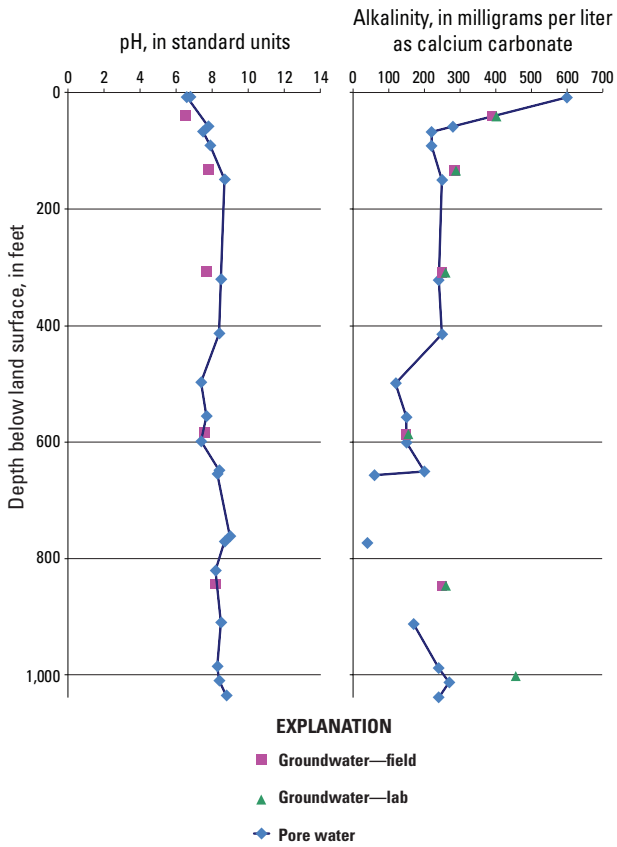

Figure 8. Graph showing cComparison of the water-quality indicators pH and alkalinity between pore water and groundwater from the East Bay Bayside Monitoring Site (EBAY) core and EBAY piezometers, respectively.

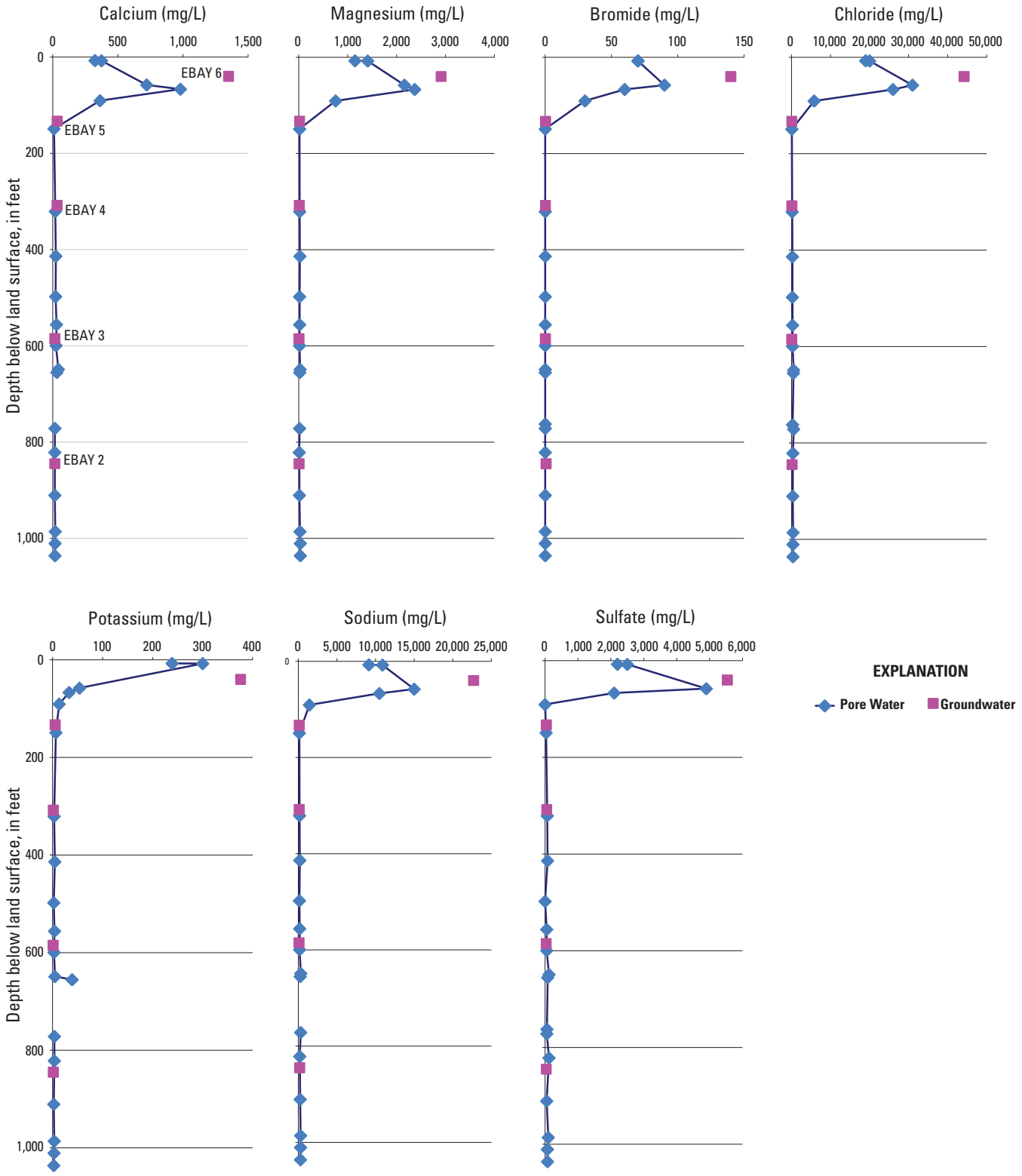

Figure 9. Graphs showing cComparison of selected major-ion concentrations between pore water and groundwater from the East Bay Bayside Monitoring Site (EBAY) core and EBAY piezometers, respectively.

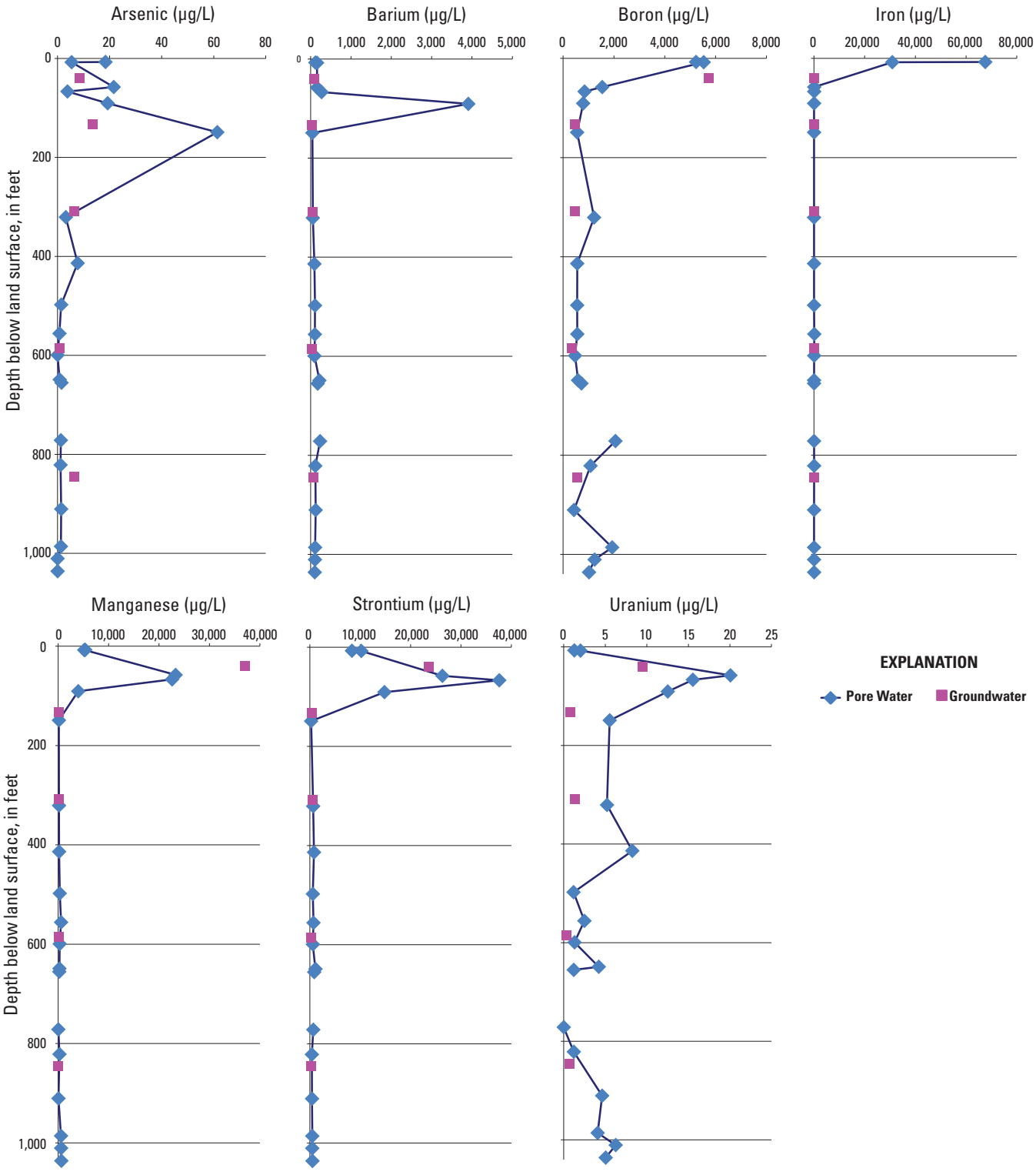

Figure 10. Graphs showing cComparison of selected trace-metal concentrations between pore water and groundwater from the East Bay Bayside Monitoring Site (EBAY) core and EBAY piezometers, respectively.

Sample depth and selected water-quality indicators (pH, salinity, and alkalinity), and dissolved inorganic carbon (DIC) in pore-water are presented in *table 24*. Values of pH ranged from 6.6 to 9.0 and had a mean and median of 8.1 and 8.35, respectively. The two shallowest of the 20 samples (within 8 ft of land surface) were circumneutral, having a pH of around 7, whereas the remaining 18 samples were more basic. Pore-water samples ranged in salinity from 0.05 to 4.4 percent and showed a marked drop in salinity below 67 fbls. Alkalinity, as calculated from DIC, ranged from 40 to 600 mg/L as calcium carbonate and had an average concentration of about 220 mg/L. DIC was detected in all of the pore-water samples. Concentrations of DIC ranged from about 9 to 215 mg/L and averaged about 57 mg/L. Comparison of pH and alkalinity results between groundwater and pore-water from the EBAY piezometers and cores showed similar patterns with depth (*fig. 8*).

Pore-water samples were analyzed for 12 major ions (*table 25*). Of the major ions, four cations (calcium, magnesium, potassium, and sodium) and three anions (bromine, chloride, and iodine) were detected at all depths sampled. Sulfate was detected in 90 percent of the samples and had concentrations ranging from 33 to 4900 mg/L. Nitrate was detected in 50 percent of the samples and had concentrations ranging from about 1 to 3 mg/L. Bromide was detected only in samples collected within 91 ft of land surface, and concentrations ranged from 30 to 90 mg/L. Nitrite was detected only in the sample collected from 414 fbls. Orthophosphate was not detected in any of the samples.

Seven of these ions (calcium, magnesium, bromide, chloride, potassium, sodium, and sulfate) were analyzed in both pore-water and groundwater (*fig. 9*). Groundwater and pore-water sampled from EBAY piezometers and cores, respectively, showed similar patterns in concentration with increasing depth for these seven constituents. Bromide in pore-water was not detected deeper than 91 fbls, but was detected in all piezometer depths sampled at Bayside.

Pore-water samples were analyzed for eight trace metals (*table 26*). In all samples analyzed, the trace metals barium, boron, iron, manganese, and strontium were detected and ranged in concentration from about 45 to 3,910 µg/L, 429 to 5,530 µg/L, 16 to 67,600 µg/L, 26 to 23,300 µg/L, and 240 to 37,600 µg/L, respectively. Arsenic was detected in 84 percent of the samples and had concentrations ranging from 0.73 to 61.4 µg/L. Uranium was detected in 95 percent of the samples and had concentrations ranging from 1.18 to 20.06 µg/L. Lead was not detected in any of the samples. As with major ions, the highest trace metal concentrations were generally within 91 ft of land surface.

Pore-water and groundwater samples from EBAY core and piezometers, respectively, were compared for eight of the same trace elements (*tables 9* and *26*), and the results generally agree (*fig. 10*). Results showed higher concentrations at shallower depths in both groundwater and pore-water samples. Lead was not detected in either pore-water or groundwater samples. Iron was detected in only 69 percent of the groundwater samples, whereas it was detected in all of the pore-water samples; concentrations of iron in pore-water samples were 3 to 10 times higher than in groundwater samples.

The isotopic ratios of oxygen and hydrogen in water can be used as tracers of hydrologic processes. These ratios aid in interpretation of the source of groundwater recharge because they reflect the altitude, latitude, and temperature of precipitation as well as the extent of evaporation of the water (Clark and Fritz, 1997; Kendall and McDonnell, 1998). Groundwater samples collected from EBAY piezometers showed similar isotopic ratios for hydrogen and oxygen to the pore-water samples collected from the EBAY core at similar depths (*tables 10* and *27*; *fig. 5*). The one exception to this was a groundwater sample collected from the EBAY3 piezometer situated at a depth of 585 fbls, which showed an isotopic ratio of hydrogen and oxygen lighter than its pore-water counterparts at similar depths.

Table 24. Summary of water quality indicators, alkalinity, and dissolved inorganic carbon for pore water extracted from selected East Bay Bayside Monitoring Site (EBAY) core.

[The five digit number in parentheses below the constituent name is the U.S. Geological Survey (USGS) parameter code used to uniquely identify a specific constituent or property. **Abbreviations**: $CaCO_3$, calcium carbonate; ft, feet; LSD, land surface datum; mg/L, milligrams per liter; NaCl, sodium chloride; —, not collected]

Core number	Sample depth (ft below LSD)	Water-quality indicators			Dissolved inorganic carbon (mg/L) (00691)
		pH (standard units) (00400)	Salinity (percent NaCl)	Alkalinity (mg/L as $CaCO_3$)	
EBAY_2	7.2	6.8	2.94	—	—
EBAY_2	7.6	6.6	3.2	600	215
EBAY_12	57.8	7.8	4.4	280	70.5
EBAY_14	66.8	7.5	3.5	220	57.0
EBAY_19	90.6	7.9	0.91	220	54.1
EBAY_30	149.1	8.7	0.05	250	60.0
EBAY_39	320.7	8.5	0.07	240	56.7
EBAY_41	413.6	8.4	0.1	250	59.0
EBAY_44	497.6	7.4	0.07	120	30.3
EBAY_48	555.8	7.7	0.14	150	37.9
EBAY_51	599.4	7.4	0.14	150	37.8
EBAY_54	648.9	8.4	0.17	200	48.4
EBAY_56	655.3	8.3	0.13	60	14.2
EBAY_58	762.3	9.0	0.17	—	—
EBAY_60	771.5	8.7	0.14	40	8.9
EBAY_62	821.4	8.2	0.11	—	—
EBAY_66	910.5	8.5	0.13	170	41.7
EBAY_68	986.0	8.3	0.19	240	58.4
EBAY_71	1,010.6	8.4	0.19	270	63.7
EBAY_74	1,036.1	8.8	0.15	240	57.4

Table 25. Concentrations of major ions in pore water extracted from selected East Bay Bayside Monitoring Site (EBAY) core.

[The five digit number in parentheses below the constituent name is the U.S. Geological Survey parameter code used to uniquely identify a specific constituent or property. **Abbreviations**: E, estimated value; ft, feet; LSD, land surface datum; mg/L, milligrams per liter; N, nitrogen; <, less than minimum detection limit; —, not collected]

Core number	Sample depth (ft below LSD)	Major ions											
		Calcium (mg/L) (00915)	Magnesium (mg/L) (00925)	Potassium (mg/L) (00935)	Sodium (mg/L) (00930)	Bromide (mg/L) (71870)	Bromine (mg/L) (71871)	Chloride (mg/L) (00940)	Iodine (mg/L) (71866)	Sulfate (mg/L) (00945)	Nitrate (mg/L as N) (00618)	Nitrite (mg/L as N) (00613)	Ortho-phosphate (mg/L as phosphorous) (00671)
EBAY_2	7.2	324	1,150	239	9,140	70	74	19,000	5.94	2,200	<6	<3	<50
EBAY_2	7.6	374	1,410	300	10,900	70	88	20,000	8.06	2,500	E2	<3	<50
EBAY_12	57.8	721	2,160	53.9	15,000	90	110	31,000	E0.740	4,900	<6	<3	<50
EBAY_14	66.8	980	2,370	33.1	10,500	60	91	26,000	E0.807	2,100	<6	<3	<50
EBAY_19	90.6	363	753	13.2	1,440	30	24	5,800	0.811	<300	<6	<3	<50
EBAY_30	149.1	8.96	17.2	6.69	138	<3	0.27	81	0.248	33	1.1	<0.3	<5
EBAY_39	320.7	19.2	19.6	3.14	167	<3	0.56	170	0.184	67	1.8	<0.3	<5
EBAY_41	413.6	23.1	24.3	4.55	203	<15	0.79	230	0.322	E77	<3	1.7	<25
EBAY_44	497.6	22.0	17.5	2.47	151	<15	0.75	220	0.373	<150	E2	<1.5	<25
EBAY_48	555.8	28.4	17.8	3.91	181	<15	0.84	270	0.409	E50	<3	<1.5	<25
EBAY_51	599.4	24.7	15.5	3.03	170	<15	0.74	260	0.336	E50	<3	<1.5	<25
EBAY_54	648.9	42.4	28.8	4.65	328	<15	1.7	540	0.554	E120	E1	<1.5	<25
EBAY_56	655.3	31.3	21.0	39.1	249	<15	1.6	480	E0.068	E80	E2	<1.5	<25
EBAY_58	762.3	—	—	—	—	<15	—	270	—	E57	3	<1.5	<25
EBAY_60	771.5	16.6	17.3	3.71	312	<15	2.1	540	E0.051	E53	<3	<1.5	<25
EBAY_62	821.4	15.4	10.7	3.64	193	<15	0.84	350	0.596	E120	E2	<1.5	<25
EBAY_66	910.5	15.8	14.2	2.45	246	<15	1.0	310	0.295	E50	E1	<1.5	<25
EBAY_68	986.0	18.6	25.6	3.33	309	<15	1.3	400	0.805	E98	<3	<1.5	<25
EBAY_71	1,010.6	17.3	31.71	3.03	300	<15	1.3	370	1.26	E72	<3	<1.5	<25
EBAY_74	1,036.1	16.7	33.0	2.45	287	<15	1.3	370	1.07	E75	E1	<1.5	<25

Table 26. Trace metals in pore water extracted from selected East Bay Bayside Monitoring Site (EBAY) core and analyzed by the U.S. Geological Survey (USGS) National Water Quality Laboratory, Denver, Colorado.

[The five digit number in parentheses below the constituent name is the USGS parameter code used to uniquely identify a specific constituent or property. **Abbreviations**: E, estimated value; LSD, land surface datum; µg/L, microgram per liter; <, less than minimum detection limit; —, not collected]

Core number	Sample depth (feet below LSD)	Trace metals							
		Arsenic (µg/L) (01000)	Barium (µg/L) (01005)	Boron (µg/L) (01020)	Iron (µg/L) (01046)	Lead (µg/L) (01049)	Manganese (µg/L) (01056)	Strontium (µg/L) (01080)	Uranium (µg/L) (22703)
EBAY_2	7.2	18.4	119	E5,230	67,600	<1.6	5,360	8,340	1.27
EBAY_2	7.6	5.4	160	E5,530	30,900	<1.6	5,160	10,200	2.01
EBAY_12	57.8	21.6	160	1,540	91.3	<2.4	23,300	26,300	20.06
EBAY_14	66.8	3.8	273	845	75.5	<2	22,600	37,600	15.54
EBAY_19	90.6	19.2	3,910	791	38.5	<0.8	3,980	14,800	12.52
EBAY_30	149.1	61.4	45	552	E36.5	<1.6	140	240	5.53
EBAY_39	320.7	3.2	56	1,220	E17.5	<0.8	160	648	5.21
EBAY_41	413.6	7.7	96	557	21.7	<0.8	183	817	8.25
EBAY_44	497.6	1.4	111	555	E15.9	<0.8	306	583	1.18
EBAY_48	555.8	E0.73	107	560	128	<0.8	572	710	2.48
EBAY_51	599.4	<1.2	97	470	62.3	<0.8	292	587	1.30
EBAY_54	648.9	E0.80	219	589	21.2	<0.8	244	1,100	4.21
EBAY_56	655.3	E1.5	177	722	41.1	<1.6	213	850	1.20
EBAY_58	762.3	—	—	—	—	—	—	—	—
EBAY_60	771.5	E1.25	235	2,060	E32.8	<1.6	26.3	666	<0.8
EBAY_62	821.4	E1.15	117	1,080	58.8	<0.8	254	387	1.21
EBAY_66	910.5	E1.39	127	429	E27.5	<1.6	54.1	420	4.62
EBAY_68	986.0	E1.28	113	1,930	E31.9	<1.6	557	472	4.08
EBAY_71	1,010.6	<2.4	109	1,240	E28.7	<1.6	583	463	6.25
EBAY_74	1,036.1	<2.4	104	1,020	53.5	<1.6	619	506	5.05

Table 27. Stable isotope ratios of hydrogen and oxygen in pore water extracted from selected East Bay Bayside Monitoring Site (EBAY) core and analyzed by U.S. Geological Survey-National Research Program (USGS-NRP), Stable Isotope Laboratory, Reston, Virginia.

[The five digit number in parentheses below the constituent name is the U.S. Geological Survey parameter code used to uniquely identify a specific constituent or property. Stable isotope ratios are reported in the standard delta notation (δ), the ratio of a heavier isotope to the more common lighter isotope of that element, relative to a standard reference material. **Abbreviations**: ft, feet; LSD, land surface datum; H, hydrogen; O, oxygen]

Core number	Sample depth (ft below LSD)	Stable isotopes	
		$\delta^{2}H$ of water (per mil) (82082)	$\delta^{18}O$ of water (per mil) (82085)
EBAY_2	7.2	-29.3	-5.16
EBAY_2	7.6	-28.2	-3.7
EBAY_12	57.8	-21.6	-2.41
EBAY_14	66.8	-27.2	-3.35
EBAY_19	90.6	-40.7	-5.88
EBAY_30	149.1	-39.2	-5.94
EBAY_39	320.7	-47.1	-6.96
EBAY_41	413.6	-51.9	-7.13
EBAY_44	497.6	-49.3	-7.27
EBAY_48	555.8	-49.8	-7.18
EBAY_51	599.4	-50.2	-7.33
EBAY_54	648.9	-53.7	-7.48
EBAY_56	655.3	-50.3	-7.14
EBAY_58	762.3	-52	-7.18
EBAY_60	771.5	-53.2	-7.43
EBAY_62	821.4	-51.6	-7.57
EBAY_66	910.5	-53.1	-7.75
EBAY_68	986.0	-51.5	-7.4
EBAY_71	1,010.6	-49.7	-7.28
EBAY_74	1,036.1	-48.5	-7.22

Summary

Aquifer-system deformation associated with groundwater-level changes was investigated cooperatively by the USGS and the EBMUD at the BGP, in San Lorenzo, California, where managed aquifer storage and recovery is planned. Water from this source can be used to help meet short-term needs arising from drought or seismic and other water-supply emergencies, or imported water can be injected, stored, and later recovered for public supply. This investigation focused on collecting and analyzing subsurface data obtained during and after drilling at four sites at and near the BGP.

Fourteen piezometers and two extensometers were installed among six boreholes at the four sites. Drill cuttings were collected and described, and a suite of borehole geophysical logs was made in each borehole. At the Bayside site, next to the BGP, samples from selected sections of core were analyzed to determine pore-water chemistry, vertical hydraulic conductivity, physical and mechanical properties, depositional environment, age determinations, and mineral composition. Groundwater samples were collected from all 14 piezometers for water-quality analyses. Groundwater-level and aquifer-system-compaction measurements were made at the Bayside site, and slug tests were performed at the Bayside piezometers and nine pre-existing sites to determine aquifer characteristics.

The lithologic and geophysical logs compiled for this study indicated unconsolidated to partially consolidated continental and marine alluvial deposits consisting of mostly silt and clay. Shear wave velocities in the upper 100 ft indicated a stiff soil. A laterally extensive zone, consisting of three coarse sand and gravel beds 98 ft thick, in total, between 508 and 650 fbls, known as the Deep aquifer, is the focus of this ASR project.

Groundwater levels monitored in the piezometers at the EBAY site exhibited diurnal fluctuations. Groundwater levels measured in piezometer EBAY3, screened within the Deep aquifer, exhibited the greatest diurnal fluctuation. Groundwater levels measured in piezometers EBAY3, EBAY4, and EBAY5 exhibited seasonal fluctuations where groundwater levels were higher in the winter and spring and lower in the summer and fall. Seasonal fluctuations were not apparent in groundwater levels measured in EBAY2 and EBAY6.

Aquifer-system compaction and expansion in the shallow and deep extensometers corresponded to groundwater-level drawdown and recovery, respectively. The connection between compaction and expansion of the aquifer system and drawdown and recovery of groundwater levels was demonstrated by diurnal and seasonal fluctuations in the extensometer data. In addition, the magnitude of the values of compaction and expansion between the shallow and deep extensometers was similar, indicating that the deformation was occurring above the shallow extensometer.

Slug test estimates of hydraulic conductivity of the hydrogeologic units next to the screened zones, performed at 14 sites, ranged from 0.34 to 120 ft/d. A hydraulic conductivity of 32 ft/d, estimated at EBAY3, was the highest conductivity estimated from the piezometers at the EBAY site.

Groundwater-quality results summarized here focus on the noteworthy attributes associated with the Deep aquifer. Groundwater samples collected from piezometer EBAY3, situated in the Deep aquifer, exhibited the lowest concentrations of water-quality indicators for specific conductance and alkalinity and had a non-detect for dissolved oxygen. Nutrient concentrations in the Deep aquifer were the lowest among the EBAY piezometers for nitrogen (non-detect) and orthophosphate as phosphorous. In addition, EBAY3 stood out as the only piezometer with a detection for nitrate plus nitrite. Major and minor ion concentrations were the lowest in groundwater samples from EBAY3 for calcium, magnesium, potassium, bromide, chloride, sulfate, and total dissolved solids. In addition, groundwater samples from EBAY3 exhibited the lowest trace-metal concentrations of aluminum, arsenic, barium, cadmium, copper, lithium, strontium, and uranium. Stable-isotope values from groundwater samples from EBAY3 exhibited a low ratio. Tritium values were generally elevated compared to the remaining samples.

Analysis of core samples collected for the Bayside site revealed sediments are normally consolidated below a depth of about 135 ft. They showed greater elastic specific storage and less inelastic specific storage than samples collected from the San Joaquin Valley. Mineralogical analysis of two core samples within the Deep aquifer zone showed an abundance of total clay consisting mainly of smectite and illite. Elemental analysis showed relatively high concentrations of major and trace elements within the Deep aquifer zone. The analysis of pore-water chemistry demonstrated a decrease in salinity and ion concentration below 90 ft. Results from the analysis of the pore-water chemistry also revealed elevated concentrations of iron and magnesium in the Deep aquifer zone. The data derived from the extensive analyses can be used by EBMUD and other agencies to evaluate the chemical and mechanical responses of aquifers underlying the East Bay Plain to the injection and recovery of imported water from the Sierra Nevada of California.

References Cited

Aitken, M.J., 1998, An introduction to optical dating: The dating of Quaternary sediments by the use of photon-stimulated luminescence: New York, Oxford University Press, 267 p.

American Society for Testing and Materials, 2003, Standard test methods for measurement of hydraulic conductivity of saturated porous materials using a flexible wall permeameter, D5084–03: West Conshohocken, Penn., ASTM International, DOI: 10.1520/D5084–00R03, *www.astm.org*.

Anderson, C.W., 2005, Turbidity (version 2.1): U.S. Geological Survey Techniques of Water-Resources Investigations, book 9, chap. A6., section 6.7, accessed September 30, 2009, *http://pubs.water.usgs.gov/twri9A6*/.

Arnal, R.E., Quinterno, P.J., Conomos, T.J., and Gram, R., 1980, Trends in the distribution of recent foraminifera in San Francisco Bay, *in* Sliter, W.V., ed., Studies in marine micropaleontology and paleoecology. A memorial volume to Orville L. Bandy: Cushman Foundation for Foraminiferal Research Special Publication 19, p. 17–39.

Atwater, B.G., Ross, B.E., Wehmiller, J.F., 1981, Stratigraphy of the late Quaternary estuarine deposits and amino acid stereochemistry of oyster shells beneath San Francisco Bay, California: Quaternary Research, v. 16, p. 181–200, *http://dx.doi.org/10.1016/0033-5894(81)90044-2*.

Battarbee, R.A., 1986, Diatom analysis, in Berglund, B.E., ed., Handbook of holocene palaeoecology and palaeohydrology: New York, John Wiley & Sons, p. 527–570.

Bennett, M.J., Sneed, M., Noce, T.E., and Tinsley, J. III, 2009, Cone penetration test and soil boring at the Bayside Groundwater Project Site in San Lorenzo, Alameda County, California: U.S. Geological Survey Open-File Report 2009–1050, 30 p., *http://pubs.er.usgs.gov/publication/ofr20091050*.

Brocher, T.M., Borchers J.W., Sneed, M., and Tinsley, J.C., 2007, New 300-m deep vs suspension log helps characterize seismic hazards posed by the San Leandro Basin, East Bay, Northern California: Seismological Research Letters, v. 78, no. 2, p. 270–271.

Brown and Caldwell, Inc., 1986, Evaluation of groundwater resources and proposed design for emergency water supply wells: Pleasant Hill, California, [variously paged].

Budahn, J.R., and Wandless, G.A., 2002, Instrumental neutron activation by abbreviated count: Chapter Y, U.S. Geological Survey Open-File Report 02–233–Y, *http://pubs.usgs.gov/of/2002/ofr-02-0223/Y15INAA-SHORT_M.pdf*.

Butler, J.J., Jr., and Garnett, E.J., 2000, Simple procedures for analysis of slug tests in formations of high hydraulic conductivity using spreadsheet and scientific graphics software: Kansas Geological Survey Open-File Report 2000–40, 21 p., *http://www.kgs.ku.edu/Hydro/Publications/OFR00_40/index.html*.

Casagrande, A., 1936, The determination of the pre-consolidation load and its practical significance *in* A. Casagrande, ed., Proceeding of the 1st International Soil Mechanics and Foundation Engineering Conference, Cambridge, Mass., June 22–26, 1936: Harvard University, Cambridge, Mass., Graduate School of Engineering, v. 3, p. 60–64.

Castagna, J.P, Batzle, M.L., and Eastwood, R.L., 1985, Relationships between compressional-wave and shear-wave velocities in clastic silicate rocks: Geophysics, v. 50, no. 4, p. 571–581, *http://dx.doi.org/10.1190/1.1441933*.

Catchings, R.D., Borchers, J.W., Goldman, M.R., Gandhok, G., Ponce, D.A., and Steedman, C.E., 2006, Subsurface structure of the East Bay Plain ground-water basin: San Francisco Bay to the Hayward fault, Alameda County, California: U.S. Geological Survey Open-File Report 2006–1084, 68 p., *http://pubs.er.usgs.gov/publication/ofr20061084*.

CH2M-Hill, Inc., 2000, Regional hydrogeologic investigation of the south East Bay Plain, Oakland, Calif., [variously paged].

Clark, I.D., and Fritz, P., 1997, Environmental isotopes in hydrogeology: Boca Raton, CRC Press, 328 p.

Connor, C.L., 1975, Holocene sedimentation history of Richardson Bay, California: Stanford, Calif., Stanford University, M.S. thesis, 112 p.

Coplen, T.B., Wildman, J.D., and Chen, J., 1991, Improvements in the gaseous hydrogen-water equilibraton technique for hydrogen isotope ratio analysis: Analytical Chemistry, v. 63, no. 9, p. 910–912.

Cumming, B.F., Wilson, S.E., Hall, R.J., and Smol, J.P., 1995, Diatoms from British Columbia (Canada) lakes and their relationship to salinity, nutrients and other limnological variables: Bibliotheca Diatomologica, v. 31, 207 p.

Fugro West, Inc., 1998, East Bay injection/extraction groundwater pilot project well construction and performance testing Oro Loma Phase III injection/extraction demonstration well—Summary of operations report: Ventura, Calif., Fugro West, Inc., [variously paged].

Fugro West, Inc., 1999, East Bay injection/extraction pilot project, demonstration test operations report, [variously paged].

Galbraith, R.F., Roberts, R.G., Laslett, G.M., Yoshida, H., and Olley, J.M., 1999, Optical dating of single and multiple grains of quartz from Jinmium rock shelter, Northern Australia: Part I, Experimental design and statistical models: Archaeometry, v. 41, no. 2, p. 339–364, *http://dx.doi.org/10.1111/j.1475-4754.1999.tb00987.x*.

Galloway, D.L., Jones, D.R., and Ingebritsen, S.E., 1999, Land subsidence in the United States: U.S. Geological Survey Circular 1182, 175 p., *http://pubs.er.usgs.gov/publication/cir1182*.

Garbarino, J.R., Kanagy, L.K., and Cree, M.E., 2006, Determination of elements in natural-water, biota, sediment, and soil samples using collision/reaction cell inductively coupled plasma-mass spectrometry: U.S. Geological Survey Techniques and Methods, book 5, sec. B, chap. 1, 87 p., *http://pubs.er.usgs.gov/publication/tm5B1*.

Gasse, F., 1986, East African diatoms: Taxonomy, ecological distribution: Bibliotheca Diatomologica, v. 11, 201 p.

Graymer, R.W., 2000, Geologic map and map database of the Oakland metropolitan area, Alameda, Contra Costa, and San Francisco Counties, California: U.S. Geological Survey, Misc. Field Studies Map MF–2342, 1 sheet, scale 1:50,000, *http://pubs.usgs.gov/mf/2000/2342*.

Halford, K.J., and Kuniansky, E.L., 2002, Documentation of spreadsheets for the analysis of aquifer-test and slug-test data: U.S. Geological Survey Open-File Report 2002–197, 51 p., *http://pubs.er.usgs.gov/publication/ofr02197*.

Hille, D., 1980, Environmental soil physics: San Diego, California, Academic Press, 413 p.

Howard, A.D., 1979, Geologic history of middle California: California Natural History Guides, v. 43, 113 p.

Izbicki, J.A., Borchers, J.W., Leighton, D.A., Kulongoski, Justin, Fields, Latoya, Galloway, D.L., and Michel, R.L., 2003, Hydrogeology and geochemistry of aquifers underlying the San Lorenzo and San Leandro areas of the East Bay Plain, Alameda County, California: U.S. Geological Survey Water-Resources Investigations Report 2002–4259, 71 p., *http://pubs.er.usgs.gov/publication/wri024259*.

Jennings, A.E., and Nelson, A.R., 1992, Foraminiferal assemblage zones in Oregon tidal marshes—Relation to marsh floral zones and sea level: Journal of Foraminiferal Research, v. 22, no. 1, p. 13–29, *http://dx.doi.org/10.2113/gsjfr.22.1.13*.

Kendall, C., and McDonnell, J.J., eds., 1998, Isotope tracers in catchment hydrology: Amsterdam, Elsevier Science, 839 p.

Koltermann, C.E., and Gorelick, S.M., 1992, Paleoclimatic signature in terrestrial flood deposits: Science, v. 256, no. 5065, p. 1775–1782, *http://dx.doi.org/10.1126/science.256.5065.1775*.

Koterba, M.T., Wilde, F.D., and Lapham, W.W., 1995, Groundwater data-collection protocols and procedures for the National Water-Quality Assessment Program: Collection and documentation of water-quality samples and related data: U.S. Geological Survey Open-File Report 95–399, 114 p., *http://pubs.er.usgs.gov/publication/ofr95399*.

Krammer, Kurt, 1997a, Die cymbelloiden Diatomeen. Eine Monographie der weltweit bekannten Taxa, Teil 1, Allgemeines und Encyonema part: Stuttgart, Germany, J. Cramer, Bibliotheca Diatomologica Band 36, 382 p.

Krammer, Kurt, 1997b, Die cymbelloiden Diatomeen. Eine Monographie der weltweit bekannten Taxa, Teil 2, Encyonema part, Encyonopsis und Cymbellopsis: Stuttgart, Germany, J. Cramer, Bibliotheca Diatomologica Band 37, 469 p.

Krammer, Kurt, 2000, The genus Pinnularia, v. 1 of Lange-Bertalot, Horst, ed., Diatoms of Europe: Diatoms of the European inland waters and comparable habitats: Germany, A.R.G. Ganter Verlag K.G., 703 p.

Krammer, Kurt, 2002, Cymbella, v. 3 of Lange-Bertalot, Horst, ed., Diatoms of Europe: Diatoms of the European inland waters and comparable habitats: Germany, A.R.G. Ganter Verlag K.G., 514 p.

Krammer, Kurt and Lange-Bertalot, Horst, 1986, Bacillariophyceae, 1, Teil: Naviculaceae, *in* Ettl, H., Gerloff, J., Heynig, H., and Mollenhauer, D., eds., Süsswasser flora von Mitteleuropa, Band 2/1: New York, Gustav Fischer Verlag, 876 p.

Krammer, Kurt and Lange-Bertalot, Horst, 1988, Bacillariophyceae, 2, Teil: Bacillariaceae, Epithemiaceae, Surirellaceae, *in* Ettl, H., Gerloff, J., Heynig, H., and Mollenhauer, D., eds., Süsswasserflora von Mitteleuropa, Band 2/2: Jena, Germany, VEB Gustav Fischer Verlag, 596 p.

Krammer, Kurt and Lange-Bertalot, Horst, 1991a, Bacillariophyceae, 3, Teil: Centrales, Fragilariaceae, Eunotiaceae, *in* Ettl, H., Gerloff, J., Heynig, H., and Mollenhauer, D., eds., Süsswasserflora von Mitteleuropa, Band 2/3: Stuttgart, Germany, Gustav Fischer Verlag, 576 p.

Krammer, Kurt and Lange-Bertalot, Horst, 1991b, Bacillariophyceae, 4, Teil: Achnanthaceae, Kritische Ergänzungen zu Navicula (Lineolatae) und Gomphonema, Gesamtliteraturverzeichnis Teil 1–4, *in* Ettl, H., Gärtner, G., Gerloff, J., Heynig, H., and Mollenhauer, D., eds., Süsswasserflora von Mitteleuropa, Band 2/4: Stuttgart, Germany, Gustav Fischer Verlag, 437 p.

Lambe, W.T. and Whitman, R.V., 1969, Soil mechanics (3d ed.), John Wiley and Sons, 553 p.

Lane. E.W., 1947, Report on the subcommittee on sediment terminology: Eos Transactions, American Geophysical Union, v. 28, no. 6, p. 936–938, *http://onlinelibrary.wiley.com/doi/10.1029/TR028i006p00936/abstract*.

Lange-Bertalot, Horst, 2001, Diatoms of Europe . Diatoms of the European inland waters and comparable habitats, v. 2, Navicula sensu stricto, 10 Genera Separated from Navicula sensu lato: Frustulia: Ruggell, Liechenstein, A.R.G. Gantner Verlag K.G., 526 p.

Lange-Bertalot, Horst, and Krammer, Kurt, 1987, Bacillariaceae, Epithemiaceae, Surirellaceae: Bibliotheca Diatomologica v. 15: Stuttgart, Germany, J. Cramer, 289 p.

Lange-Bertalot, Horst, and Krammer, Kurt, 1989, Achnanthes eine Monographie der Gattungen. Bibliotheca Diatomologica v. 18: Stuttgart, Germany, J. Cramer, 393 p.

Lepper, K., 2001, Development of an objective dose distribution analysis method for luminescence dating and pilot studies for planetary applications: Stillwater, Okla., Oklahoma State University, Ph.D. dissertation, 288 p.

Lepper, K., and McKeever, S.W.S., 2002, An objective methodology for dose distribution analysis: Radiation Protection Dosimetry, v. 101, no. 1–4, p. 349–352.

Locke, J.L., 1971, Sedimentation and foraminiferal aspects of the recent sediments of San Pablo Bay: San Jose, Calif., San Jose State College, M.S. thesis, 100 p.

Lowe, R.L., 1974, Environmental requirements and pollution tolerance of freshwater diatoms: U.S. Environmental Protection Agency Report EPA–670/4–74–005, National Environmental Research Center, Cincinnati, Ohio, 334 p.

Manheim, F.T., Brooks, E.G., and Winters, W.J., 1994, Description of a hydraulic sediment squeezer: U.S. Geological Survey Open-File Report 94–584, 39 p., *http://pubs.er.usgs.gov/publication/ofr94584*.

Marlow, M.S., Jachens, R.C., Hart, P.e., Carlson, P.R., Anima, R.J., and Childs, J.R., 1999, Development of San Leandro synform and neotectonics of the San Francisco Bay block, California: Marine and Petroleum Geology, v. 16, no. 5, p. 431–442, *http://dx.doi.org/10.1016/S0264-8172(99)00002-1*.

Maslonkowski, D. P., 1984, Groundwater in the San Leandro and San Lorenzo alluvial cones of the East Bay plain of Alameda County: Alameda County Flood Control and Water Conservation District, 31 p.

Maslonkowski, D.P., 1988, Hydrogeology of the San Leandro and San Lorenzo alluvial cones of the bay plain groundwater basin, Alameda County, California: San Jose, Calif., San Jose State College, M.S. thesis, 143 p.

McCormick, J.M., Severin, K.P., and Lipps, J.H., 1994, Summer and winter distribution of foraminifera in Tomales Bay, northern California: Cushman Foundation for Foraminiferal Research Special Publication, v. 32, p. 69–101.

McGann, M., 2007, Foraminiferida *in* Carlton, J.T., ed., The Light and Smith Manual (4th ed.): Intertidal invertebrates from central California to Oregon: Berkeley and Los Angeles, Calif., University of California Press, p. 46–69.

McGann, M., Sloan, Doris, and Wan, Elmira, 2002, Biostratigraphy beneath central San Francisco Bay along the San Francisco–Oakland Bay Bridge transect, *in* Parsons, Tom, eds., Crustal Structure of the Coastal and Marine San Francisco Bay Region, California: U.S. Geological Survey Professional Paper 1658, p. 11–28, *http://pubs.er.usgs.gov/publication/pp1658*.

Means, K.D., 1965, Sediments and foraminifera of Richardson Bay, California: Los Angeles, Calif., University of Southern California, M.A. thesis, 80 p.

Michel, R.M., 1989, Tritium deposition in the continental United States, 1953–83: U.S. Geological Survey Water-Resources Investigations Report 89–4072, 46 p., *http://pubs.er.usgs.gov/publication/wri894072*.

Muir, K.S., 1997, Ground water quality in the East Bay Plain: Hayward, Calif., Alameda County Department of Public Works, 7 p.

Murray, A.S., Olley, J.M., and Caitcheon, G.G., 1995, Measurement of equivalent doses in quartz from contemporary water-lain sediments using optically stimulated luminescence: Quaternary Science Reviews, v. 14, no. 4, p. 365–371, *http://dx.doi.org/10.1016/0277-3791(95)00030-5*.

Murray, J.W., 1973, Distribution and ecology of living benthic foraminiferids: NewYork, Crane, Russak and Company, 274 p.

Nesse, W.D., 2000, Introduction to mineralogy: New York, Oxford University Press Inc.

Nightingale, H.I., and Bianchi, W.C., 1977, Ground-water turbidity resulting from artificial recharge: Groundwater, v. 15, no. 2, p. 146–152, *http://dx.doi.org/10.1111/j.1745-6584.1977.tb03159.x*.

Olley, Jon, Caitcheon, Gary, and Murray, Andrew, 1998, The distribution of apparent dose as determined by optically stimulated luminescence in small aliquots of fluvial quartz: Implications for dating young sediments: Quaternary Science Review, v. 17, no. 11, p. 1033–1040, *http://dx.doi.org/10.1016/S0277-3791(97)00090-5*.

Parker, F.L., and Athearn, W.D., 1959, Ecology of marsh foraminifera in Poponesset Bay, Massachusetts: Journal of Paleontology, v. 33, no. 2, p. 333–343, *http://www.jstor.org/stable/1300762*.

Pavelko, M.T., 2000, Ground-water and aquifer-system-compaction data from the Lorenzi Site, Las Vegas, Nevada, 1994–99: U.S. Geological Survey Open-File Report 2000–362, 26 p., *http://pubs.er.usgs.gov/publication/ofr00362*.

Phleger, F.B., 1967, Marsh foraminiferal patterns, Pacific Coast of North America: Ann. Institute Biolologie Universita National Auton. Mexico 38, Series Cienco Del Mar y Limnolologie, v. 1, p. 11–38.

Phleger, F.B., 1970, Foraminiferal populations and marine marsh processes: Limnology and Oceanography, v. 15, no. 4, p. 522–534, *http://aslo.org/lo/toc/vol_15/issue_4/0522.pdf*.

Prescott, J.R., and Hutton, J.T., 1994, Cosmic ray contributions to dose rates for luminescence and ESR dating: Large depths and long-term time variations: Radiation Measurements, v. 23, no. 2–3, p. 497–500, *http://dx.doi.org/10.1016/1350-4487(94)90086-8*.

Puls, R.W., and Powell, R.M., 1992, Acquisition of representative ground water quality samples for metals: Groundwater Monitoring & Remediation, v. 12, no. 3, p. 167–176, *http://dx.doi.org/10.1111/j.1745-6592.1992.tb00057.x*.

Quinterno, P.J., 1968, Distribution of recent foraminifera in central and south San Francisco Bay: San Jose, Calif., San Jose State College, M.S. thesis, 83 p.

Ray, M.C., Kulongoski, J.T., and Belitz, Kenneth, 2009, Ground-water quality data in the San Francisco Bay study unit, 2007: Results from the California GAMA Program: U.S. Geological Survey Data Series 396, 93 p., *http://pubs.er.usgs.gov/publication/ds396*.

Riley, F.S., 1984, Developments of borehole extensometry *in* Johnson, A.I., Carbognin, L., and Ubertini, L., eds., Land subsidence: International Association of Hydrological Sciences Publication no. 151, p. 169–186.

Rogers, J.D., and Figuers, S.H., 1991, Engineering geologic site characterization of the greater Oakland–Alameda area, Alameda and San Francisco Counties, California: Pleasant Hill, Calif,. Rogers/Pacific, Inc., 59 p.

Rosenberry, D.O., 1990, Effect of sensor error on interpretation of long-term water-level data: Groundwater, v. 28, no. 6, p. 927–936, *http://dx.doi.org/ 10.1111/j.1745-6584.1990.tb01729.x*.

Ross, B.E., 1977, The Pleistocene history of San Francisco Bay along the southern crossing: San Jose, Calif., San Jose State College, M.S. thesis, 121 p.

Round, F.E., and Bukhtiyarova, Ludmila, 1996, Four new genera based on *Achnanthes* (*Achnanthidium*) together with a re-definition of *Achnanthidium*: Diatom Research, v. 11, no. 2, p. 345–361, *http://dx.doi.org/10.1080/0269249X.1996.9705389*.

San Francisco Bay Regional Water Quality Control Board, 1999, East Bay Plain groundwater basin beneficial use evaluation report: Oakland, Calif. [variously paged].

Schmertmann, J.H., 1954, The undisturbed consolidation behavior of clay: Transactions, American Society of Civil Engineers, v. 120, no. 2775, p. 1201–1227.

Schrader, H.J., and Gersonde, R., 1978, Diatoms and silicoflagellates, *in* Zachariasse, W.J., and others (eds.), Micropaleontological counting methods and techniques: An exercise of an eight metres section of the lower Pliocene of Capo Rossello, Sicily: Utrecht Micropaleontological Bulletin 17, p. 129–176.

Scott, D.B., and Medioli, F.S., 1980, Living vs. total foraminiferal populations: Their relative usefulness in paleoecology: Journal of Paleontology, v. 54, no. 4, p. 814–831.

Scott, D.B., Mudie, P.J., and Bradshaw, J.S., 1976, Benthonic foraminifera of three southern Californian lagoons; Ecology and recent stratigraphy: Journal of Foraminiferal Research, v. 6, no. 1, p. 59–75, *http://dx.doi.org/10.2113/gsjfr.6.1.59*.

Scott, D.B., Williamson, M.A., and Duffett, T.E., 1981, Marsh foraminifera of Prince Edward Island—Their recent distribution and application for former sea level studies: Maritime Sediments and Maritime Geology, v. 17, no. 3, p. 98–129, *http://journals.hil.unb.ca/index.php/ag/article/view/1380*.

Sedlock, R.L., 1995, Tectonic framework, origin, and evolution of the San Francisco Bay region, *in* Sangines, E.M., Andersen, D.W., and Buising, A.V., eds., Recent geologic studies in the San Franciso Bay area: Pacific Section of the Society of Economic Paleontologists and Mineralogists, Book 76, p. 1–17.

Slater, R.A., 1965, Sedimentary environments in Suisun Bay, California: Los Angeles, Calif., University of Southern California, M.A. thesis, 104 p.

Sloan, Doris, 1992, The Yerba Buena mud: Record of the last-interglacial predecessor of San Francisco Bay, California: Geological Society of America Bulletin, v. 104, no. 6, p. 716–727.

Sneed, Michelle, 2001, Hydraulic and mechanical properties affecting ground-water flow and aquifer-system compaction, San Joaquin Valley, California: U.S. Geological Survey Open File 2001–35, 26 p., *http://pubs.er.usgs.gov/publication/ofr0135*.

Sneed, Michelle, and Galloway, D.L., 2000, Aquifer-system compaction and land subsidence: Measurements, analyses, and simulations—The Holly site, Edwards Air Force Base, Antelope Valley, California: U.S. Geological Survey Water-Resources Investigations Report 2000–4015, 65 p., *http://pubs.er.usgs.gov/publication/wri20004015*.

Sneed, Michelle, Borchers, J.W., Kayen, R.E., Carkin, B.A., Ellett, K.M., Wheeler, G.A., and Brocher, T.M, 2007, Hydromechanical response characterization by integration of geophysical and hydrological data, San Lorenzo, California, Eos, Transactions, American Geophysical Union, v. 88, no. 52, Fall Meeting Supplement, Abstract H23A–1007.

Strausberg, S.I., 1983, Turbidity interferes with accuracy in heavy metal concentrations: Industrial Wastes, v. 29, no. 2, p. 16–21.

Trask, P.D., and Rolston, J.W., 1951, Engineering geology of San Francisco Bay, California: Geological Society of America Bulletin, v. 62, no. 9, p. 1079–1110, *http://dx.doi.org/10.1130/0016-7606(1951)62[1079:EGOSFB]2.0.CO;2*.

U.S. Geological Survey, 2012, Earthquake Hazards Program, Soil type and shaking hazard in the San Francisco Bay area, accessed December 11, 2012, *http://earthquake.usgs.gov/regional/nca/soiltype/*.

U.S. Geological Survey, [various dates], National field manual for the collection of water-quality data: U.S. Geoloigical Survey Techniques of Water-Resources Investigations, book 9, chap. A1–A9, *http://water.usgs.gov/owq/FieldManual/*.

Waters Corporation, 1992, Method A-103, Anion analysis using IC-Pak a HR column with borate/gluconate eluent: Waters Innovative Methods, 12 p.

Wilde, F.D., Radtke, D.B., Gibbs, J., and Iwatsubo, R.T., 2006, Collection of water samples: U.S. Geological Survey Techniques of Water-Resources Investigations, book 9, chap. A4, accessed June 28, 2007, *http://pubs.water.usgs.gov/twri9A4/*.

Wolf, R.E., Introduction to ICP-MS, U.S. Geological Survey, March 2005, accessed February 24, 2009, *http://minerals.cr.usgs.gov/icpms/intro.html*.

Prepared by the Sacramento Publishing Service Center.

For more information concerning this report, contact:

Director
U.S. Geological Survey
California Water Science Center
6000 J Street, Placer Hall
Sacramento, CA 95829

or visit our Web site at:
http://ca.water.usgs.gov

ISSN 2327-638X (online)
http://dx.doi.org/10.3133/ds890

Michelle Sneed and others—**Lithostratigraphic, Borehole-Geophysical, Hydrogeologic, and Hydrochemical Data from the East Bay Plain, Alameda County, California**—Data Series 890